UNIVERSITÀ DEGLI STUDI DI NAPOLI

FEDERICO II

DIPARTIMENTO DI INGEGNERIA INDUSTRIALE

Dottorato di Ricerca in Ingegneria Aerospaziale, Navale e della Qualità

SIGNIFICANT IMPROVEMENT OF THE SHIP ENERGY EFFICIENCY VIA DESIGN OF EXPERIMENTS AND REGRESSION ANALYSIS

Luigi Vitiello

Tutor
Prof. Ing. Salvatore Miranda
Prof. Ing. Biagio Palumbo

Coordinatore
Prof. Ing. Luigi De Luca

XXVI Ciclo

SIGNIFICANT IMPROVEMENT OF THE SHIP ENERGY EFFICIENCY VIA DESIGN OF EXPERIMENTS AND REGRESSION ANALYSIS

luigi.vitiello@unina.it

Department of Industrial Engineering, University of Naples Federico II, P.le V. Tecchio n. 80, 80125 Napoli (ITALY)

ABSTRACT

The main goal of the Ph.D. dissertation is to underline how a statistical approach in the planning and executive phases of the experimental activities, as well as the monitoring of complex systems can both bring real innovations in the maritime field and a higher efficiency in the results.

After drawing up the Kyoto protocol, the International Maritime Organization (IMO), the UN Agency in charge for legal questions dealing with the maritime sector, has approved and ratified many measures to reduce the CO2 emissions of ships. For this reason since January 1st, 2013 a higher energy efficiency for ships is required, to be achieved through design and operation choices. During the study for the dissertation it could be shown how the application of appropriate statistical frameworks allowed to meet the goals of recent requirements.

In the design step the experiment planning allowed to give designers of high speed crafts information about geometrical details of the stepped hulls. Moreover, the Design Phase has shown the strategic role that a systematic approach to planning for a design industrial experiment plays in technological process innovation. The team approach is the real driving force of pre-experimental activities.

In order to predict fuel consumption and therefore carbon dioxide emission by exploiting the navigation information usually available on modern ships, a statistical model is introduced based on multiple regression analysis. For each voyage the actual fuel consumption can be compared with the consumption prediction and the prediction limits obtained through the proposed model. If the prediction interval does not included the actual fuel consumption, the management would be alerted of any change (improvement/decrease) in ship performance or the possible need for further data analysis.

In fact, only with a proper and continuous monitoring of specific variables, it is possible to support sail management in making decisions.

In the Operation Phase, the statistical approach presented in this thesis helps practitioners to exploit navigation information usually available on modern ships in order to predict fuel consumption, and therefore CO2 emissions, for given specific set of sailing parameters.

Using these models it is possible to estimate both the reduction of fuel consumption through the improvement in energy efficiency and to estimate the CO2 emissions which is useful to get the carbon credit.

During the Ph.D. a new experimental proof protocol in the towing tank test was developed: a method for the measurement of the thrust of outboard marine engines, an innovative type of construction for propeller, boat appendages and clear composite hulls to see the water flows during the experiments in the towing tank test.

This study shows how engineering and statistical knowledge can be integrated and catalyses process innovation. Moreover, it allows for a continuous learning from data, which produces a significant improvement of the ship energy efficiency via design of experiments and regression analysis.

.

CONTENTS

ABSTRACT

The main goal of the Ph.D. dissertation is to underline how a statistical approach in the planning and executive phases of the experimental activities, as well as the monitoring of complex systems can both bring real innovations in the maritime field and a higher efficiency in the results.

After drawing up the Kyoto protocol, the International Maritime Organization (IMO), the UN Agency in charge for legal questions dealing with the maritime sector, has approved and ratified many measures to reduce the CO2 emissions of ships. For this reason since January 1st, 2013 a higher energy efficiency for ships is required, to be achieved through design and operation choices. During the study for the dissertation it could be shown how the application of appropriate statistical frameworks allowed to meet the goals of recent requirements.

In the design step the experiment planning allowed to give designers of high speed crafts information about geometrical details of the stepped hulls. Moreover, the Design Phase has shown the strategic role that a systematic approach to planning for a design industrial experiment plays in technological process innovation. The team approach is the real driving force of pre-experimental activities.

In order to predict fuel consumption and therefore carbon dioxide emission by exploiting the navigation information usually available on modern ships, a statistical model is introduced based on multiple regression analysis. For each voyage the actual fuel consumption can be compared with the consumption prediction and the prediction limits obtained through the proposed model. If the prediction interval does not included the actual fuel consumption, the management would be alerted of any change (improvement/decrease) in ship performance or the possible need for further data analysis.

In fact, only with a proper and continuous monitoring of specific variables, it is possible to support sail management in making decisions.

In the Operation Phase, the statistical approach presented in this thesis helps practitioners to exploit navigation information usually available on modern ships in order to predict fuel consumption, and therefore CO2 emissions, for given specific set of sailing parameters.

Using these models it is possible to estimate both the reduction of fuel consumption through the improvement in energy efficiency and to estimate the CO2 emissions which is useful to get the carbon credit.

During the Ph.D. a new experimental proof protocol in the towing tank test was developed: a method for the measurement of the thrust of outboard marine engines, an innovative type of construction for propeller, boat appendages and clear composite hulls to see the water flows during the experiments in the towing tank test.

In this study we have shown how engineering and statistical knowledge can be integrated, how it catalyses process innovation, and, moreover how, it allows an effective cycle of step-by-step learning to be implemented in order to produce a significant improvement of the ship energy efficiency via design of experiments and regression analysis.

INTRODUCTION

The main goal of the Ph.D. dissertation is to underline how a statistical approach in the planning and executive phases of the experimental activities, as well as the monitoring of complex systems can both bring real innovations in the maritime field and a higher efficiency in the results.
The developed methods are of an experimental and theoretical kind.
After drawing up the Kyoto protocol, the International Maritime Organization (IMO), the UN Agency in charge for legal questions dealing with the maritime sector, has approved and ratified many measures to reduce the CO2 emissions of ships. For this reason since January 1st, 2013 a higher energy efficiency for ships is required, to be achieved through design and operation choices. During the study for the dissertation it could be shown how the application of appropriate statistical frameworks allowed to meet the goals of recent requirements.
In particular it was possible to characterize the stepped hull design and to monitor the fuel consumption of the RO-RO Pax through the Design of Experiments and the development and implementation of an adequate regression model.
The main results obtained concern the following points:
In the design step the experiment planning allowed to give designers of high speed crafts information about geometrical details of the stepped hulls. In the operation step, the implementation of regression models for monitoring the fuel consumption of the RO-RO Pax allowed the fuel consumption prediction on a specific course and the estimation of the prediction intervals according to some sailing parameters. Using these models it is possible to estimate both the reduction of fuel consumption through the improvement in energy efficiency and to estimate the CO_2 emissions which is useful to get the carbon credit.
During the Ph.D. a new experimental proof protocol in the towing tank test was developed: a method for the measurement of the thrust of outboard marine engines, an innovative type of construction for propeller, boat appendages and clear composite hulls to see the water flows during the experiments in the towing tank test.

1. Problem definition

The economic development of the modern society is based on an increasing demand for the transport of goods and people. As mentioned in [1] and [2], the demand growing is estimated at about 10 times per generation.
90% of the world commerce today is operated by 100.243 ships [3]. In 1885 the last maritime transport on long course with a sailing ship was operated. The sailing ships, which had a leading role up to that time in the world maritime transport, were replaced by steam ships. The fastest sailing clippers, which could sail at a speed of 20 knots, although faster than the stream ships, always depended on the wind. Further on the East-Europe course the sailing clippers couldn't cross the Suez Canal. The new stream-

operated ships, over that limit, reduced drastically the travelling time, and the sailing clippers were less competitive.

The sailing clippers had limits regarding the stowage, the loading and needed a big crew to operate the sails. This meant higher costs for the crew. Differently from the ships operated with fossil fuel, the environmental effects of the wind driven ships during the navigation was next to zero.

During the 20th century, following the technological development and the increasing demand and necessity to reduce the transport time of goods, the "naval gigantism" began. The construction of bigger and bigger, faster and faster ships needed the installation on board of huge power, which meant a higher fuel consumption and influence on the environment.

According to the second IMO Green House Gas study final 2009 [3], the international transport produces about 870 million tons of CO_2, i.e. 2,7% of the global emissions of carbon dioxide in 2007. The exhaust gases of engines are the main source of greenhouse gases from ships and among them carbon dioxide is the most important not only regarding to the quantity but also for the global warming.

2. Comparison of CO_2 emissions for various transport modes

Gabrielli and von Kármán in [1] assembled a collection of data for installed power, maximum speed and gross weight for a wide variety of transport modes.

The log-scale graph shows for different kinds of means of transport what is the necessary power for a weight unit to move a mass at a given speed.

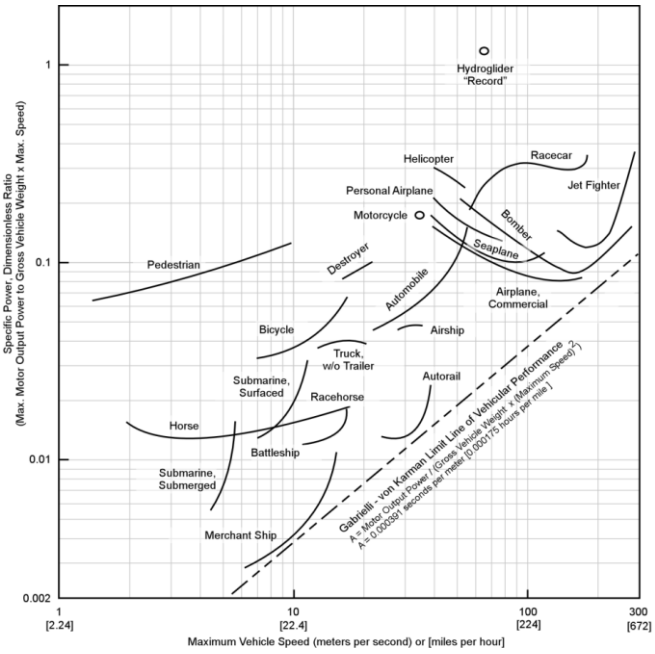

Figure 1: Gabrielli Von Karman Diagram

The Gabrielli Von-Karman diagram *Figure 1* quotes on abscissa the maximum vehicle speed and on ordinate the specific power for weight unit necessary to develop that speed. Similar to this the value on

ordinate can be read like the energy (see y-axis on the diagram) necessary to cover a given distance with different means of transport. This diagram can also be interpreted for the environmental effects, e.g. for the CO_2 emissions, as there is a direct correlation between the fuel consumption, delivered power and CO_2 emissions.

In *Figure 1* you can see the technological limit curve for different means of transport "Gabrielli Von Karman limit"; next to this curve there are the means of transport with a higher energetic efficiency, e.g. merchant ships and trains. These have the lowest CO_2 emissions compared with the loaded tons and speed.

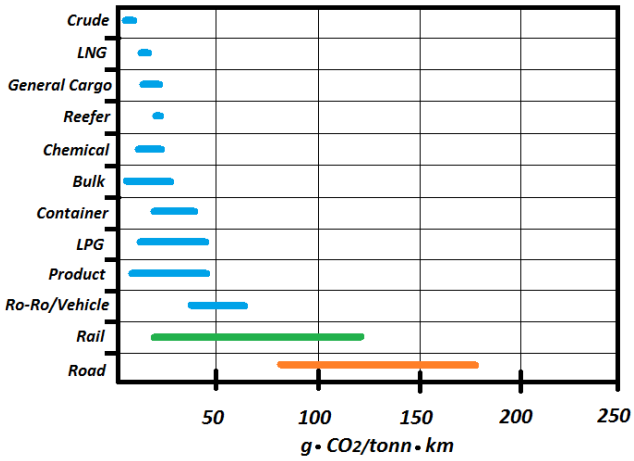

Figure 2: comparison between CO_2 emissions of ships and carriage by rail and on the road

Figure 2 shows the CO_2 emissions of different kinds of ships compared with the carriage by rail and on the road. *Figure 2* also shows that the means of carriage with the lowest environmental effects are the crude oil ships and the bulk carrier ship, e.g. ships which can carry a huge quantity of goods at a low speed.

The studies carried out by IMO [3] assert that in the next 40 years the emissions of greenhouse gases will increase of 150-200% compared to today.

3. Legal framework

After signing up the Kyoto protocol, IMO presented in 2009 a survey of the greenhouse emissions produced by the shipping sector [3]. It also approved and ratified some measures to reduce the CO_2 emissions coming from ships.

IMO through the MEPC (Maritime Environmental Protection Commitee) has focused its attention on the problem of polluting emissions and required from the shipping companies to maximize the energy efficiency of a ship both during the design and the operation with different activities as shown in *Figure 3*.

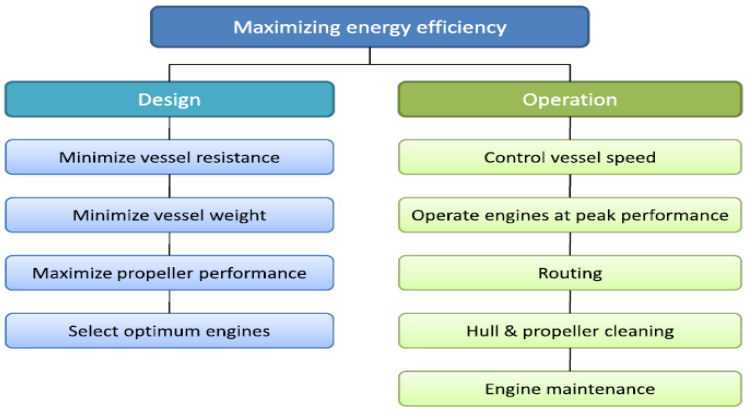

Figure 3: main measures to maximize the energy efficiency [3]

During the *design* phase, to maximize the energy efficiency it is necessary to minimize the vessel resistance, to maximize the thrust efficiency, to reduce the vessel weight and to choose the right power plants so that the energy consumptions are low and that the main and auxiliary engines can work to the best output possible.

During the *operation phase*, to maximize the energy efficiency it is necessary to ensure that the ship is driven in the best way possible by the crew, respecting the mission profile for which it was built and a right maintenance of engine, hull and propeller must be carried out.

To face the a.m. problems the shipping companies are trying to build ships which are more and more efficient from an energy point of view, with flexible mission profiles and with a remote monitoring.

In fact, since January 2013 the IMO (International Maritime Organization) through the MEPC (Maritime Environmental Protection Committee) [3] [4], has been imposing on shipping companies a significant improvement in ship energy efficiency. That not only during the sailing, but also from the design process, onwards through the definition of the Energy Efficiency Design Index (EEDI) [5] [6] [7] and the editing of the Ship Energy Efficiency Management Plan (SEEMP) manual [8] [9] to regulate the CO_2 emissions [10].

4. EEDI

The EEDI [6] [5] [7] [11] indicates a merchant ship's CO_2 output in relation to its value for society measured in transport work capacity.

The EEDI is calculated on a large number of parameters. It is based on the installed main engine power, the speed obtained at 75% of Maximum Continuous Rating and scantling draft, the engine specific fuel oil consumption (main and auxiliary engine) and the type of fuel burned (via the fuel's CO_2 emission factor). The results are expressed in CO_2 emission in gram per tonne of cargo transported over one nautical mile (g CO_2/ton mile). The EEDI calculation formula is presented and explained in Figure 4

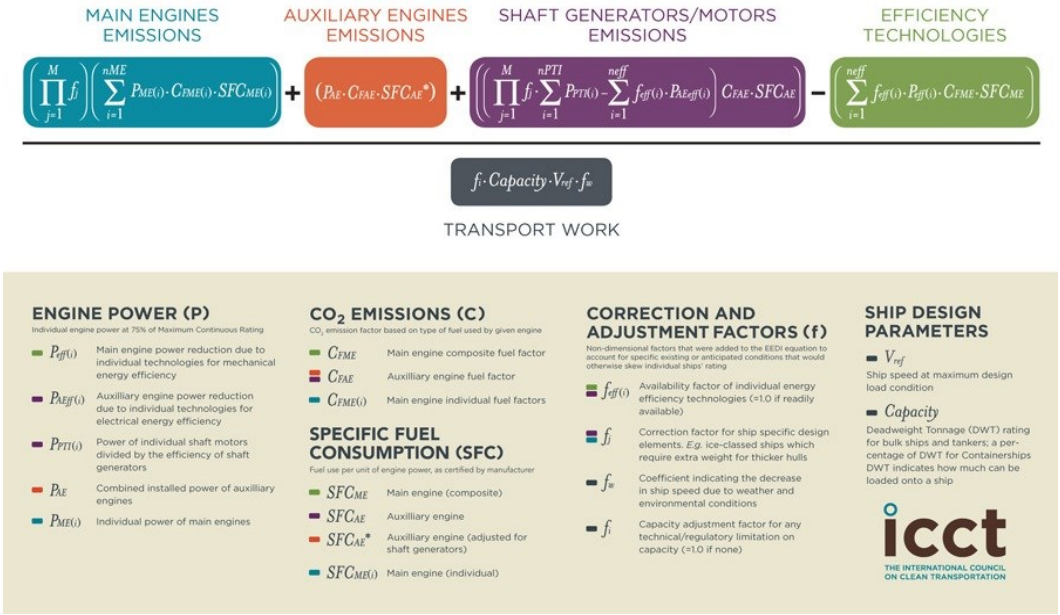

Figure 4: formula for the calculation of the EEDI Index and label explaining the sizes used [11]

5. SEEMP

The SEEMP [8] [9] [11] should be developed as a ship-specific plan by the ship owner, operator or any other party concerned, e.g., charterer. The SEEMP seeks to improve a ship's energy efficiency through four steps: planning, implementation, monitoring, and self-evaluation and improvement. These components play a critical role in the continuous cycle to improve ship energy management.

A possible approach to the monitoring step is suggested through the use of the EEOI Index and the operator is urged to adopt new technologies and practices to optimize the ship performances.

6. EEOI

The EEOI [11] [12] is an index for monitoring fuel consumption and CO_2 emission (CO_2-Index) for ships in operation. However, it is a recommended part of the SEEMP which is required on all ships after January 1st, 2013.

Like the EEDI the EEOI is expressed in gram CO_2 emitted per tonne cargo transported over the distance of one nautical mile (gram CO_2/ton mile). As opposed to the EEDI, its calculation is based on the real fuel consumption and cargo load of the vessel:

$$\text{EEOI} = \frac{\text{Total Fuel Consumption} \times \text{Fuel Carbon Content}}{\text{Cargo mass} \times \text{Sailed Distance}} \quad (1)$$

This index changes according to the time and depends on the fuel consumption, the course and the cargo loaded. The EEOI as defined does not take into account of some factors on which the ship consumption depends, e.g. the speed. The same load can be carried on the same course and then taking in

consideration the same miles with two different ships which use up the same quantity of fuel though sailing at different speeds. Consequently this kind of index doesn't take into account the efficiency of the ship.

Despite legal framework requirement for EEOI are not feasible for CO_2 emission monitoring in real conditions.

Conversely, in this study a model for consumption prediction (as well as CO_2 emission prediction) on the basis of real navigation data, which has not taken into consideration from the literature before.

SECTION 1: DESIGN PHASE

INTRODUCTION

In this section of the study we will find out the best design details of an unconventional hull through the use of statistical methodologies with the goal to reduce the vessel resistance, the fuel consumption and the CO_2 emissions. The obtained results are used as design guidelines.

This approach can be used for the design of any kind of ship hull or a part of it.

In particular, after the assignment of the design data, first the design details were found out through the conventional bibliographical analysis and then an experimental methodology in a towing tank test was developed to measure the hull total resistance R_{TM}, the dynamic trim angle τ and the dynamic sink age S_K. At the end, design of experiments in a towing tank test will be carried out on different hulls to find out the geometrical detail of the stepped hull.

1. Setting of the stepped hull among the hulls, state of the art

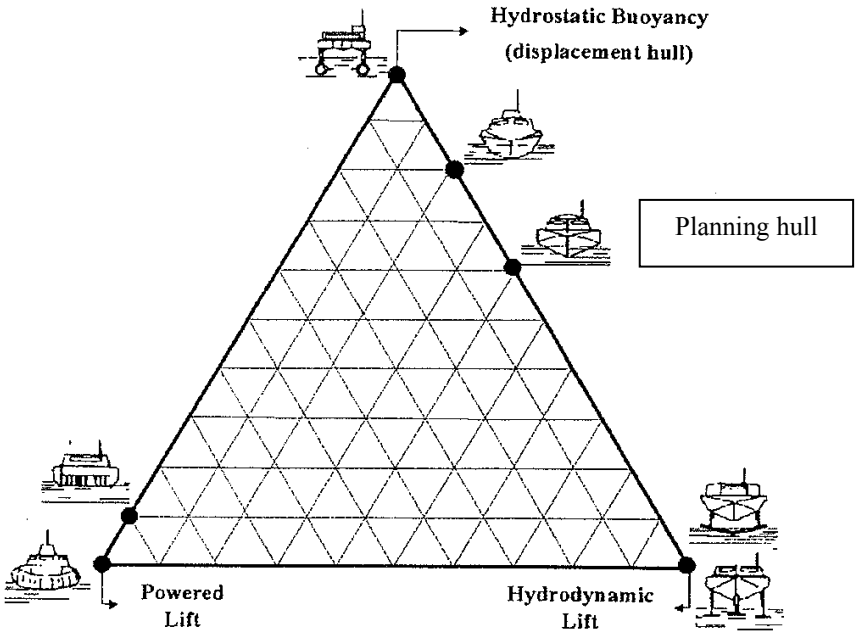

Figure 5: sustention triangle

The classification of advanced vehicles and their hybrid derivation usually follows the classical sustention triangle, Jewell (1973). The corners of this triangle represent the vessels supported by hydrostatic buoyancy, hydrodynamic lift and powered lift. The edges and the inside of the triangle represent the hybrids, *Figure 5*.

Planning boats and therefore the stepped hull move to the right side of the triangle as a speed variation occurs.

The state-of-the-art regarding transport efficiency is described in the *Figure 55* below. This figure is shown in many scientific publications, among them (Donald Blount et al…).

On the abscissa we see the Volumetric Froude Number F_∇, the non-dimensional parameter of speed; on the ordinate we see the transport efficiency E_T defined as:

$$E_T = \frac{W \cdot V}{0{,}102 \cdot P_d} \tag{1}$$

Where speed V is expressed in m/s, the displacement of the unit W is expressed in metric tonnes and the power delivered to the propeller P_D is expressed in kW.

This parameter is the weight/power ratio and represents the quality of the whole means of transport.

Its curves are the result of a statistical analysis of many points where each of them represents a boat at the top of its performance. For example the rigid inflatable boats Mito 31 (RIB) built by MVmarine, a mono hull with two steps, have a top speed of 60 knots and 442 kW (600 HP) as well as a displacement of 31392 N, is represented by the point that shows $F_\nabla = 8{,}1$ and $E_T = 2{,}2$. The *Figure 55* represented scales are log-scales.

If you analyse the graph you see that at an operating speed with very low Froude numbers, up to 0,8, the hard chine hulls obtain the best results. In an operating range at a Froude number between 0,8 and 1,5 the round bilge hulls have better results and over a Froude number of 1,5 up to 6 the surface effect ship (SES) have the best results. If the speeds grow and the Froude number is more than 6 the stepped hulls have an undisputed supremacy.

2. History of the stepped hull

The first stepped hulls were originally proposed by Rev. Ramus of Sussex England in 1872. Probably the first systematic and scientific data, also useful for planning hulls, was obtained by the experimental tests on the model stepped hulls of seaplanes between the two world wars. In this regard, it is worth to remembering the research institutes of Langley Field (USA), Farnborough (England), Hamburg (Germany) and Guidonia (Italy). The last two were destroyed following the events of the last world war.

At the beginning of the 1900s the stepped hulls were used for seaplane skids. They had considerable takeoff and landing speeds, much higher than the speed of marine vehicles of that time. That's why many studies were carried out in USA and published by Society of Naval Architect and Marine Engine in 1911 on Transaction [13], where different flat plates, V-shaped plates as well as stepped plates were tested to analyze their performance.

In the past the only hulls able to develop high speeds were the few operating in the marine and in racing. For this reason the study of the first of them was kept a secret and for the second ones the experiences of naval architects and boat yards were well protected.

Today it's easy to find low cost high powered engines, especially as boats are lighter and lighter and thanks to new building technologies with composite materials it's easy to reach quite high speeds (F_N high Froude numbers).

3. Hydrodynamic operational principle of a stepped hull

The usual high speed planning crafts have V-shaped and hard chinned hulls; sometimes, one or more steps are adopted in the hulls.

The steps are sharp discontinuities located in the bottom surface of the hulls; usually they run transversally and they are V-shaped, with the vertex facing aft ward; on the outboard sides the steps terminate with large apertures.

When the craft travels at high speeds, the air sucked through the outboard side apertures leads to flow separation and the formation of gas cavities. If the steps are ventilated enough by the sucked air, the phenomenon stabilizes and the effects may be two effects: a reduction of the total wetted surface and an increase in the hull lift-drag ratio. The results show values of the hydrodynamic resistance significantly lower than those of the stepless mono-hulls.

Dynamically, the water flow crossing the step finds a vacuum zone in which the hull dries up, with a reduction of wetted hull surface and the frictional resistance. In *Figure 6* the total wetted hull surface on the ship (hatch area) at 50 knots speed should be about 5 m^2.

In general every hard chine hull in planning will be in $n+1$ fluid triangles with decreasing pressure from water stagnation line.

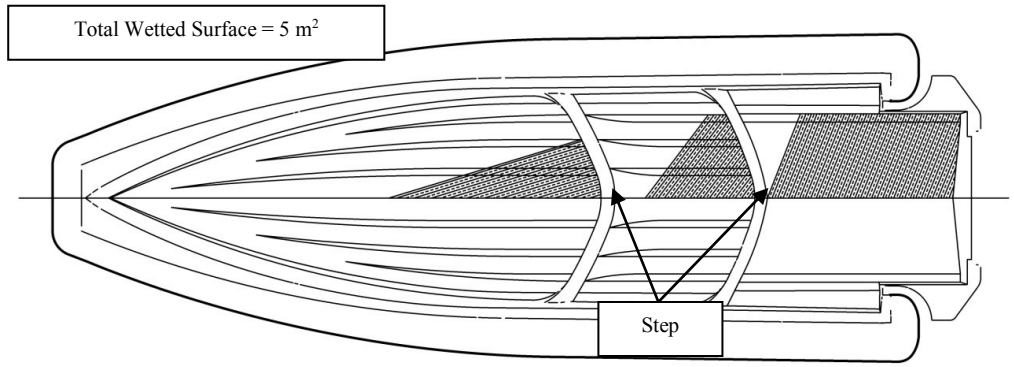

Figure 6: stepped hull, wetted surface at 50 knots speed

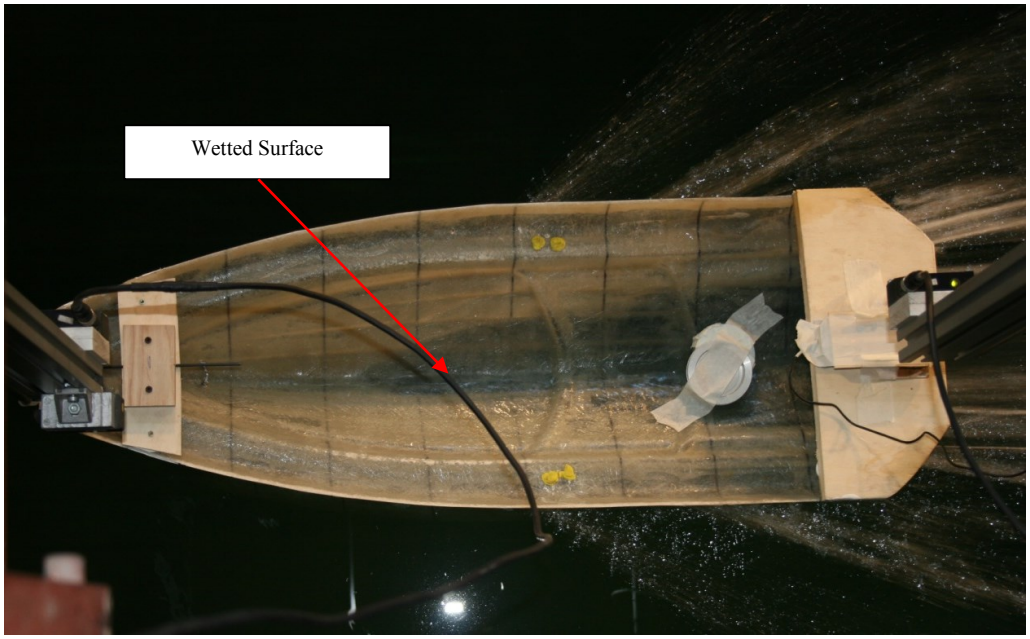

Figure 7: stepped hull model, wetted surface at 50 knots speed, model basin photo, Naples March 2012

According to the previous rule, if we consider a hull with two steps, in planning it will be on 3 water triangles of lift (see *Figure 6 and Figure 7*), while the same stepless hull will be on une water triangle of lift (*Figure 8 and Figure 9*). In the case of stepless hull running at 50 knots the water plane surface area will be 8,6 m^2, *Figure 8 and Figure 9.*

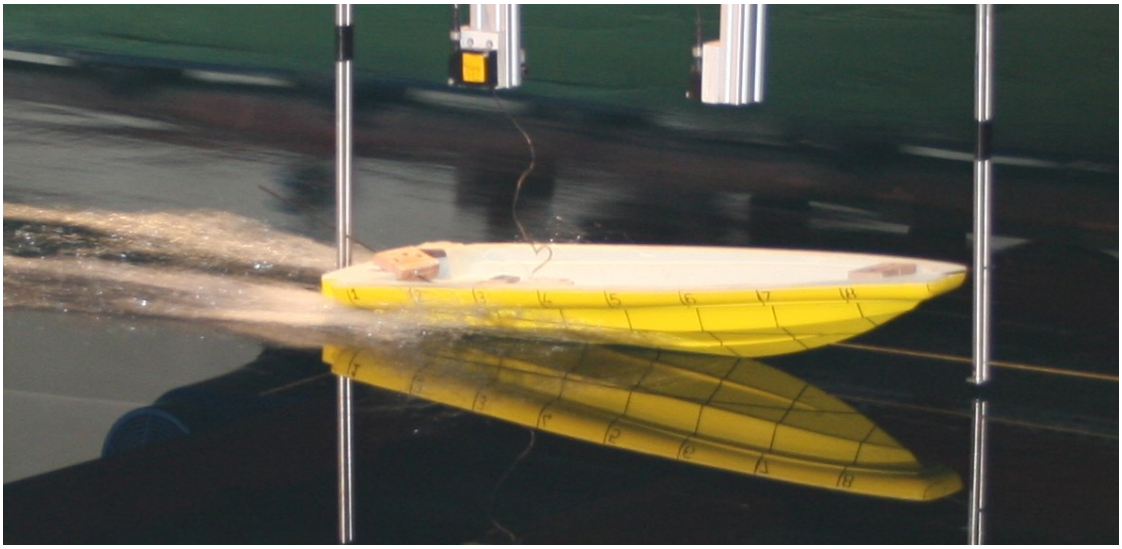

Figure 8: stepless hull model at 50 knots speed, model basin photo, Naples March 2012

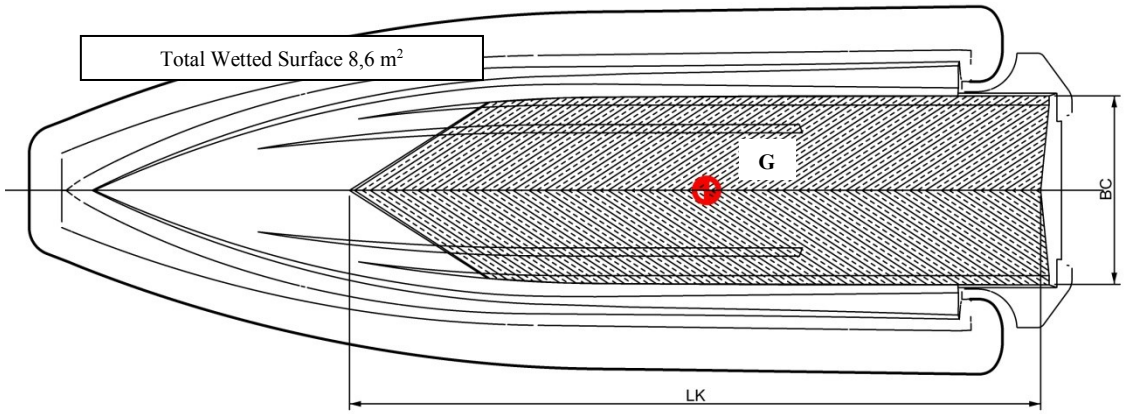

Figure 9: stepless hull, wetted surface at 50 knots

CHAPTER 1 – CONVENTIONAL DESIGN

1. Design issues

When you have to carry out a boat design to analyse the performances referring to vessel resistance and trim, you may use three methods of investigation: the towing tank tests, the computing fluid dynamics (CFD) and the systematic series. In the case of the high speed crafts (HSC) (high Froude number), with the detachment of the confined flow and the two-phase flows, the CFD analysis still doesn't produce good results.

Today if you wish to design a hard chine hull for a small craft, the only complete and reliable data at disposal of designers is the systematic series 62 and 64, designed and tested by Eugene Clement, Donald Bount, and so others the David Taylor Model Basin (DTMB, USA) from the early 50s until 1964. They are hard chine hulls with different geometries, displacements and dead rise angles.

The hard chine hulls have an intrinsic limit given by their geometric shape; indeed the higher the speed, the higher also the vessel resistance compared with a simple chine stepped hull. Instability and dynamic phenomena occur more easily.

But if a designer wishes to build a stepped hull, he has no systematic series from which to obtain reliable data and information.

Assignment of the following design data

Hull Type	*Hard chined, stepped hull*
Length Overall (m)	*10*
Chine Beam (m)	*2*
Deadrise Angle (°)	*23*
Displacement (N)	*31392*
Maximum Speed (knots)	*50*
Propulsion type	*Outboard engine*

Table 1: design data

Whit these design data has been conducted a bibliography analysis.

The study of the factors involved in the experimentation is a crucial task and requires intensive knowledge transfer. The first brainstorm in step involved listing all of the factors that, according to different technological points of view and competencies, came out during team discussion. The second step consisted of classifying each factor as a control, held-constant or nuisance factor [14]

Control factors in the screening experimental phase, the following control factors have been selected: numbers of the steps (N_S), step height (H_S), longitudinal position of the step (LSP), longitudinal position of the gravity centre (LCG), and model speed (V_M). All the factors are quantitative parameters.

Table 2 shows normal and generally good values, as reported in technical literature.

Control Factor	Optimum value	Unit	Paper
Numbers of the steps (Ns)	2	N°	**[15] [16]**
Step height (Hs)	40	mm	**[15] [16]**
Longitudinal position of the step (LSP)	LCG between aft and fore step		[15] [16] [17]
	LSP is function of boat geometry		[18]
	LCG is forward the first step		[19]
Static Tau	0, -1	Deg.	**[20]**
Model speed (Vm)		m/s	

Table 2: control factor

Step Number (Ns) is 2 because this hulls have a high L/B ratio. In accordance with Peters in [16] and Akers in [15], single or twin step decisions depend on length-to-beam ratio, and speed. The low aspect ratio lifting surface of boat with narrow beam requires two steps for lift.

Step Height (Hs) is 40 mm but is difficult to define because it is different for every hull and is based on the angle of attack. Peters in [16] defines a minimum and maximum value for Step Height (31,8 mm, 65,5 mm). Akers in [15] in accordance with the author Norman Skene specifies that high steps are not necessary and that experience shows steps as low as 16 mm could be effective. The real issue with high speed steps is that you may have to put an S-curve in the buttock line behind the step to control the angle of attack of next step

Longitudinal Step Position (LSP) have different solutions.

First in accordance with Acampora in [17], Akers in [15] and Peters in [16] a solution is based on the concept that it is necessary to have a middle surface close to the LCG, with the forward and aft portions of the hull stabilizing the craft longitudinally. This solution has a problem: if you put the steps too close to each other, the water attaching to the second step is contaminated by the aerated low-density water from the first step.

Second, Clement and Pope [18] define a procedure to obtain LSP in function of hull geometric parameters. However, the step is always forward with respect to the LCG.

The third solution is in accordance with Clement in [19], is based on the utilization of a design approach for a stepped hull similar to a design of a hydrofoil boat or an airplane. Therefore this approach is able to find the optimum configuration of a lifting surface to obtain a maximum lift-drag ratio, but, as consequence, the CG is closed in a forward lifting surface. On the other hand the LCG is near the fore step but further forward respect it. Where you put the LCG, so that weight is balanced across the steps, only a small change in the relative locations of LCG and centre of pressure will change your boat from stable to unstable.

Referring to the trim angle static at rest τ_0, as shown in [20], a boat by the trim by stern presents a higher resistance at low Froude numbers, while at high Froude numbers resistance will be lower.

2. Design of a stepped hull according to the literature

According to the literature, the following design parameters are considered:

- number of step 2
- step height 40 mm
- longitudinal centre of gravity close between the fore and the aft step.

CHAPTER 2 – TESTING METHODOLOGY

When carrying out a power prediction, it is known that the power delivered P_D of the engine is equal to:

$$P_D = \frac{P_E}{\eta_D} \tag{2}$$

Where:

- $P_E = R_T \cdot V$ represents the effective power of the hull, calculated through the total resistance R_{TM} measured with a towing tank test, and the test speed V_M.
- $\eta_D = \eta_0 \cdot \eta_r \cdot \eta_h$ where $\eta_h = \frac{1-t}{1-w}$ and represents the quasi-propulsive efficiency considering the hull, the propeller and the interaction between them.

As our research was made on a planning hull, it's justifiable to suppose that efficiency $\eta_r = 1$.

In literature, there are not self-propulsion tests with propellers similar to them installed on the outboard engines, and there are no towing tank tests of such small and fast hulls. It has been necessary to define a different approach: first of all we had to research a new experimental methodology to obtain good results for the measure of R_{TM}; then we had to make instruments to measure the thrust of the engines and to calculate $1-t$; finally we had to build a model propeller like the one used for the experiment to gain a survey of the necessary values to calculate the coefficients η_0 and $1-w$.

1. Experimental methodology to the hull resistance measure

Power prediction through the towing tank tests was conducted at the Department of Industrial Engineering section of Naval Architecture and Marine Engineering of the University "Federico II" in Naples. Dimensions of the basin are: length 137,5 m, width 9 m, deep 4,25 m. The tow carriage is able to develop a maximum speed of 10 m/s with a maximum acceleration of 1 m/s^2.

The test used Froude methodology for effective power calculation; the scale model has considered the maximum ship and the maximum carriage velocities.

The first test series has been done with R47 by Kempf & Remmers equipment *(Figure 11)* which constrains the model by system force shown in *Figure 10*. The thrust T, that is the shot force which happens in the hinge, is located in a higher position compared to the centre of gravity and higher with respect to hydrodynamics centre. The R47 instrumental gravity centre is located in the same longitudinal abscissa of the buoyancy centre. We have also done many tests reducing the instruments' weights by a tackle, but the results have been poor because the values of τ angle and running resistance obtained by model experiments were too different of sea trial results.

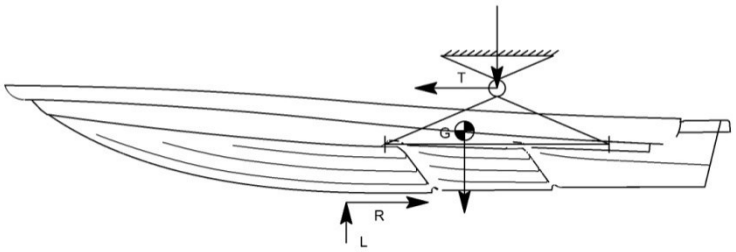

Figure 10: R47 system forces

2. Experimental issues

The development and diffusion of stepped hull forms, even in widespread use, can take great advantage from towing tank tests. For power prediction, towing tank tests were carried out with scale model of standard Rigid Inflatable Boats (RIB), Mito 31 built by MVmarine S.r.l., with different testing methodologies.

The small model dimension makes the experimentation and towing tank-sea correlation difficult, because of scale effect problems and high ship speed (50 Knots, Fn 3,0 and F_∇ 7,0). However, a particular test system has been setup which reproduces in the towing tank the same dynamic condition as at sea. This new setup has been developed to reproduce in the towing tank test the same angles measured in sea trial. Since the trim angle is a fundamental quality for the dynamical similarity between model and ship flows.

The speed and resistance measurements have been transferred with Froude methodology, up to a speed of 50 knots.

The angle τ is a direct consequence of the forces system acting on the running hull and influencing the relationship between lift and drug L/D, dynamic stability, porpoising and sea keeping.

Many different models in scale ratio 1:10 were built using different construction techniques and materials in order to reproduce forms as accurately as possible.

3. Sea trial tests to dynamic trim angle measure

The need to start our research from sea trial tests comes from the difficulty of the towing tank tests with R47 Kempf & Remmers instruments (see *Figure 11*), generally used for planning hull. The tests showed that the model was unable to lift itself from the water at high speed, with high resistance value.

Contrariwise the full scale RIB Mito 31 behaved differently and this suggested the carrying out of a series of sea trial tests on Mito 31 RIB.

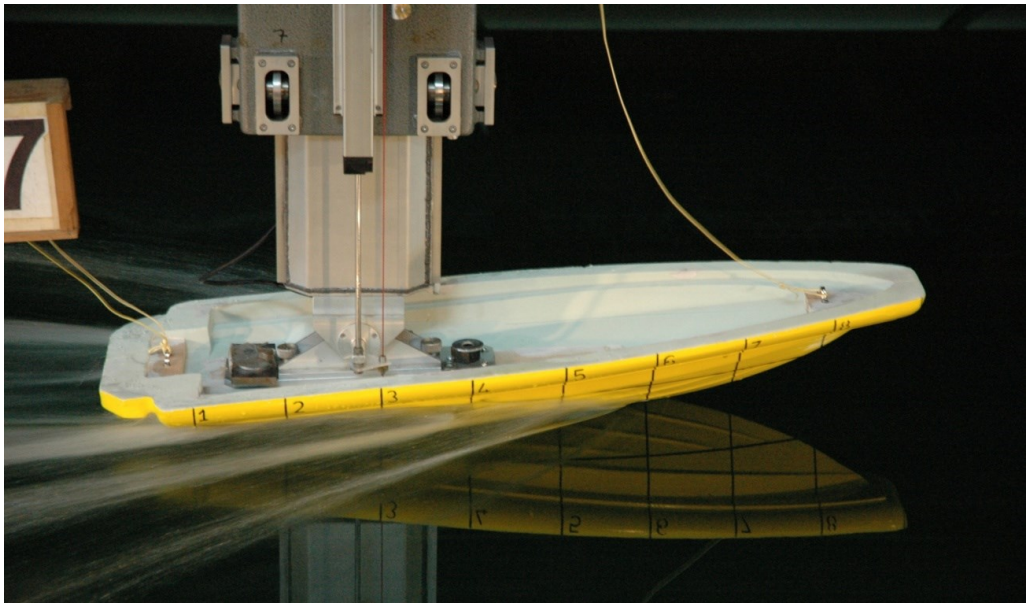

Figure 11: R47 Towing tank test, stepped hull 50 knots speed, Model Basin photo, Naples August 2011

In sea trial tests, an inertial platform was installed with as output data Euler angle and acceleration measures (*Figure 14*). Using board instruments fuel consumption and rpm engines (*Figure 13*) were acquired for each speed.

Figure 12: inertial platform

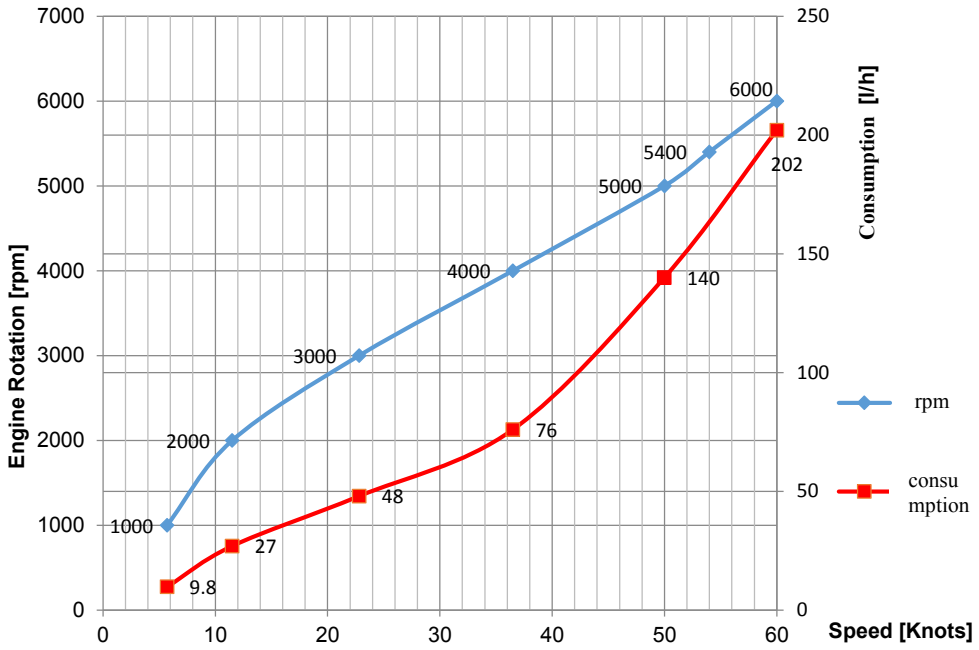

Figure 13: sea trial test, speed, rpm, fuel consumption curve

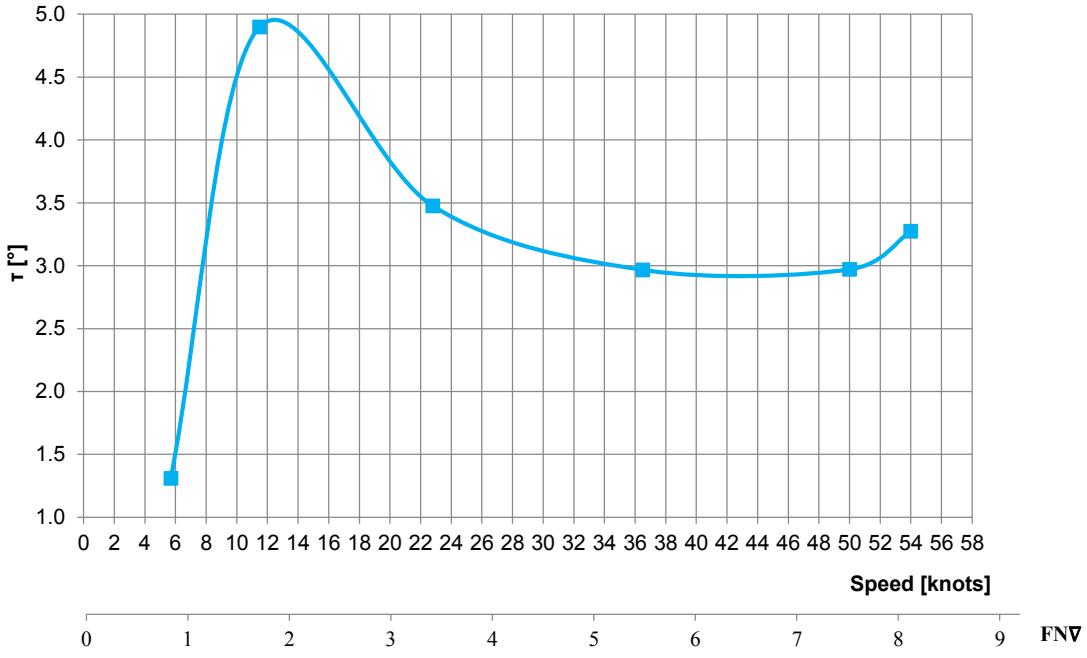

Figure 14: sea trial test τ Vs speed curve

4. Trim Engine effect

All outboard engines are equipped with power trim and tilt systems, in order to direct thrust in the

centerplane with, consequently, a variation in the moment that the engine transfers on the transom; however, this system modifies forces and causes additional difficulties that must be considered.
The effects of this regulation at maximum engine rotation allow for the gaining of 4 knots at maximum speed and 0,5° of dynamic trim angle τ influencing hump speed.
Accordingly, to reduce the number of variables, all sea trial tests were performed with RIB ships and the thrust direction in a horizontal position in static condition, with zero trim and zero thrust angle (figure 12, T vector parallel to WL).

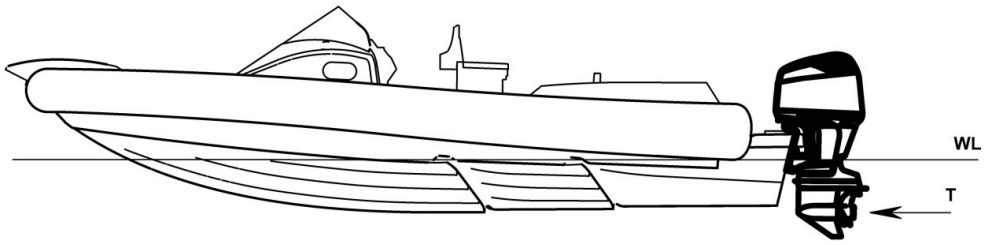

Figure 15: outboard engine thrust

5. Experimental Studies – Down Thrust Methodology

We analysed the true forces system (*Figure 16*) and we tried to reproduce a similar system in towing tank test to obtain the same τ angle.

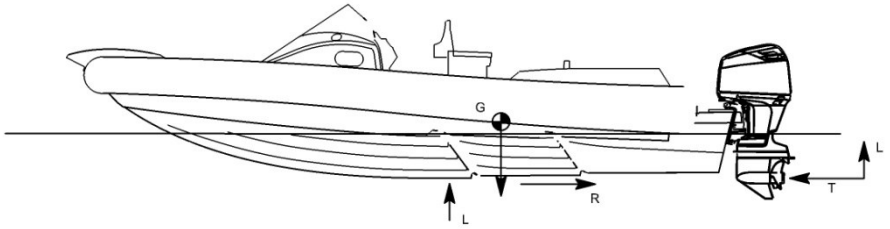

Figure 16: true forces system

To reproduce at best the system forces we started again from real RIB, the two outboards engines have been constrained to the transom trough four bolts for every engine, two in highest bracket zone and the other two in the lowest bracket zone *(Figure 17).* The engine, when going forward transfers the T Thrust to the transom through F1 Force applied in lowest brackets area and the T thrust moment, as regards the lowest brackets area through traction force F2, applied in the highest part, of the bracket (*Figure 18*).

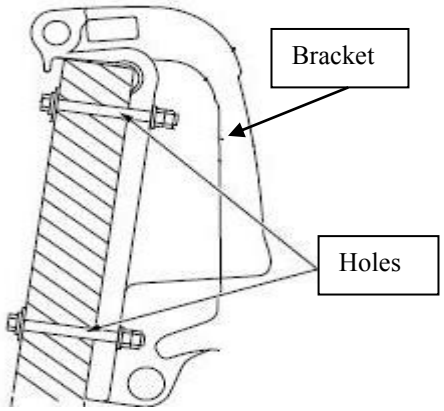

Figure 17: engine bracket

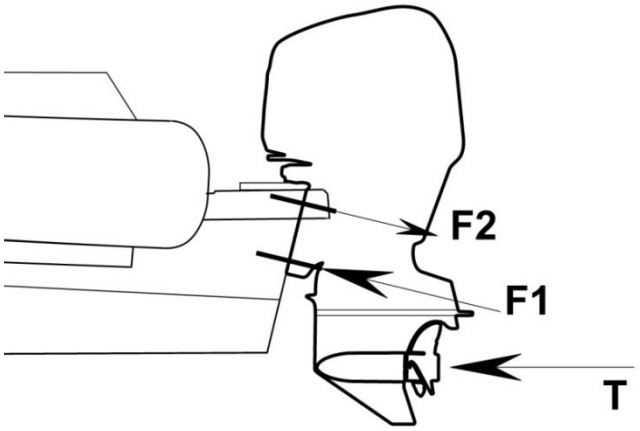

Figure 18: engine forces

Consequently, the system forces engine/RIB is similar to a beam supported by a pin and a roller (*Figure 19*). In fact, the propeller thrust is transmitted to stern through a moment generated by the thrust vector with respect to the lowest brackets area, while the highest holes are in contrast (*Figure 20*).

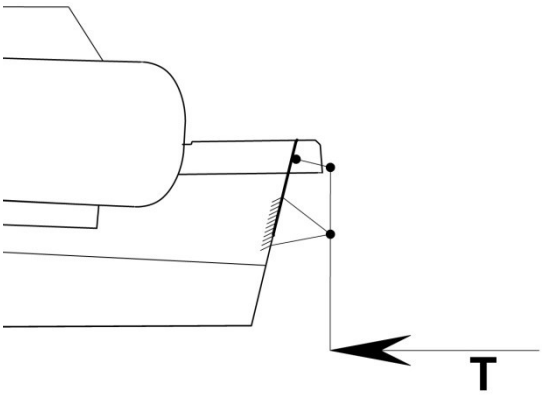

Figure 19: engine thrust 1

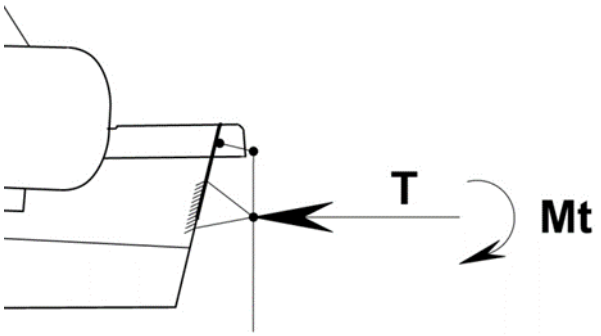

Figure 20: engine thrust 2

The last observation is based on the location of the model point thrust. In fact the thrust to the transom is transmitted entirely from the lowest bracket area.

In a horizontal position in a static trim angle at rest τ_0 equal at zero, the towing tank thrust force is applied in the point P intersection between engine thrust direction and keel line at bow (*Figure 21*)

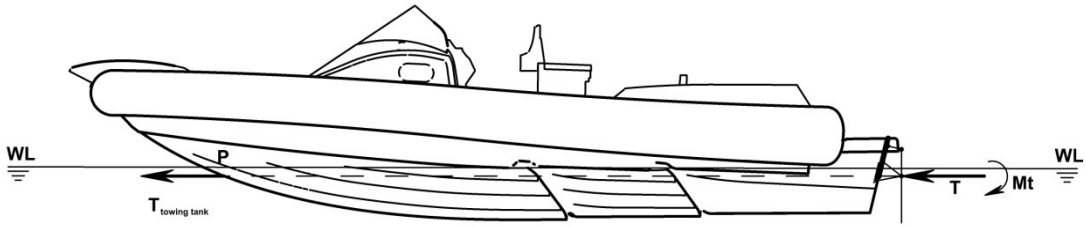

Figure 21: towing tank thrust force

:

This methodology, called "Down Thrust" (DT) does not consider the M_T moment effect, which could generate on the RIB an increasing of the τ angle.

There is a fixed orthogonal reference axis with origin in the aft perpendicular. The X-axis is parallel to the base line and positive toward the bow, the Z-axis is orthogonal to the steel water plane and positive going upwards, and the Y-axis is positive towards the RIB right side.

With R47 instruments the model had just 3 degrees of freedom, moving along X and Y-axis and rotating around Y-axis. In the case of "Down Thrust" it has all the six degrees of freedom. In fact, to avoid the instability phenomena, the model has been realized with two guide model masts; one located in the bow and the other at stern, which engage in two forks. (*Figure 22*).

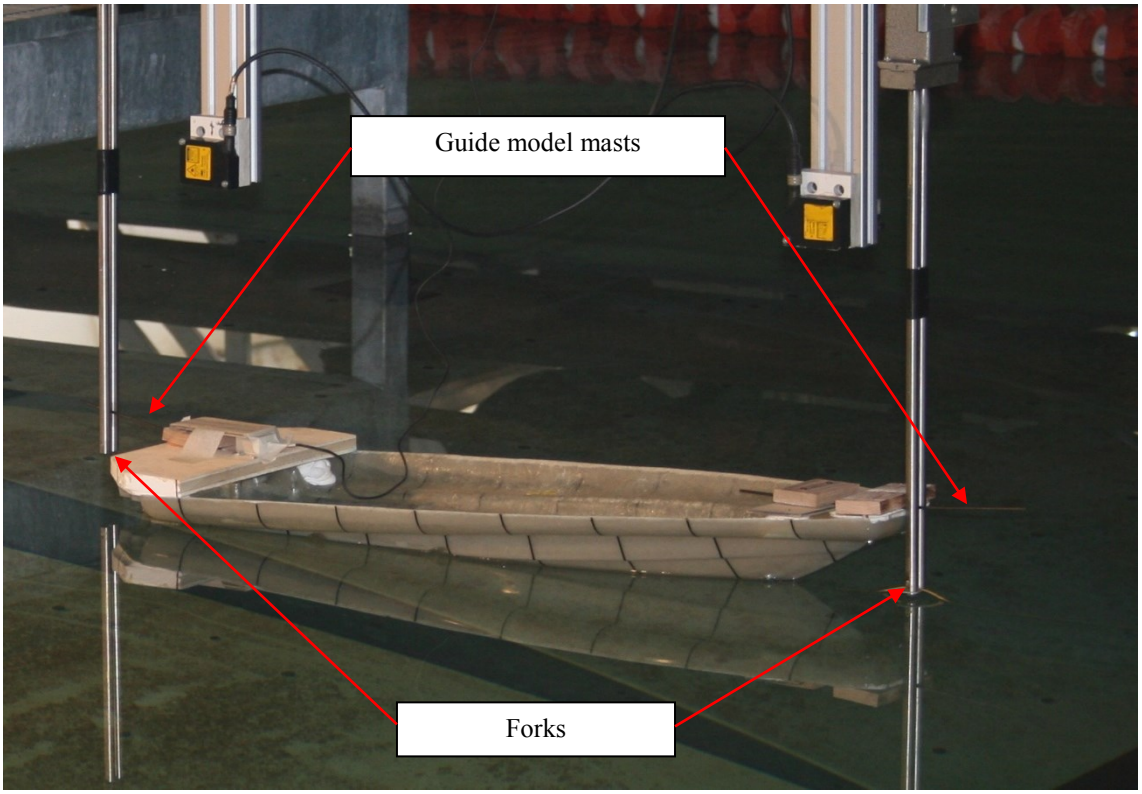

Figure 22: towing tank DT Test, stepped hull, Model Basin photo, Naples March 2012

Down Thrust allows the model to move along the X and Z-axis but not along the Y-axis, and allows for rotation around the Y and X-axis but not around Z-axis. Consequently only the yaw and drift motion are constrained.

We reached this solution releasing the model from each instrument, because with such a small model displacement (3,13 Kg) the RIB model becomes sensitive to every external force.

All the towing tank tests have been executed with zero trim in static condition $\tau_0 = 0$.

Consequently, the towing tank and sea trials test results are compare in *Figure 23 and Figure 24*. The first chart, *Figure 23*, shows the τ angle versus the speed. It has been noticed that $\tau - V$ curve obtained by Down Thrust test shows the same trend as the sea trial test curve. Conversely, the R47 instrument has registered the τ lowest values because, having the highest thrust respect to the hydrodynamic resistance centre; it produces a bow pitch moment which it transfers to the small model.

In the speed range between 30 and 50 knots, the difference between the τ_M angle measured in towing tank test with respect to the sea trial test τ_S angle is an average of 0,3°.

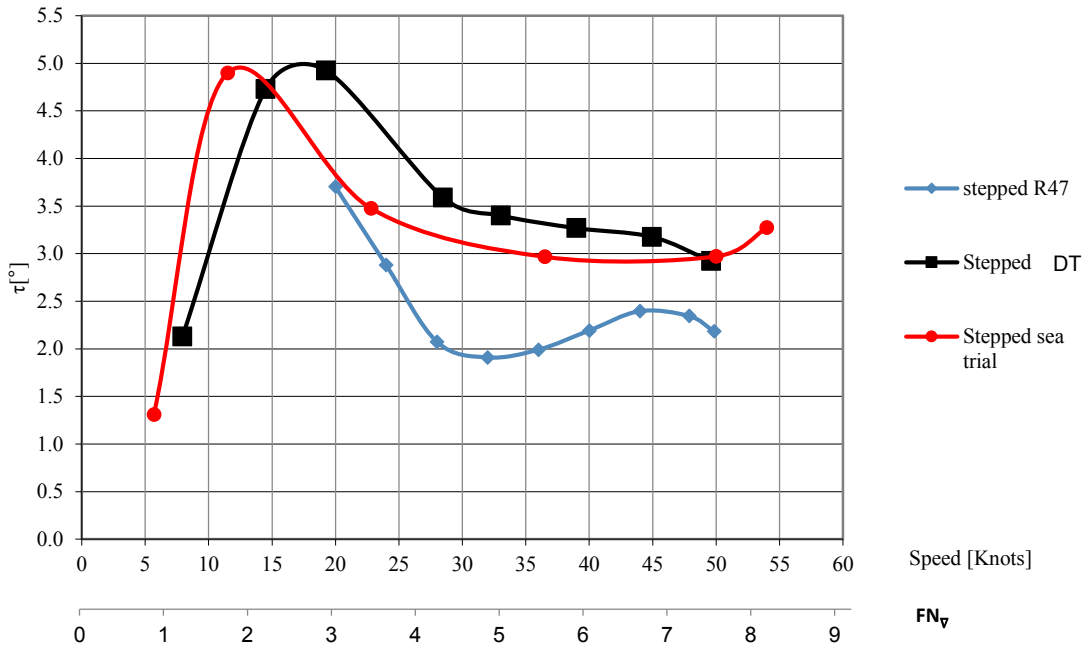

Figure 23: sea trial and towing tank tests, τ Vs V curve

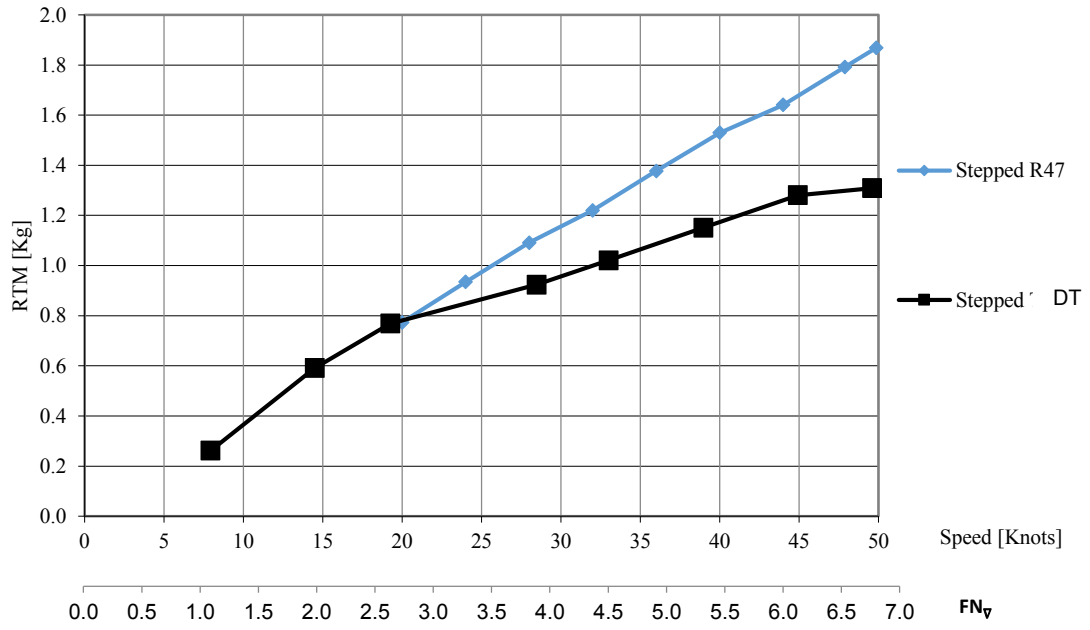

Figure 24: towing tank tests compare results, R_{TM} measure with Down Thrust and R47

The Down Thrust Methodology gives a value of the maximum standard deviation equal to 1% of resistance and trim angle τ values.

With R47 instruments the standard deviation values are higher than the Down Thrust Methodology and consequently the experimental measure of the resistance and trim angle value can be considered reliable.

This methodology has been used to measure R_{TM} in all experiments in the towing tank. P_E was calculated according to the Froude method.

6. Experimental methodology for the measure of the thrust

In our case the propeller thrust T_S was measured through tests at sea on RIB Mito 31 of MVmarine.
According to the logic scheme of the outboard engine $(figure 17 \div 22)$ to measure the propeller thrust behind the transom for the RIB, it was necessary to connect the load cells with the upper holes (*Figure 17*), which constrain the engine to measure the F2 forces (*Figure 18*)
The F2 force lets the upper pins work on traction; that is why two circular load cells were built, similar to cylinder which, working with compression, measure the F2 force.
The load cells were built in aluminium and equipped with two biaxial strain gauges (*Figure 25*) and are able to measure both the axial deformation and the centerplane component. The signals have been acquired from a watertight DaQ (*Figure 26*), specially made, and the data was processed by a dedicated software program sponsored by HP-System S.r.l.

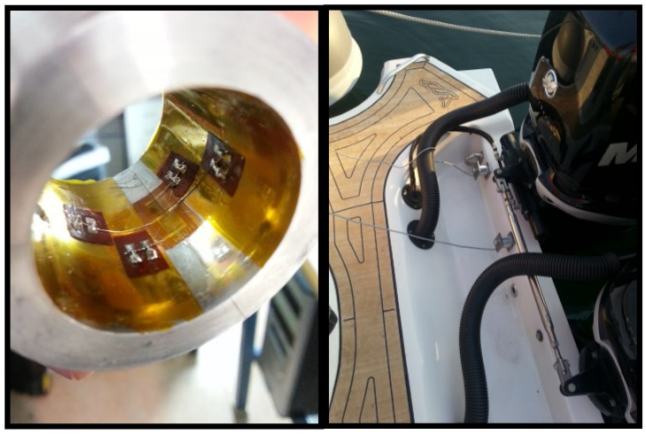

Figure 25: load cells and installation

Figure 26: data acquired hardware

The measurements were acquired several times and in still sea conditions so that the results were not very far from the towing tank test conditions. The results are shown in the graph below.

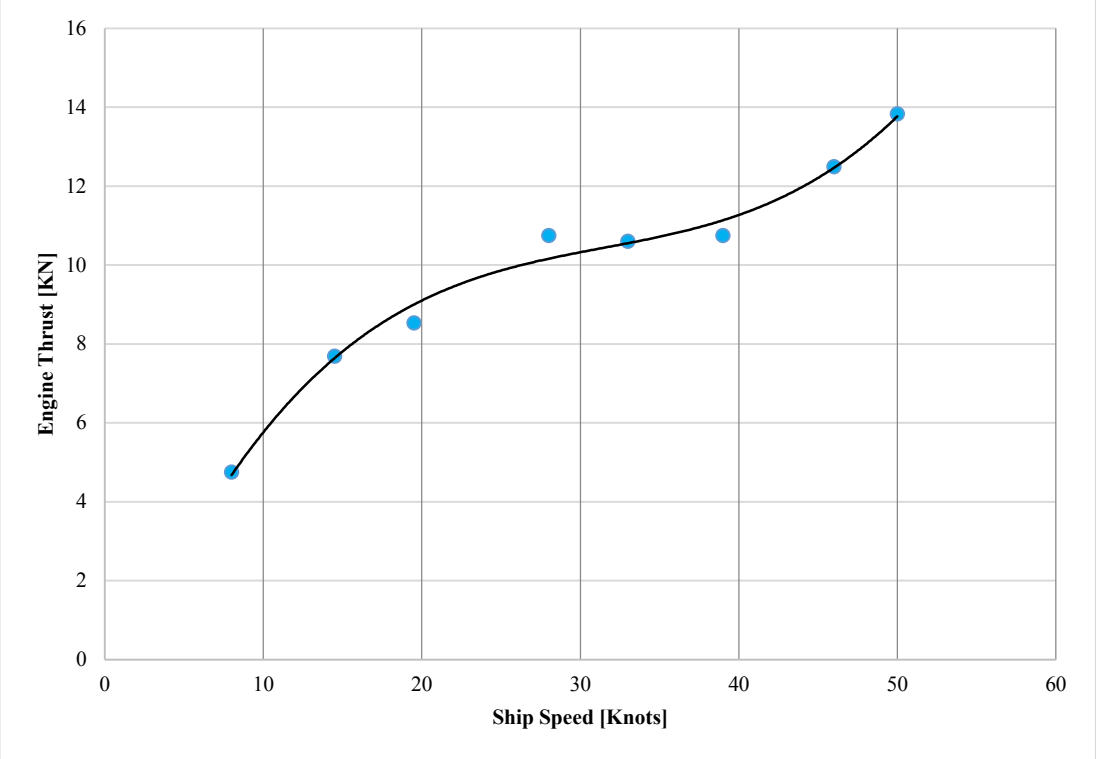

Figure 27: sea trial test, engine thrust Vs ship speed curve

7. Experimental methodology for the propeller open water efficiency calculation

The open water efficiency is calculated through experimental measurements in the towing tank test during the open water test with instruments H29 of Kemp & Remmers.
The open water efficiency is as follows:

$$\eta_0 = \frac{T \cdot V_A}{2\pi \cdot n \cdot Q} \tag{3}$$

Where: T represents the thrust, Q represents the torque and n the propeller revolutions per minutes. The values ware acquired with the change of V_A, which represents the speed of advance of the dynamometric carriage during the tests.
The test with the open water propeller test was made on a scale model propeller used during the sea trial tests on RIB Mito 31. The propeller was redesigned in a 3D-CAD with techniques of reverse engineering *Figure 28*, reduced on a geometric scale and made with 3D rapid prototyping of polymeric materials i.e. nylon and glass fibres *Figure 29*.

Figure 28: propeller reverse engineering

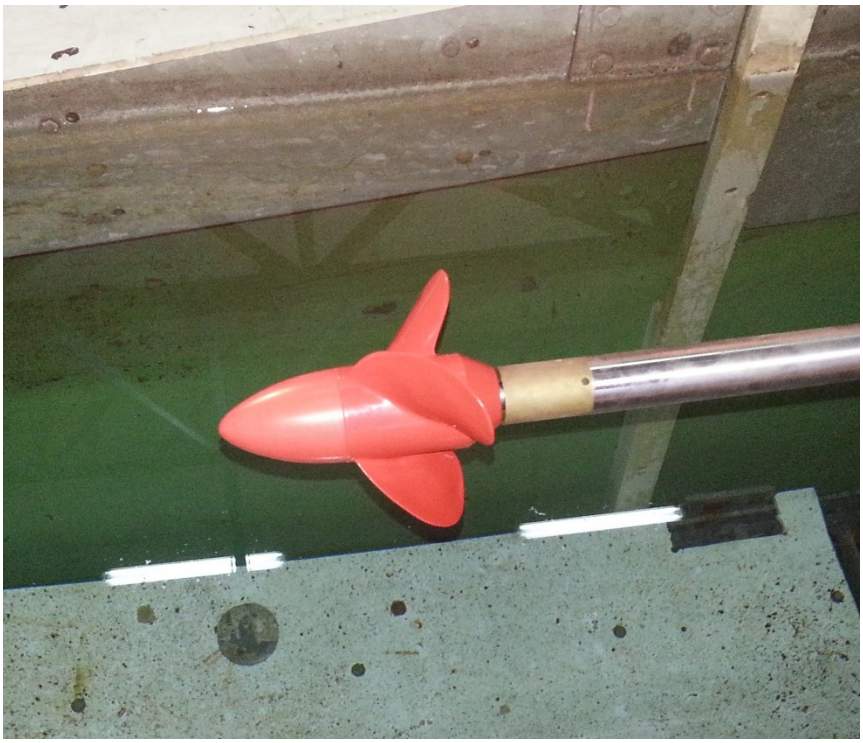

Figure 29: propeller during oper water test

To test the materials and their mechanical properties, the propeller was first tested in an induced cavitation regime, then at the maximum thrust. The results were more than satisfying; the blades did not vibrate.

The production of this kind of propeller with this technology made possible a reduction of costs of 90% compared with conventional technology.

The characteristic curve for the propeller is the following:

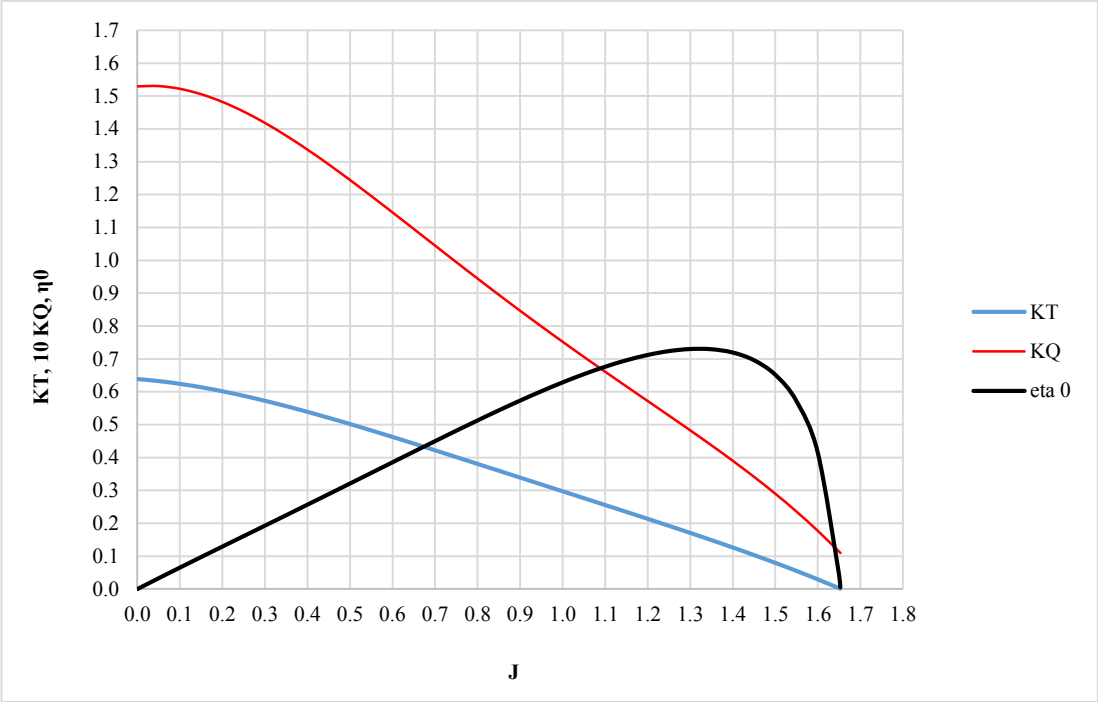

Figure 30: propeller open water test

8. Experimental methodology to calculate η_h

The hull efficiency η_h seems to be:

$$\eta_h = \frac{1-t}{1-w} \tag{4}$$

Where

$1-t$ is the thrust deduction factor

$1-w$ is the wake factor

$1-t$ was calculated as:

$$1-t = \frac{R_{TS}^{+}}{Ts} \tag{5}$$

Where:

T_S is equal to the thrust propeller.

R_{TS}^{+} is calculated according Froude Method by R_{TM}^{+}

$$R_{TM}^{+} = R_{TM} + R_{AP} \tag{6}$$

Were R_{TM} is the experimental model resistance and R_{AP} is the resistance of stern drive calculate on the model scale

1-w was calculated as:

$$1 - w = \frac{V_A}{V} \tag{7}$$

Where V is the test speed and V_A is the advance speed.

To calculate V_A we used as input data $KT_S = KT_M = KT_0 = \frac{T_S}{\rho_S n^2 D_S^4}$.

J and η_0 are read from the model propeller characteristics curve *Figure 31* and the wake fraction W_T is calculated.

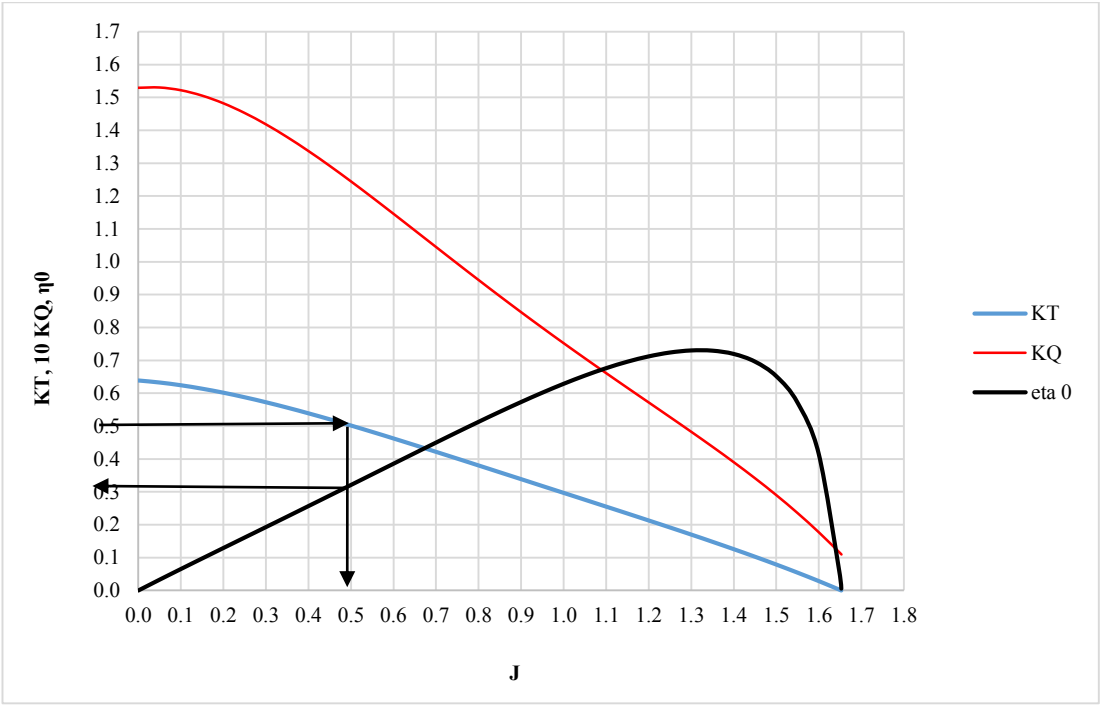

Figure 31: propeller open ware test for J and η_0 calc.

9. Results

The results of the towing tank test and sea trial are shown in the following *Table 3.* For confidentiality reasons we will show only some of the values.

V_S *[Knots]*	η_0	$1-w$	$1-t$	η_D	P_D *[CV]*
19,5	0,645	1,064	0,882	0,534	131,6
28	0,671	0,917	0,822	0,602	189,3
33	0,717	0,973	0,913	0,673	214,8
39	0,729	0,933	0,870	0,679	273,8
46	0,729	1,002	0,904	0,658	358,4
50	0,730	0,954	0,903	0,691	362,3

Table 3: towing tank test and sea trial results

CHAPTER 3 – Design of Experiment

Experimental model tests can be a valuable source of information for the design, even if, for a given hull form, There are many factors that can affect the hydrodynamic performance. So the model testing which is already difficult for the high speed could become more complex and expensive.

In this chapter, statistical approach based on Design of Experiment (DoE) is applied to the testing program of stepped models of planning boat in order to evaluate the factors that influence the hydrodynamic resistance. The obtained results help the designers to find the "best solution".

Traditional design usually applies a OFAT (one-factor-at-a-time) approach, using tools of an experimental and analytical type, so it is possible to change one project parameter at a time.

In order to reach a solution more quickly and with a minimum amount of data, the authors apply the technique of Design of Experiment (DOE) to stepped hull design by experimental model tests carried out in the towing tank.

This technique, already widespread in industrial design for several years, has been applied in the marine field.

A key stage in ship design is the definition of the ship power performance.

Up to today this problem has been solved by performing experimental tests on ship models in the towing tank, according to international standards recommended by the International Towing Tank Conference (ITTC).

The case study is the determination of the resistance of a high speed planning craft by experimental model tests and its dependence on the steps geometry.

In this respect, the relevant background information derives from previous activities carried out by the experimental laboratories of Department on Industrial Engineering (DII), Section of Naval Engineering, Naples University Federico II. However, previous experiments performed by DII adopted an OFAT approach.

In *Table 1* there are the design data.

According to the systematic approach to planning a design industrial experiment proposed in [14], two pre-design sheets (i.e. the main and secondary sheets) were conceived and implemented.

1. Response Variables.

The objective of the experimental work is to minimize the advancing resistance of the hull by an appropriate combination of the design parameters. Therefore, the total resistance R_T, the dynamic trim angle τ and the sinkage S_K are the response variables adopted.

The study of the factors involved in the experimentation phase is a crucial task and requires intensive knowledge transfer. The first brainstorm involved listing all of the factors that, according to different technological points of view and competencies, came out during team discussion. The second step consisted of classifying each factor as a control, held-constant or nuisance factor [14].

2. Control Factors

In the screening experimental phase, the following control factors have been selected: numbers of the steps (N_S), step height (H_S), longitudinal position of the step (LSP), longitudinal position of the gravity centre (LCG), and model speed (V_M). All the factors are quantitative parameters and have been presented in chapter 1.

As regard the other factor are listed below.

3. Constant factors

Constant factors are controllable factors whose effects are not of interest in the experimental phase. In particular, resistance tests are performed with a constant displacement Δ_M , step shape and aspect ratio. The model displacement has the constant values $\Delta_M = 30,61N$ for all the models, fixed based on testing facilities.

There are three basic possibilities for the step shape shown in Figure 2: step pointed aft, transverse step ([21], [22], [23], [24]) and the sweep-back step ([24], [15], [25]). The *step pointed aft* variant is the most common choice in practical design. Most recreational boats have the step pointed aft because it is easier to ventilate. If ventilation is not achieved, regardless of whether or not the vessel is moving fast enough to induce flow separation, flow can get sucked up in the region directly behind of the step. This can cause eddies, additional turbulence, and huge amounts of resistance that would make a step design disadvantageous. The sweep-back step is the most efficient step type, but it is also the hardest to ventilate. It is the step type used for Clement's in Dynaplane model [25].

The stepless hull is the parent of all the stepped ones. The steps are obtained by dividing the hull transversally in two (one step) or three (two steps) bodies.

The fore body is in a position somewhat forward of the mid ship section; the aft body are behind. The steps are obtained by slightly rising the aft body above the fore body keel, creating steps in the hull profile *Figure 32*.

The aspect ratio is $AR = \frac{L_{WL}}{B_{WL}} = 3,34 \pm 0,02$; all the steps shape are forward.

4. The nuisance factors

Are the conditions of the tank water and its mass density that depend on water temperature. However, all the experimental tests are performed according to ITTC standard recommendations [26].

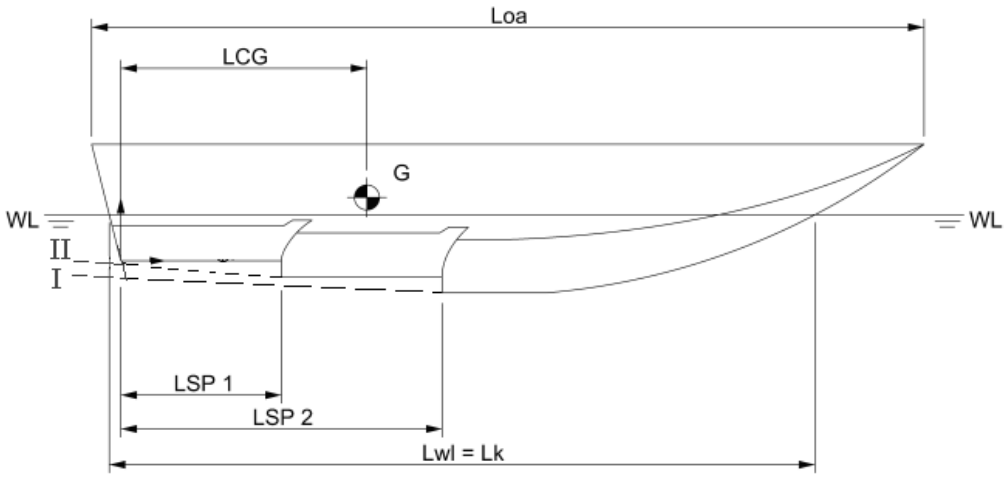

Figure 32: stepped hull geometry

5. Limits due to the experimental layout

All the limits of the experimental layout are verified for each trial.
Considering the towing length, the distance for the carriage acceleration, the minimum time for data acquisition and the distance for deceleration, the model maximum speed limit is 8,05 m/s.
The test used Froude methodology and the model scale ratio has considered the maximum ship and the maximum carriage velocities. It follows that

$$\frac{V_S}{V_M} = \sqrt{\lambda} \ . \tag{8}$$

Where in accordance with design data, the maximum ship speed V_S is about 50 knots and maximum towing tank carriage speed V_M is 8,05 m/s, the λ scale is

$$\lambda = \left(\frac{V_S}{V_M}\right)^2 = \left(\frac{25,72}{8,05}\right)^2 = (3,20)^2 = 10,24 \, . \tag{9}$$

In accordance with design data, assuming a model scale ratio 1:10, the model displacement is

$$\frac{\Delta_S}{\Delta_M} = \gamma_S \cdot \lambda^3 = \frac{31392\,N}{\Delta_M} \Rightarrow \Delta_M = 31,392\,N \, . \tag{10}$$

All models were built by MVmarine RIB yard in glass reinforced plastic on the side and the hull bottom was made with only resin. The finish in transparent gel-coat to obtain a transparent hull bottom and to see the running wetted hull surface. Further the materials chosen allow us to obtain a defined corner to avoid water flow adherences at the surface instead of releasing *Figure 33*.

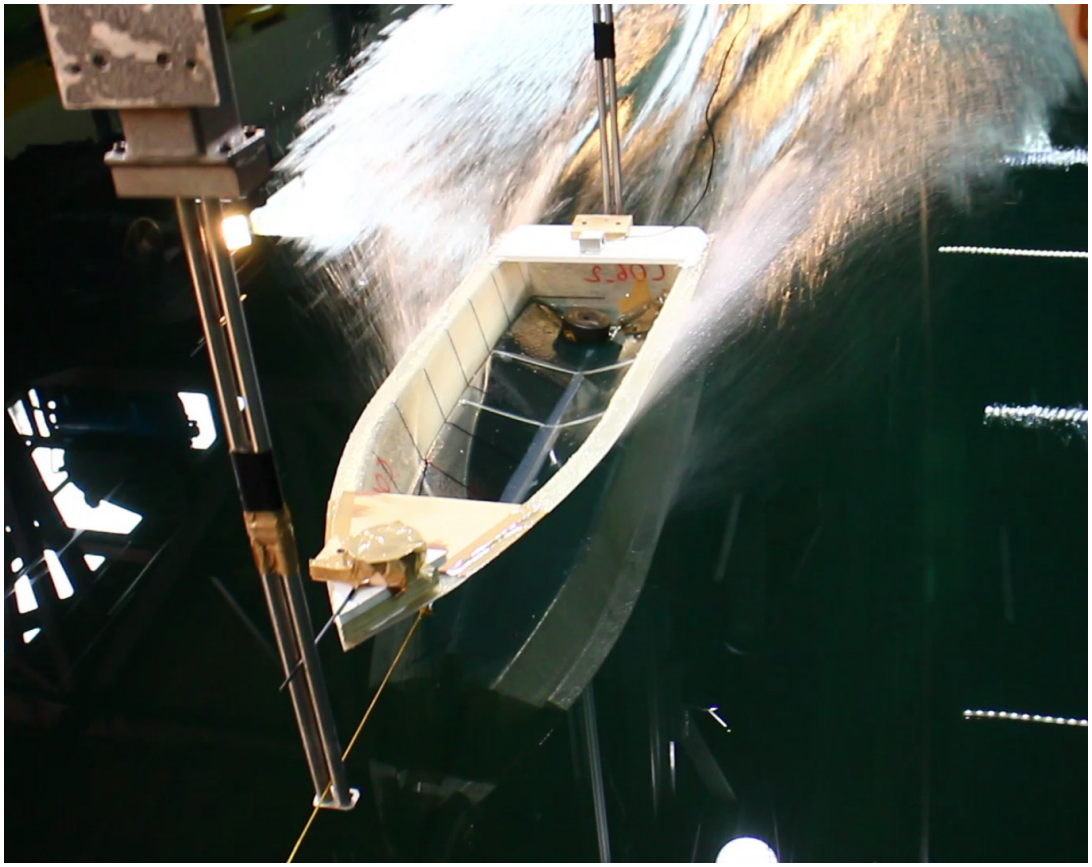

Figure 33: model test

The standard equipment used in model basin for resistance test, Kempf & Remmers model R47, change the system forces. In fact in consequence, the longitudinal running angle is different between the towing tank test and the sea trial test [27]. These phenomenon changes the hydrodynamic resistance.
For this particular high speed experimentation with smaller and lighter models, in accordance with [27] test methodology "down thrust" has been used.

6. Experimental Design

During the pre-experimental phase, 5 control factors were considered important on two levels and an experimental plan 2^5 was adopted. The 32 experimental tests were conducted with a replication and no repetitions because resources were limited. An obvious risk when conducting an experiment that has only one run at each test combination is that we may be fitting a model noise. When analysing data from unreplicated factorial design, occasionally real high order interaction occurs. A method of analysis attributed to Daniel (1959) [28] provides a simple way to overcome this problem.
During the experimentation the interactions of the main effects were analyzed, up to two elements.
In *Table 4* the control factors and the corresponding levels considered are reported.

Control Factor	Labels	Low (-)	High (+)	Unit
Step number	A	1	2	N°
Step height	B	2	6	mm
Longitudinal step position	C	0	1,4	m
Static Tau	D	-1	+1	Deg.
Model speed	E	4,63	8,05	m/s

Table 4: control factors

During the planning of the scale models of the 8 hulls, the step height was set at 2 and 6 mm on model scale, which means 20-60 mm in ship scale, as these are considered the limit values suggested by Peters in [16] e by Akers in [15].

Referring to the longitudinal step position, inspiration was taken from the two planning ideas suggested by Clement & Pope in [18] and Clement in [19], then the hulls designed with a value of longitudinal step position equal to 0 m were made with a step corresponding exactly with the centre of gravity G as in [19]. While the ones with a value of the longitudinal step position equal to 1.4 meters have the step on forward of the center of gravity as shown in [18].

Table 5 shows the experimental matrix with no repetition.

StdOrder	N_s	H_s	LSP	τ_0	V_m
1	1	2	0	-1	4,631
2	2	2	0	-1	4,631
3	1	6	0	-1	4,631
4	2	6	0	-1	4,631
5	1	2	1,4	-1	4,631
6	2	2	1,4	-1	4,631
7	1	6	1,4	-1	4,631
8	2	6	1,4	-1	4,631
9	1	2	0	1	4,631
10	2	2	0	1	4,631
11	1	6	0	1	4,631
12	2	6	0	1	4,631
13	1	2	1,4	1	4,631
14	2	2	1,4	1	4,631
15	1	6	1,4	1	4,631
16	2	6	1,4	1	4,631
17	1	2	0	-1	8,05
18	2	2	0	-1	8,05
19	1	6	0	-1	8,05
20	2	6	0	-1	8,05
21	1	2	1,4	-1	8,05
22	2	2	1,4	-1	8,05
23	1	6	1,4	-1	8,05
24	2	6	1,4	-1	8,05
25	1	2	0	1	8,05
26	2	2	0	1	8,05
27	1	6	0	1	8,05
28	2	6	0	1	8,05
29	1	2	1,4	1	8,05
30	2	2	1,4	1	8,05
31	1	6	1,4	1	8,05
32	2	6	1,4	1	8,05

Table 5: experimental matrix

To perform the experiments, 8 hull models were built with different geometries according to the change of the control factors, and 32 runs of the dynamometric carriage were carried out in the towing tank. During each run the DaQ measured the response variables, i.e. the total resistance R_{TM} through a load cell, the τ angle with an accelerometer and the sink age S_K with two lasers.

Hereafter there are some pictures of the different construction phases of the models.

Figure 34: stepped hull model construction

7. Analysis and technological interpretation of the results

The technological interpretation of the results is a very important phase. Comparing the technological "expectation", elicited in the pre-experimental phase with the statistical results allows practitioners to gain technological knowledge and to determine the added value of a systematic approach to planning a design industrial experiment.

The Anova method was applied in order to test the statistical significance of the main effects and the three-factor interaction for the taper and the recast layer. Diagnostic checking was successfully performed via graphical analysis of the residuals. The experimental results for the Total Resistance *Figure 35* and the dynamic trim angle are shown in *Figure 36*, using Pareto charts of standardized effects ($\alpha = 0{,}05$).

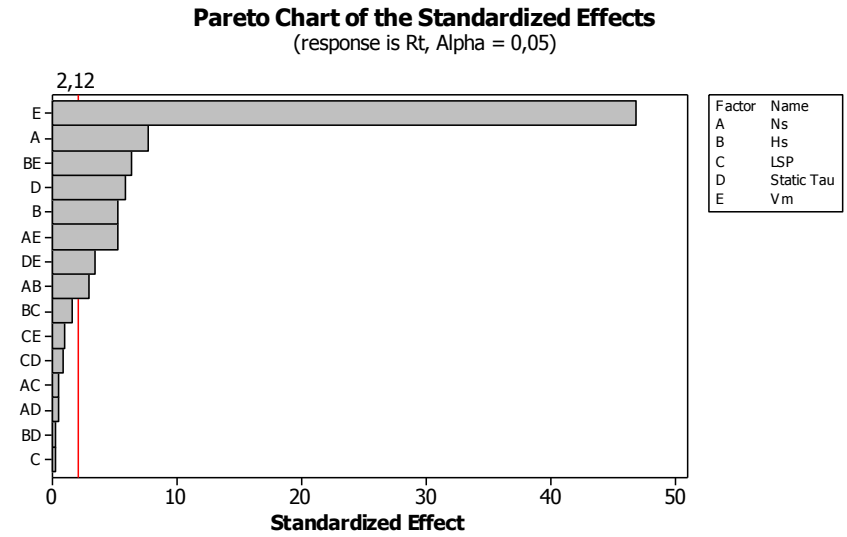

Figure 35: total resistance, Pareto chart

As expected, and confirming the reliability of the results, the speed Vm is the most significant control factor on hull resistance. In order we have: the number of steps, the interaction between speed Vm and the height of step Hs, the static tau angle, the height of step Hs, the interactions between the number of step Ns and the height of step Hs, between the static tau angle and the speed Vm, between the number of step Ns and the height of step Hs.

From *Figure 35* we can infer that the longitudinal step position, widely discussed in the literature, in this experimentation had no statistically significant effects on the total resistance, neither did its interactions with speed, static tau angle at rest and step number.

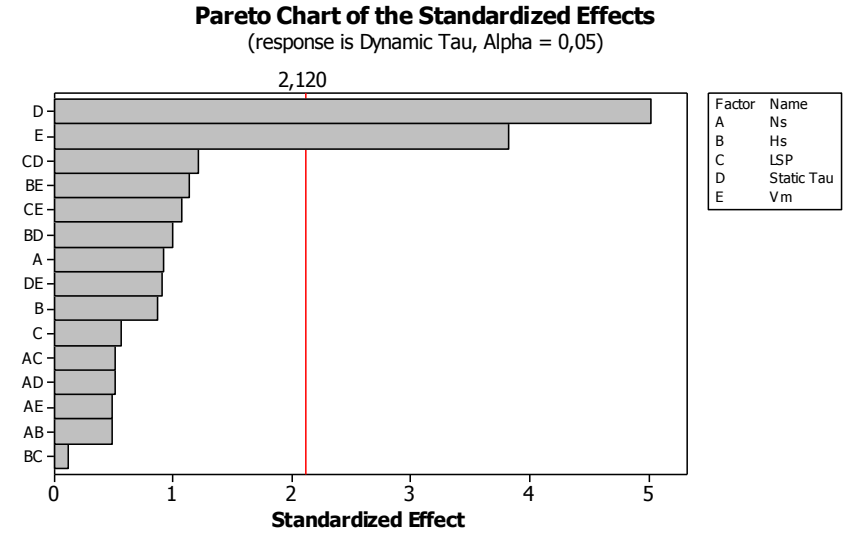

Figure 36: dynamic trim angle, Pareto chart

Also in this analysis the results confirm the expected previsions based on the theory. Actually we see that when referring to the τ angle; are really significant the τ_0 angle and the V_M. The non relevance of all other factors was neither known nor predictable.

The best results in terms of hydrodynamic resistance can be obtained with the best combination of control factors. We can use the Pareto charts of the effects *Figure 35 and Figure 36* to compare the relative magnitude and the statistical significance and interaction effect between control factor as (N_s, H_s, LSP, τ_0 , V_M) and response variable (R_T, τ).

After identifying the statistically significant factors, we are able to determine their effect on the response variables through the following graphs *Figure 37*.

In the following graphs, for each control factor are shown on the abscissa the two levels it adopts and for each level on the ordinate the resistance values registered during the tests, where the horizontal straight line represents the mean.

From the *Figure 37* we can deduce that referring to the R_T, the more the speed increase the more the resistance grows as expected. In addition the hulls with a number of steps equal to one have registered a lower resistance toward the hulls with two steps. In the same way the hulls with a step height equal to two millimetres have on average a better performance and finally the one with a $\tau_0 = -1°$ has on average lower resistance values. At the end we can assert that the best design combination of the control factors which minimizes the total resistance R_T is N_S 1, H_S 2 mm and $\tau_0 = -1°$.

Please remember that from the bibliographic analysis following design parameters it emerged that with a: number of step equal to 2, height of step equal to 40 mm, longitudinal distance of the center of gravity between the fore step and the aft step. In static trim angle at rest, a boat by stern presents a higher resistance at low Froude numbers.

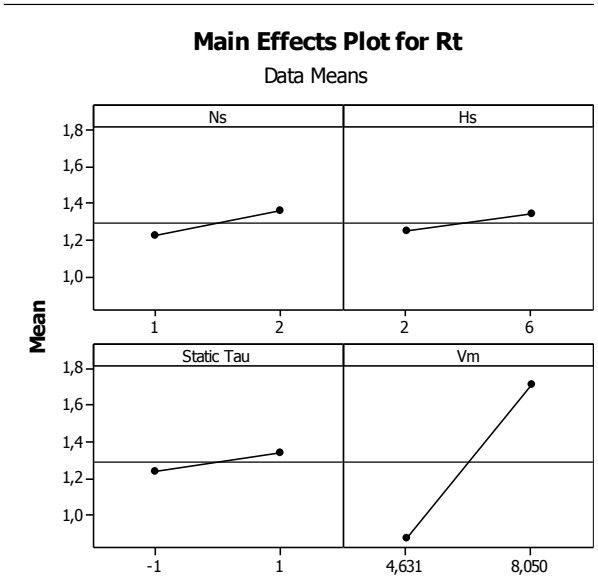

Figure 37: main effects plot for R_T

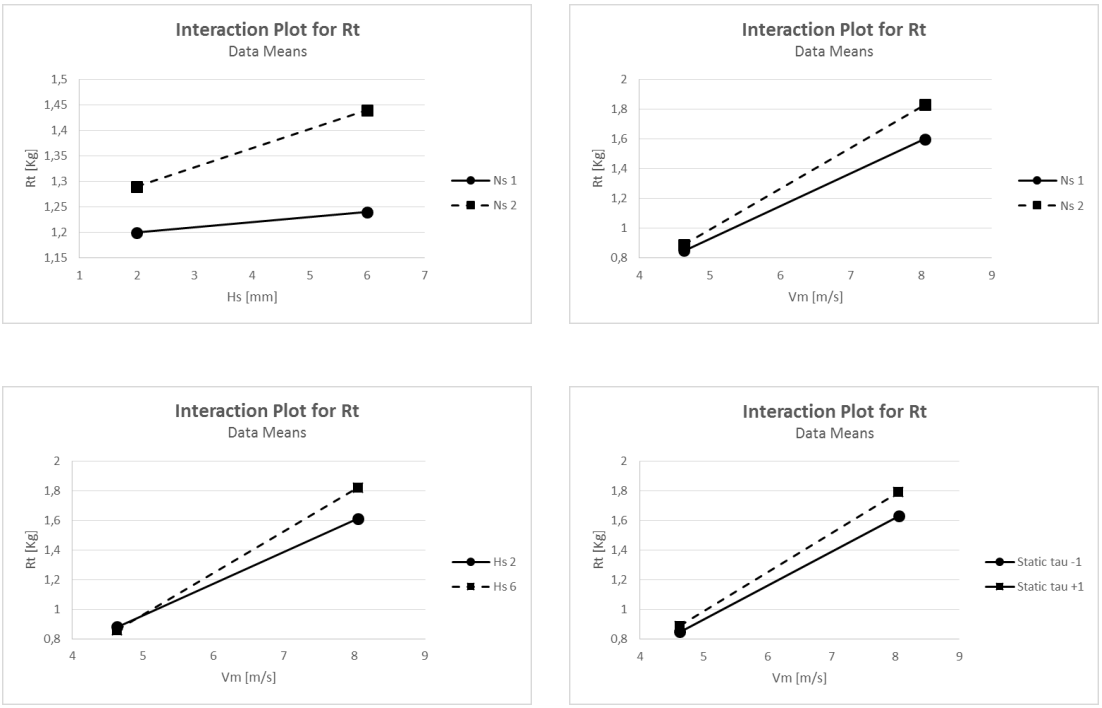

Figure 38: interaction plot for R_T

The *Figure 38* shows the interactions between two control factors referring to the total resistance R_T, in all graphs on the abscissa there is the value supposed by the control factor (i.e. the geometric parameter fixed for that particular design solution), and on the ordinate there is the total resistance R_T measured in the towing tank test.

In the first line there are the graphs referring to the interactions between the number of step Ns and the other control factors. Please note that all design solutions with 2 steps on average have registered higher total resistance values and such values increase the higher the step height and the speed. This is not in accordance with the publication of Peters [16].

In the second line, the interesting graph is that between the step height and the speed. When the speed increases the stepped hulls with low H_S register lower resistance values on average; this is explained by the authors because in the towing tank big vortexes underneath the hulls with high steps were registered; a phenomenon that cannot be observed on hulls with low steps. This phenomenon becomes more noticeable at higher speeds.

Finally another interesting graph is the one comparing the τ_0 with the model speed. Here you can observe that the trim by stern hulls have registered on average lower total resistance values on the speed field observed.

SECTION 2: OPERATION PHASE

CHAPTER 1 – Valuation of CO_2 emissions, monitoring and measuring methods for fuel consumption

1. Valuation of CO_2 emissions for a ship during sailing, through the monitoring of energy consumption.

As required by IMO in [3], the environmental influence of a ship is evaluated through the emissions of carbon dioxide. Thus, starting with the consumption of fossil fuel it's possible to estimate the CO_2 emissions through a coefficient. Please find hereafter the value of this coefficient, which varies according to the type of fuel:

Type of fuel	Reference	Carbon content	C_F (t-CO_2/t-Fuel)
1. Diesel/Gas Oil	ISO 8217 Grades DMX through DMC	0.875	3.206000
2. Light Fuel Oil (LFO)	ISO 8217 Grades RMA through RMD	0.86	3.151040
3. Heavy Fuel Oil (HFO)	ISO 8217 Grades RME through RMK	0.85	3.114400
4. Liquified Petroleum Gas (LPG)	Propane Butane	0.819 0.827	3.000000 3.030000
5. Liquified Natural Gas (LNG)		0.75	2.750000

Table 6: fuel carbon content coefficient by [3]

The fuel used changes according to the engine architecture of the ship and the geographic zone it is sailing.

It is a convention that a generic route can be divided into three phases: port, manoeuvre and sailing. There are three types of main consumers on board, i.e. the main engines, the diesel and the auxiliary generators.

In this thesis, we are going to analyse only the fuel consumption during sailing; this represents the largest quantity of fuel for the kind of ship subject to the study.

2. Aim of the monitoring

The operating costs of a ship depend on different factors. Today the first cost item in the budget of a ship is fuel, as shown in *Figure 39*.

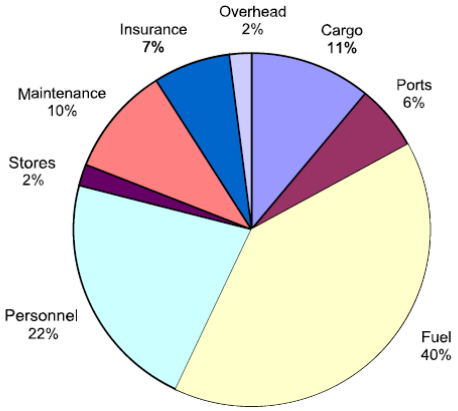

Figure 39: sharing of the operation costs of a ship, by [29]

The fuel cost is of about 40% of the total costs for a RO-RO Pax, similar to the subject of this study, i.e. about 43.000 tons of fuel corresponding to approximately 24.000.000 US dollars.

The increasingly rigorous rules regarding security, environmental protection and the constantly increasing price of fuel, led many shipping companies, the Italian first, to review their own strategies by trying to invest in new ships with low fuel consumption and emissions and adopting a correct policy of energy efficiency for the existing fleet.

In fact, only with a proper and continuous monitoring of specific variables, is it possible to support sail management in making decisions. Moreover monitoring makes it possible to estimate the failing fuel consumption and CO_2 emissions with corresponding carbon credits.

3. Description of direct and indirect measure methods

In general, on board of a ship fuel is used in the main engines to produce propulsive power, in the auxiliary engines to produce electrical energy and in the boilers to produce steam.

The logic in the three previous cases runs as follows:

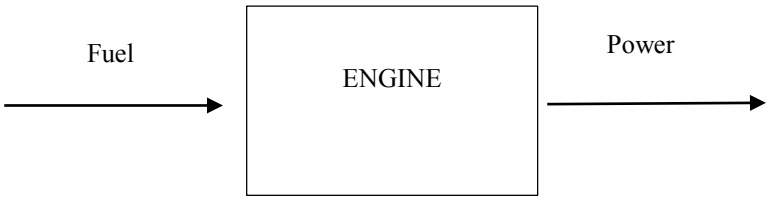

Consequently, to estimate the fuel consumption you can proceed in two ways: you can either measure directly the consumption upstream of the engine/boiler or measure the power supplied and from this calculate the fuel consumption necessary to produce the power.

In the first example we can talk of direct measuring, in the second one of indirect measuring.

The direct method is based on the measurement of volume or weight of the fuel used, made through sensors located on the delivery pipes to the engines/boilers.

The indirect method is based on the estimation of fuel consumption reading it from the power outlet of engines/boilers.

4. Direct methods for fuel consumption measure

To measure the fuel consumption of an engine on board of a ship with the direct method we can use a flow meter or make a sounding of the tanks.
On board ships, three types of flow meters are used: volumetric, coriolis and ultrasonic.
It's necessary to make a preliminary remark that the direct measurement of fuel consumption of the main and auxiliary engines on board is still subject to several difficulties/uncertainties. Please find hereafter the principal of these:

- The volumetric liter counter measures the volume of the liquid which flows in the pipe, and this is the most used method as it is also the cheapest, even if rather bulky. To measure a liquid's mass, it is necessary to know the density, which depends on temperature, and this should be delivered by each storage operation. These measurements are often not available.
- The mass litre counter uses the principle of Coriolis; it measures directly the mass flow of the liquid. But like the volumetric litre counter it is bulky as well, more expensive and sensitive to vibrations, thus it carries the risk of producing incorrect results. For this reason its use on board of ships is quite limited.
- The ultrasonic litre counter is less bulky, but to have a reliable measurement an accurate calibration of several operational parameters is needed.
- The direct sounding of the tanks, made manually by an operator, is useful only for the fuel measurement at the end of the route. This method requires a correction of the measurement according to the transversal and longitudinal trim of the ship and of the temperature through specific sounding tables delivered by the shipyards, thus it is the most inaccurate and uncertain method.
- The indirect sounding is made by reading the levels in the fuel tanks with sensors. It is more convenient because it does not require an operator, but it offers the same uncertainties as the direct method, besides the fact that the sensors must be located correctly.

5. Indirect methods for fuel consumption measure

To calculate the fuel consumption Y of an engine on a given voyage, the following formula is used:

$$Y = P \cdot SFC \cdot h \tag{11}$$

Where:

P = power in kW

SFC = specific fuel consumption in $\frac{g}{kWh}$

h = sailing time in hours

The power delivered is measured in kW with a torque meter generally positioned on the propeller axis downstream of the reduction gear, consequently reading only the power and thus the consumption will always be underestimated because the mechanical output of the gear is not considered.

The specific fuel consumption, as reported in [3] depends on the type of engine and its year of construction and is as follows:

Engine year of build	Stroke low speed	Stroke medium-/ high speed (>5000kW)	Stroke medium-/ high speed (1000-5000kW)	Stroke medium-/ high speed (<1000kW)
1970-1983	180-200	190-210	200-230	210-250
1984-2000	170-180	180-195	180-200	200-240
2001-2007	165-175	175-185	180-200	190-230

Table 7: Values of specific fuel consumption in g/kWh

The data in
Table 7 is the result of statistic researches and consequently they could change according to the engine used.

6. Description of the methods

On the ships in this study, we have also installed volumetric flow meters to measure the volume of the fuel consumed and torque meters to measure the power given by the main engines to the propeller axis. The fuel consumption of the auxiliary engines and boilers is excluded from the study as they are usually turned off during sailing and in this phase they seem to be irrelevant with respect to total engine consumption.

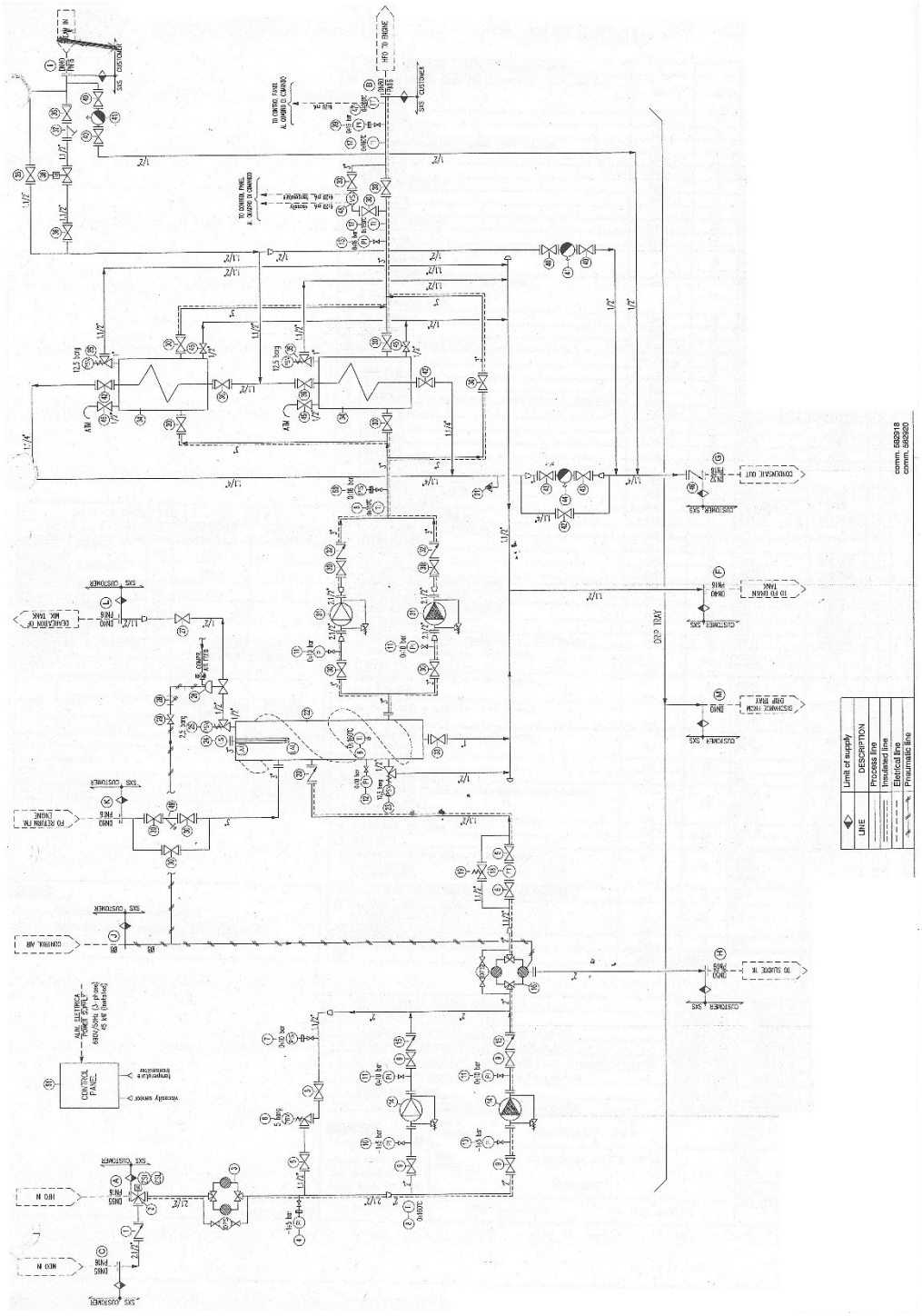

Figure 40: fuel pipeline scheme

Legend:

18	*Flow meter & Thermometer*
22	*Steel Pressure Vessel Capacity 186 lt*
34	*Steam Heater*

During navigation, fuel is extracted from the daily tank through the “HFO IN” pipe. Then, according to *Figure 40*. The fuel flows through the volumetric flow meter 18, is convoyed to tank 22 and then is heated through 34, before it is sent to the main engines. As we have installed diesel engines, there is a back flow pipe which returns to 22.
However, even without considering the back flow pipe return a the overestimation of fuel consumption is not severe.
Therefore, we will not measure the fuel quantity coming back from the main engines and consequently it will be impossible to measure the instant consumption.
The consumption data collected by the volumetric flow meters was not taken into account for the following reasons:

- due to technical problems, such data not over always available;
- temperature and certificate of the chemical analysis of fuel is not sometimes available too.

The approach adopted for the calculation of fuel consumption is indirect and deducted from the engine delivered power the shaft propeller. Through the estimation of the engine performances and the specific consumption, it has been possible to estimate the fuel consumption for the engines installed.

CHAPTER 2 -The case study:

1. Description of the two ships

a. Mission Profile

Data is collected from twin cruise ships, namely SHIP 1 and SHIP 2, property of Grimaldi Group. Both ships are used on a commercial route to link two European ports, namely PORT A and PORT B, and make a stopover in PORT C during summertime.
Ships, port names and data are intentionally omitted for confidentiality reasons.
The twin ships are RO-RO Pax and have the same technical characteristics: diesel propulsion, two variable pitch propellers, two rudders, bulbous bow, and a transom stern.

b. Technical specification

The main technical characteristics are:

Length over all	225 m
Length between perpendicular	202 m
Max bam	30,40 m
Scantling draft	7 m
Max draft	7,15 m
Maximum power for propulsion (MCR)	55.440 kW
Speed at 66% MCR	25 Kn
Speed at 90% MCR	27,5 Kn

Table 8: Main technical specifications

Main and auxiliary engines
The ship has a main engine with variable pitch propeller and four diesel engines Wärtsilä, Type 12V46D 12 V cylinder, four stroke with a maximum continuous rating of 13,860 kW at 500 rpm.
The engines are powered with three types of fuel: Heavy Fuel Oil (HFO), Marine Diesel Oil (MDO) and Marine Diesel Oil with a Low Sulphur level (LS).
Ships in the different geographic areas use the three different types of fuel.
Electrical system
The electrical system of the ships consist of: three Diesel generators (DG) of 2,500 kW at 690 V, two shaft alternators (AA) of 2,875 kVA at 690 V and one emergency diesel generator (DGE) of 480 kW.
Gearbox

The gearbox has two fast inlet shafts powered by the engine shaft, a (slow) outlet shaft for the propeller and a faster one to which the shaft alternator is connected. The gear ratio between the engine shaft and the propeller shaft is equal to 3.24. The gear ratio between the engine shaft and the shaft alternator is equal to 0.32.

2. Engine room layout

The twin cruise ships considered in this paper have four main engines for propulsion with two variable pitch propellers, three diesel generators and two shaft generators for electric power.
The main engine power is used both for propulsion and electrical generation through the shaft generators, which are themselves keyed on a gearbox, as outlined in *Figure 41*.

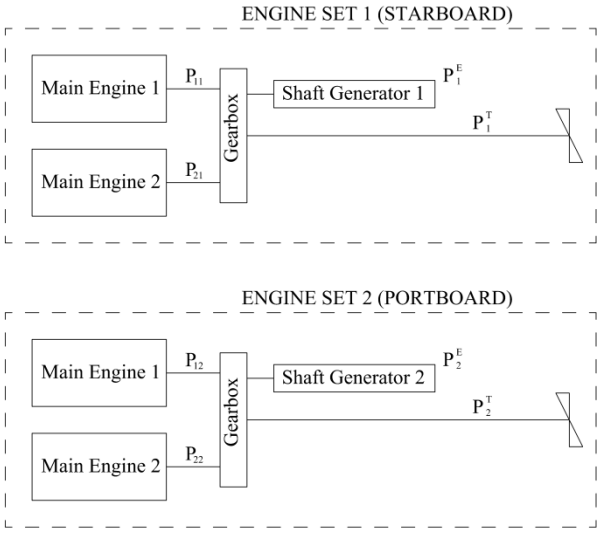

Figure 41: engine room layout

The on-board electrical energy production is critical and a black out should always be avoided.
The engine system can drive propulsion at fixed RPM (constant mode) and at variable RPM (combinator mode).
The constant RPM mode is needed when a shaft generator must be engaged for electric power. However, in this mode, the ship speed is regulated only by changing the pitch propeller and it is not possible to reach the max vessel speed.
Conversely, in combinator mode the ship speed is regulated by increasing both the pitch propeller and engine rpm. Unfortunately, in this mode it is not possible to engage the shaft generator.
With the first operation option, electrical energy production is more expensive than with diesel generators.
The main engine power is utilized both for propulsion and electrical generation through the shaft generators, which are themselves keyed on a gearbox, as outlined in *Figure 41*.
On the j-th engine set ($j = 1, 2$) of each ship, the sensor network is equipped with

— a torque meter (placed on the shaft between gearbox and propeller) to measure the thrust power P_j^T on the shaft propeller

— a power meter (placed on the shaft generator) to measure the electrical power P_j^E.

P_j^T and P_j^E represent the only available measurements we could use in order to calculate the main engine power load. Main engines and shaft generators must be considered separately because, for example, when the operation mode is "combinator" the shaft generator must be off during the voyage. However, not to underestimate the output power P_j of the j-th engine set, we need to consider the gearbox mechanical efficiency η_j^m and shaft generator electrical efficiency η_j^e the following relation

$$P_j = \frac{P_j^E}{\eta_j^e \eta_j^m} + \frac{P_j^T}{\eta_j^m} \tag{12}$$

Where the performance of the technical sheets of equipment are as follows:

$$\begin{cases} \eta_m^{AA} = 0,95 \\ \eta_e = 0,96 \\ \eta_m^G = 0,95 \end{cases}$$

Therefore, the output power P_{ij} of the i-th main engine of the j-th engine set can be calculated as follows:

$$P_{ij} = \begin{cases} 0 & if\ x_{ij} = 0 \,\forall i \\ \dfrac{x_{ij}}{\sum_{i=1}^{n} x_{ij}} P_j & otherwise \end{cases} \tag{13}$$

3. Data Acquisition

Data is collected both manually (by the master through the voyage report) and automatically by the Data Acquisition System (DAQ). The four timing sections into which a generic route from Port A to Port B can be divided, is showed in *Table 9*.

The four phases are defined by the moment when the crew change the status "Sailing/Manoeuvre", and this moment can be defined by the *Start With Engine* (SWE) and *Finish With Engine* (FWE).

FWE is the date and time when the manoeuvre begins at departure and arrival, SWE is the date and time when the manoeuvre ends at departure and arrival.

Stay in port	From the engine stop to FWE at departure
Departure manoeuvre	From FWE to SWE at departure
Sailing	From FWE at departure to SWE at arrival
Arrival manoeuvre	From FWE to SWE at arrival

Table 9: list of timing sections

a. Manually voyage report

For each voyage, according to international laws, the master and the chief engineer must fill in the voyage report end of each voyage and send it to the Energy Saving Department (ESD) of the Shipping Company. The Excel-file contains among others the following information which have been analysed: starting port, FEW, SWE, arrival port, power, sailing time [h], average speed [knots], miles sailed [M], direction and speed of wind, sea force and direction, stabilizer fin operating time, fore and aft drafts, HFO consumption [t], MDO consumption [t], LS consumption [t].
The collected data is transferred into a table report where each line contains information about each voyage. In particular the average speed is calculated as a relation between sailing miles and sailing time.

b. DAQ

The first step in analysing the fuel consumption is to acquire data about the two ships, namely Ship 1 and Ship 2 for confidentially reasons.
To avoid problems with manual transcriptions, the shipping company installed a sensor network on board able to measure and collect automatically all the voyage data.
The DAQ acquires data from the sailing instruments, from the automation systems and from the ad hoc on board sensors.
The data coming from the sailing instruments are: date, time, gps position, speed over ground, course over ground, wind speed and direction, magnetic bow, wave radar.
The signals coming from the automation system are: rpm and power, fuel consumption, main engine state (on/off), tank level, drafts, manoeuvring/sailing mode.
The signals coming from the ad hoc sensors are: longitudinal (static/dynamic) running angle, vertical acceleration, stabilizer fin operating status (on/off).

4. DAQ sensors and operation

a. Software Description

The software was developed for a continuous operation, i.e. 24 h / 7 d in a completely automatic way and unmanned.

The system was designed from two different software forms named: “data collector” and “optimum trim”.

The first form “Data Collector” process the signals and save them in a text file (csv). If the signals coming from the sensors are reliable, with these files it’s possible to develop an accurate report about consumption and propulsive performance of the ship for each route/voyage.

If available, the Data Collector has an interface with the board system, automatic system and sailing system, so that it’s not necessary to install redundant sensors.

b. DAQ Operation

All data are temporarily stored and at intervals of 300 seconds (5 min), mean and sum values of the operations is calculated and saved.

The database has a text format with commas separating the columns – standard format “CSV” (Comma-Separated Values), is made of 108 columns and can be imported into each spreadsheet.

The file name is composed of data and time of creation, for example:

2013-08-27_05-36.csv

2013-08-27_18-46.csv

The report files are based on the voyage and are called T_Report. The weekly report files are called W_Report;

The T_Report contains the following sections: stay in port, departure manoeuvre, sailing and arrival manoeuvre.

The voyage file is closed and a new one is created when the following conditions occur: all four main engines stop, speed < 0.3 knots for almost 15 minutes, arrival port different from departure port.

All files generated by the ship are sent over the internet to the Energy Save Department of the shipping company.

c. DAQ data processing

The Excel file is in csv format, with the data of all five minutes. It contains the following information which is subject to several preliminary operations, before it can be analysed: date and time, latitude [mins], longitude [mins], speed over ground [Kn], power port board [kW], power starboard [kW], electric power shaft generator port board [kW], electric power shaft generator starboard [kW], draft aft perpendicular, port board Draft at midship section, port board draft at midship section, draft forward perpendicular

On each Excel file in csv format following operations were carried out:

- Division of data into 3 categories (port, manoeuvre and sailing) according to the Speed Over Ground (S.O.G)
- Calculation of the displacement value of ship (see Chap. 3)
- Converting data about latitude and longitude to establish the departure and arrival port
- Calculation of the wind components (Chap.3)

The T_Report sent by the DaQ system, is made of an Excel sheet containing following information for each voyage: voyage number, departure port, FWE, SWE, arrival port, power measure on propeller shaft [kW], sailing time [h], average speed over ground [Kn], sailed distance [NM], wind direction [°], wind speed [kn], total fuel consumption [t]
To analyse data it was necessary to change the T_Report inserting new columns for the following variables:

- *Sailing time adjusted*
- *Speed Over Ground cube (V^3)*
- *Magnitude wind speed in Beaufort scale*
- *Wind component (W_h, W_f, W_s)*
- *Draft in leave and arrival port*
- *Displacement (Δ)*
- *Sailing mode (E)*
- *Stabilizer fin operating time (F)*
- *Main engine power (P)*
- *% main engine power*
- *Standard fuel consumption Y_s*
- *Specific fuel consumption effective (C_{SE})*
- *Fuel Consumption (Y)*

Hereafter the changes made to insert the new variables are explained.
For *Sailing time adjusted* we mean the sailing time in decimal format.
The *Speed Over Ground cube* is raised to the power of three for technical reasons explained in detail in Chap. 3.
The variable *wind force* expresses the value of the wind force according to the Beafourt scale.
The *wind component* represents the breaking down of the real wind vector according to the direction of the ship (Chap.3).
The variable E is an indicator with two levels (0,1) which identifies the engine operation mode during sailing (Chap. 3).
The variable *F* (*Stabilizer fin operating time*) is expressed in hours in a decimal format and tell us the real operating time of stabilizer fins during sailing.
The *total power (P)* coming from the main engines is calculated with the relation (12) and (13).

The *Standard fuel consumption* Y_s is calculated with the equation (11), through the constant value of SFC equal to $190\frac{g}{kW \cdot h}$ as reported by the shipping company.

As is know the Specific Fuel Consumption (*SFC*) is function of the power and the engine type. In *Table 10,* reports the *effective Specific Fuel Consumption (SFC$_e$)* values at different power load measured during the engine factory tests:

Power [kW]	Power [%]	*SFC*$_e$ [g/kWh]
13.824	25	211,3
27.720	50	194,0
39.140	71	194,9
41.580	75	194,1
47.124	85	191,7
55.520	100	196,0
60.984	110	201,4

Table 10: factory tests of the cruise ship main engines

In *Figure 42* Power [%] is plotted against *SFC$_e$* and can be fitted by the following polynomial

$$SFC_e = -9e^{-9}x^6 + 4e^{-6}x^5 - 6e^{-4}x^4 + 5e^{-2}x^3 - 2,21x^2 + 47,35x - 176,01$$

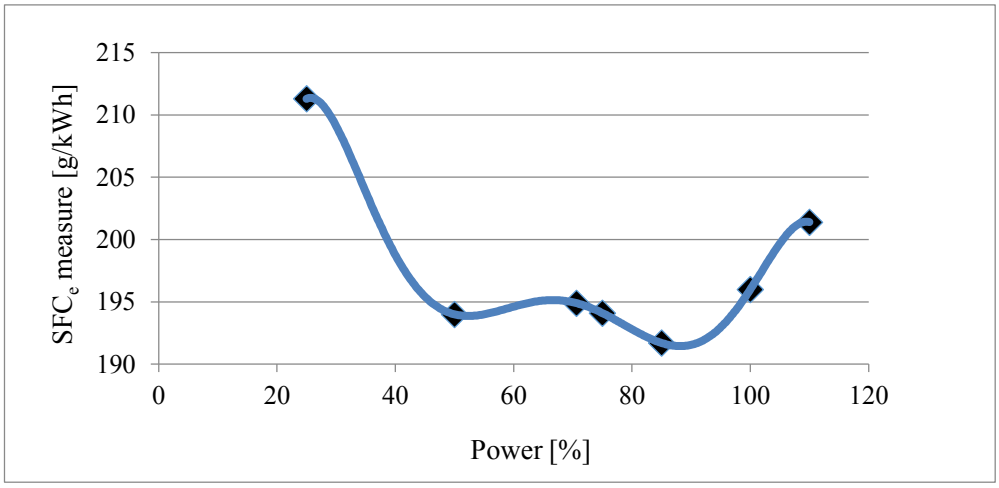

Figure 42: SFC$_e$ diagram

Differently from the literature then the effective fuel consumption Y in equation (11) can be calculated more precisely than Y_s through *SFC$_e$*

CHAPTER 3 - Adopted methodology

1. Notes on regression analysis

In this paper, for each voyage, a multiple linear regression model has been used for fuel consumption data modelling and prediction.

In a multiple linear regression model [30] and [31] with *k* regressor variables, the dependent variable or response Y may be related to q independent or regressor variables $X_k \ (k = 1, \ldots, q)$ by the following model

$$Y = \beta_0 + \beta_1 x_1 + \beta_2 x_2 + \ldots + \beta_q x_q + Z \tag{14}$$

where Z is a random error component, i.e., a random variable which is assumed to have mean zero and unknown variance σ^2.

Therefore, if n observation are available $(x_{1i}, x_{2i}, \ldots, x_{qi}, y_i)$ of $(X_1, X_2, \ldots, X_q, Y_i)$ through (14) we obtain

$$y_i = \beta_0 + \beta_1 x_{1i} + \ldots + \beta_k x_{ki} + \ldots + \beta_q x_{qi} + z_i \quad i = 1, 2, \ldots, n \tag{15}$$

where we usually assume that errors z_i's are uncorrelated. The regression coefficients estimates $(\hat{\beta}_0, \ldots, \hat{\beta}_q)$ can be obtained through the least square method. The regression function estimate

$$\hat{y} = \hat{\beta}_0 + \hat{\beta}_1 x_1 + \ldots + \hat{\beta}_k x_k + \ldots + \hat{\beta}_q x_q . \tag{16}$$

This can be then utilized for fuel consumption prediction $\hat{y}$ at each voyage *i* and sailing condition. In order to test for significance of regression of the generic model (14), we may use the coefficient of multiple determination

$$R^2 = 1 - \frac{\sum_{i=1}^{n} (y_i - \hat{y}_i)^2}{\sum_{i=1}^{n} (y_i - \bar{y})^2} = \frac{\sum_{i=1}^{n} (\hat{y}_i - \bar{y})^2}{\sum_{i=1}^{n} (y_i - \bar{y})^2} \tag{17}$$

where $\bar{y}$ is the mean fuel consumption. R^2 indicates the explicated variance of response variables and can be interpreted as a global statistic to assess the fit of the model. The R^2 statistic is somewhat problematic as a measure of the quality of the fit for a multiple regression model because it always increases when a variable is added to a model. Then if you include unnecessary terms, R^2 can be artificially high.

Therefore, we also calculate the adjusted coefficient of multiple determination

$$R^2_{Adj} = 1 - \left(\frac{n-1}{n-q-1} \right) \frac{\sum_{i=1}^{n} \left(y_i - \hat{y}_i \right)^2}{\sum_{i=1}^{n} \left(y_i - \bar{y} \right)^2} \tag{18}$$

where $\bar{y}$ is the mean fuel consumption.

We defined the $PRESS$ residuals as $e_{(i)} = y_i - \hat{y}_{(i)}$ were $\hat{y}_{(i)}$ is the predicted value of the i-th observed response based on a model fit to the remaining n -1 sample points. We noted that large PRESS residuals are potentially useful in identifying observations where the model does not fit the data well or observations for which the model is likely to provide poor future predictions. We define PRESS statistic as sum of squares, defined as the sum of the squared PRESS residuals, as a measure of model quality. The PRESS statistic is

$$PRESS = \sum_{i=1}^{n} \left[y_i - \hat{y}_{(i)} \right]^2 . \tag{19}$$

PRESS is generally regarded as a measure of how well a regression model will perform in predicting new data. A model with a small value of PRESS is desired.

The PRESS statistic can be used to compute an R^2 like statistic for prediction, say

$$R^2_{pred} = 1 - \frac{PRESS}{SS_T} . \tag{20}$$

This statistic gives some indication of the predictive capability of the regression model.

In this paper R^2, R^2_{adj} and R^2_{pred} are reported as a percentage.

Furthermore we calculate the $100 \cdot (1-\alpha)\%$ prediction interval [2, 11] for a future observation Y_0 given $x_1, x_2, \ldots, x_q$ by the following relation

$$\hat{y}_0 - t_{\alpha/2, n-q-1} \, \hat{\sigma}_{pred} \le Y_0 \le \hat{y}_0 + t_{\alpha/2, n-q-1} \, \hat{\sigma}_{pred} \tag{21}$$

where $\hat{y}_0 = \hat{\beta}_0 + \hat{\beta}_1 x_1 + \hat{\beta}_2 x_2 + \ldots + \hat{\beta}_q x_q$, $t_{\alpha/2, n-q-1}$ is the $100 \cdot \alpha/2 - \text{th}$ percentile of a Student distribution with $n-q-1$ degrees of freedom and $\hat{\sigma}_{pred}$ is an estimate of the standard deviation of the prediction error.

2. Model Adequacy Checking

In according to [30], the major assumptions that we have made thus far in our study of regression analysis are as follows:

1. The relationship between the response y and the regressors is linear, at least approximately.
2. The error term e has zero mean.
3. The error term ε has constant variance σ^2
4. The errors are uncorrelated.
5. The errors are normally distributed.

Taken together, assumptions 4 and 5 imply that the errors are independent random variables. Assumption 5 is required for hypothesis testing and interval estimation. We should always consider the validity of these assumptions to be doubtful and conduct analyses to examine the adequacy of the model we have attempted to calculate. The types of model inadequacies discussed here have potentially serious consequences. Gross violations of the assumptions may produce an unstable model in the sense that a different sample could lead to a very different model with apposite conclusions.

The residuals are defined as:

$$e_i = y_i - \hat{y}_i \quad i = 1, 2, ..., n$$

where y_i; is an observation and $\hat{y}_i$; is the corresponding fitted value. Since a residual may be viewed as the deviation between the data and the fit, it is also a measure of the variability in the response variable not explained by the regression model. It is also convenient to think of the residuals as the realized or observed values of the model errors.

Analysis of the residuals is an effective way to discover several types of model inadequacies. As we will see, plotting residuals is a very effective way to investigate how well the regression model fits the data.

The residuals have several important properties. The standardized residuals have mean zero and approximately unit variance $\hat{\sigma}^2$. Consequently, a large standardized residual ($-2 \le d_i = e_i / \sqrt{\hat{\sigma}^2} \le +2$) potentially indicates an outlier.

3. Categorical regression variables

The variables employed in regression analysis are often quantitative variables, that is, the variables that have a well-defined scale of measurement. Variables such as temperature, distance, pressure, and income are quantitative variables. In some situations, it is necessary to use qualitative or categorical variables as predictor variables in regression.

We must assign a set of levels to a qualitative variable to account for the effect that the variable may have on the response. This is done through the use of indicator variables that assume value 0 or 1. Sometimes indicator variables are called *dummy variables* [30].

4. Technological selection

To identify the variables which best explain the phenomenon of fuel consumption, we started from the physics of the problem. After establishing a mission profile, the external actions influencing the ship and the management procedures of the crew as well as the fuel consumption were observed.

In Figure 43: external actions and reactions of the ship *Figure 43* is outlined in blue the fuel required from the main engine to deliver a given power to the propeller and thus to develop the thrust, in red the external actions i.e. the resistances necessary to develop a given speed are outlined.

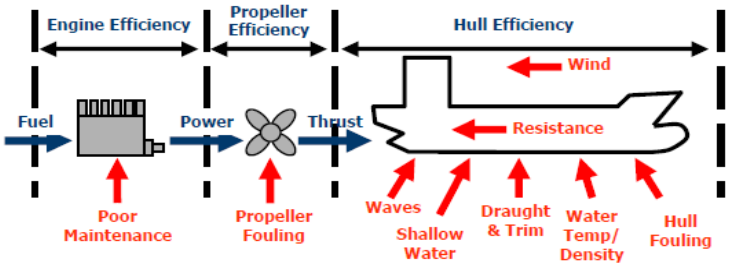

Figure 43: external actions and reactions of the ship [29]

The resistance to movement of a ship can be divided in different components:

$$R_T = R_H + R_{AP} + R_{AA} + R_{AW} + R_A \tag{22}$$

Where:

R_T: total resistance

R_H: bare hull resistance

R_{AP}: the increase in resistance relative to that of the naked, or bare hull resistance, caused by appendages;

R_{AA}: resistance of the above water form of a ship due to its motion relative to still air or wind;

R_{AW}: resistance in waves, the mean increase in resistance in wind and waves as compared with the still water resistance at the same mean speed;

R_A: The increase in resistance relative to the resistance of a hydraulically smooth hull due to the effect of roughness. Roughness caused by marine organisms depositing shell or grass.

The a.m. variables are directly proportional to speed and are described through specific values acquired from the automatically system. The initial database of "csv" counts 108 acquired variables, but only the useful variables were selected to describe the relation (22).

Moreover, from the [Principles of Naval Architecture] are follows that

$$R_T = \frac{1}{2} C_T \rho S V^2 \tag{23}$$

where R_T is the total resistance, C_T is the total resistance coefficient, ρ is the fluid density, S is the wetted surface. Moreover we have also that:

$$P = R_T \cdot V \,. \tag{24}$$

Then by (23) and (24) it follows also that

$$Y \propto V^3 \,. \tag{25}$$

The sailing speed is the value that the most influences fuel consumption and according to relation (23) it is introduced in the model like a value to the power of three.

Hull resistance R_H is directly proportional to displacement.

Resistance of appendix R_{AP} , in this model represents the additional resistance of stabilizer fins used in poor weather conditions.

Air and wind resistance R_{AA} are described through the decomposition of the real wind vector along longitudinal and transversal axles.

Additional resistance due to sea conditions R_{AW} and to hull deterioration caused by vegetation R_A, were not directly considered as there were no experimental values at disposal.

In this paper, for each ship and for each voyage, we take into consideration the following variables, which have the main technological influence on the fuel consumption Y (Mt) of the main engines and therefore characterize each *sailing condition*:

V	Speed Over Ground	(Knots)
M	Sailed Distance Over Ground	(NM)
W_h	Head Wind	(Knots)
W_s	Side Wind	(Knots)
Δ	Displacement	(Mt)
F	Stabilizer fin operating time	(h)
E	Engine operation mode	-

Table 11: variables

The SOG V is calculated from the GPS speed signal. The Sailed distance Over Ground M is calculated as the 2nd loxodromic problem based on the GPS coordinates collected every 5 minutes.

The true wind $\mathbf{W}$ as well as the *longitudinal wind* W_l and the *transversal wind* W_t, reported in fig.1, are calculated every 5 minutes through COG, SOG and apparent wind direction and speed are collected by on-board anemometer.

In particular, W_l and W_t are calculated as

$$W_l = -W \cos\left(\vartheta_W - COG\right) \tag{26}$$

$$W_t = -W\, sen\left(\vartheta_W - COG\right) \tag{27}$$

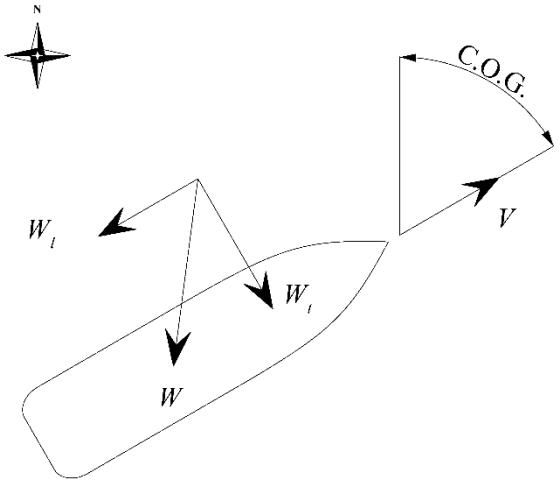

Figure 44: wind component

$W_l \geq 0$ corresponds to a wind following component, $W_l < 0$ corresponds to a head wind component.

Since the head wind force generally constitutes the largest part of the longitudinal wind induced resistance, in this paper, we consider the head wind W_h define as the mean value of

$$W_l^+ = \begin{cases} 0 & if\ W_l \geq 0 \\ -W_l & if\ W_l < 0 \end{cases} \tag{28}$$

On the other hand, the transversal wind force always causes, drift and deviation from the intended course and therefore an added resistance for the two following reasons:

- the ship's heading is not aligned with the steered course.
- the drift needs to be continuously compensated by the rudder.

Therefore, we take into consideration the side wind W_s, defined as the mean value of $|W_t|$.

For each ship, the displacement Δ is determined based on the data collected by the four draft gauges installed on fore (FP) and aft (AP) perpendiculars and on the port and starboard of the midship section. Specifically, we obtain the *midship draft* by averaging the port and starboard draft in the midship section and the *trim* as the difference between AP and FP draft, respectively.

On the basis of the midship draft and trim, we can exploit the hydrostatic data to calculate the displacement when the ship leaves the departure port Δ_l and the displacement when the ship arrives to the arrival port Δ_a.

Specifically, Δ_l and Δ_a are calculated when the ship speed is less than 0,3 knots (which characterize the steady state of the ship). Then, for each voyage, the displacement is calculated as the mean value of Δ_l and Δ_a.

The stabilizer fin operating time F takes into consideration the resistance and the fuel consumption increase which occur when stabilizer fins are in use (e.g., in poor weather condition). Differently from the above data, this information is deducted from the *noon report.*

The variable E is an indicator with two levels which identifies the engine operation mode during sailing. In fact, the engine system can drive propulsion at fixed RPM (*constant mode*) and at variable RPM (*combinator mode*).

The constant RPM mode is needed when a shaft generator has to be engaged for electric power. However in this mode the ship speed is regulated only by changing the pitch propeller and it is not possible to reach the max vessel speed.

Likewise, in combinator mode the ship speed is regulated by increasing both the pitch propeller and engine rpm. Unfortunately, in this mode it is not possible to engage the shaft generator.

Therefore, let

$$E = \begin{cases} 0 & \text{if constant mode is selected} \\ 1 & \text{if combinator mode is selected} \end{cases} \tag{29}$$

5. Statistical methods for variable selection

In most practical problems, especially those involving historical data, the analyst has a rather large pool of possible candidate regressors, of which only a few are likely to be important. Finding an appropriate subset of regressors for the model is essential. Good variable selection methods are very important in the presence of multicollinearity.

Building a regression model that includes only a subset of the available regressors involves two conflicting objectives:

1. We would like the model to include as many regressors as possible so that the information content in these factors can influence the predicted value of y.
2. We want the model to include as few regressors as possible because the variance of the prediction ì increases as the number of regressors increases. Also the more regressors there are in a model, the greater the costs of data collection and model maintenance.

The process of finding a model that is a compromise between these two objectives is called selecting the "best" regression equation.

Experience, professional judgment in the subject-matter field, and subjective considerations all enter into the variable selection problem. Variable selection procedures should be used by the analyst as methods to explore the structure of the data.

The statistics R , adjusted R , Mallows' Cp, and S (square root of MSE) are calculated by the best subsets procedure and can be used as comparison criteria

Typically, you would only consider subsets that provide the largest R value. However, R always increases with the size of the subsets. When comparing models with the same number of predictors, choosing the model with the highest R is equivalent to choosing the model with the smallest SSE

Use adjusted R and Mallows' Cp to compare models with different numbers of predictors. In this case, choosing the model with the highest adjusted R is equivalent to choosing the model with the smallest mean square error (MSE). The Mallows' Cp statistic is given by the formula

$$C_P = \frac{SS_E(p)}{\hat{\sigma}^2(FM)} - n + 2p \tag{30}$$

Where:

$SS_E(p)$ is SSE for the best model with p parameters (including the intercept, if it is in the equation);

$\hat{\sigma}^2(FM)$ is the mean square error for the model with all m predictors.

If the model is adequate (that is, fits the data well), then the expected value of Mallows' Cp is approximately equal to p (the number of parameters in the model). A small Mallows' Cp indicates that the model is relatively precise (has small variance) in estimating the true regression coefficients and predicting future responses. This precision will not improve much by adding more predictors. Models with considerable lack of fit have Mallows' Cp values larger than p.

Minitab© output table with best subset model

												E	E	E	E	E	E	E	F
												x	x	x	x	x	x	x	x
						V						V							V
						^		W	W	W		^		W	W	W			^
Vars	R-Sq	R-Sq(adj)	Mallows Cp	S	3	M	f	h	s	Δ	F	E	3	M	f	h	s	F	Δ	3
1	92,5	92,5	1774,6	7,7977		X														
1	31,0	30,8	19272,4	23,633							X									
2	95,9	95,8	820,2	5,8043	X	X														
2	93,9	93,9	1370,7	7,0280		X						X								
3	97,4	97,3	391,2	4,6321	X	X														X
3	97,4	97,3	393,6	4,6394	X	X					X									
4	98,2	98,2	148,3	3,8070	X	X		X												X
4	98,2	98,2	157,8	3,8423	X	X		X			X									
5	98,4	98,4	102,0	3,6255	X	X		X	X											X
5	98,4	98,4	105,2	3,6379	X	X		X	X		X									
6	98,5	98,5	62,3	3,4608	X	X		X	X		X	X								
6	98,5	98,5	63,3	3,4649	X	X		X	X		X							X		
7	98,6	98,6	35,0	3,3409	X	X		X	X	X	X	X								
7	98,6	98,6	36,4	3,3471	X	X		X	X	X	X							X		
8	98,7	98,7	23,5	3,2869	X	X		X	X	X	X	X		X						
8	98,7	98,7	25,2	3,2940	X	X		X	X	X	X			X				X		
9	98,7	98,7	16,1	3,2497	X	X		X	X	X	X	X		X					X	
9	98,7	98,7	17,8	3,2571	X	X		X	X	X	X			X				X	X	
10	98,7	98,7	13,4	3,2332	X	X		X	X	X	X	X		X		X			X	
10	98,7	98,7	15,0	3,2401	X	X		X	X	X	X	X	X	X					X	
11	98,8	98,7	12,0	3,2223	X	X		X	X	X	X	X	X	X		X			X	
11	98,7	98,7	13,4	3,2284	X	X		X	X	X	X	X	X	X				X	X	
12	98,8	98,7	11,2	3,2238	X	X		X	X	X	X	X	X	X		X		X	X	
12	98,8	98,7	12,6	3,2203	X	X	X	X	X	X	X	X	X	X		X			X	
13	98,8	98,7	11,8	3,2122	X	X		X	X	X	X	X	X	X		X	X	X	X	
13	98,8	98,7	12,9	3,2171	X	X	X	X	X	X	X	X	X	X		X		X	X	
14	98,8	98,7	13,5	3,2152	X	X	X	X	X	X	X	X	X	X		X		X	X	X
14	98,8	98,7	13,5	3,2154	X	X	X	X	X	X	X	X	X	X		X	X	X	X	
15	98,8	98,7	15,2	3,2183	X	X	X	X	X	X	X	X	X	X		X	X	X	X	X
15	98,8	98,7	15,2	3,2186	X	X	X	X	X	X	X	X	X	X	X	X		X	X	X
16	98,8	98,7	17,0	3,2222	X	X	X	X	X	X	X	X	X	X	X	X	X	X	X	X

Table 12: best subset

In the table above *"S"* represents the residual standard deviation.
Highlighted is the model that was chosen, with the lowest "*S*" and *Cp* value. Thus, supposing that the residual analysis is satisfying, this model is a good candidate for the best regression model.
From the table we deduce that the explaining variable W_f *"wind following"* and its interaction with the dummy variable *E* are not statistically important. This phenomenon is strictly correlated with the route of the ships subject to study and the main weather conditions found. The database seldom contains only the aft wind, it is rather accompanied by a transversal component. The second one is more relevant as it causes rolling and constrains the use of the stabilizer fins. That's why we can deduce that the aft wind has a smaller influence on fuel consumption.

6. Equation of the regression model

For each ship and for each voyage, taking into consideration the variables in tab Table 11, which have the main technological influence on the fuel consumption Y (Mt) of the main engines and therefore characterize each sailing condition, the proposed model can be expressed in the following form:

$$\begin{aligned} Y = {} & \beta_0 + \beta_1 M + \beta_2 V^3 + \beta_3 \Delta + \beta_4 W_h + \beta_5 W_s + \beta_6 F + \\ & + E \cdot \left(\beta_1 + \beta_{11} M + \beta_{12} V^3 + \beta_{13} \Delta + \beta_{14} W_h + \beta_{15} W_s + \beta_{16} F \right) + Z \end{aligned} \tag{31}$$

CHAPTER 4- Analysis of data and results

1. Analysis of sailing data

Only with a proper and continuous monitoring of specific variables, it is possible to support sail management in making decisions.

In fact we develop a statistical framework based on multiple linear regression which allows ship fuel consumption prediction for the given sailing condition of a specific voyage and prediction interval calculation which can be compared with the effective fuel consumption. Note that this approach overcomes the Speed-Power curves, which are usually used the naval architecture to predict fuel consumption only through the bi-dimensional relation between power/consumption and speed.

The regression model can be expressed in (31)

The above described model has been implemented for the ships *SHIP 1 and SHIP 2,* using the data reported in the T-Report (voyage) conveniently processed.

According to the timesheet reported in *Figure 45*, SHIP 1 and SHIP 2 have been monitored for 363 and 355 voyages respectively. Each voyage is identified by a Voyage progressive Number (VN). In particular, SHIP 1 was monitored from 1th August 2012 to 31th July 2013 $(VN157 \div VN537)$. SHIP 2 was monitored from 2nd of January 2012 to the 22nd December 2012 $(VN1 \div VN372)$. Incomplete or problem-specific data have been excluded from the analysis.

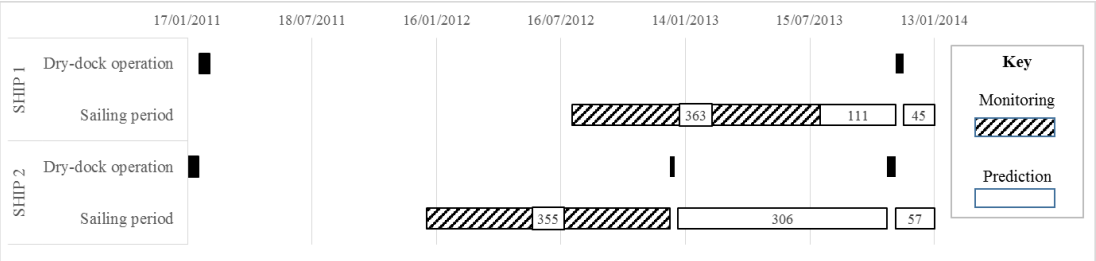

Figure 45: ships timesheet

Explicitly note, for each ship, in order to avoid any seasonality effect, are considered a monitoring periods of about one year, from *Figure 45*. Moreover, such periods do not include off-line dry-dock efficiency improvement operations.

In the next page are show the main results of the regression analysis for SHIP 1 and SHIP 2, respectively.

***SHIP 1* Analysis**

Equation model

$$\begin{aligned} Y = &-115,483 + 0,29F + 0,28Miglia + 0,04V^3 + 0,47W_f \\ &+ 0,20W_s + 0,002\Delta + 83,13E + 0,03E \cdot M - 0,0033E \cdot V^3 \\ &- 0,001E \cdot \Delta - 0,37E \cdot W_f - 0,11E \cdot W_s + 0,06E \cdot F \end{aligned} \tag{32}$$

SHIP 1	β'_{i0}	β'_{i1}	β'_{i2}	β'_{i3}	β'_{i4}	β'_{i5}	β'_{i6}
i		M	V^3	W_h	W_s	Δ	F
0	-115,480	0,275	0,004	0,470	0.203	0.002	0,293
1	-32,350	0,305	0,001	0,102	0,096	0,001	0,357
β'_{1J}	83,129	0,030	-0,003	-0,001	-0,367	-0,107	0,064
Std Dev (Mt)	2,51		R^2	99,12 %		R^2_{Adj}	99,08 %

Table 13: SHIP 1, regression analysis main results

The following table contains the estimated coefficients for each regressor according to the formula

$$\beta'_{ij} = \beta_i \quad if\ E = 0;\ \beta'_{ij} = \beta_i + \beta_{ij} \quad if\ E = 1 \quad con\ j = 1,2,...,6 \tag{33}$$

ANOVA

Source	DF	Seq SS	Adj SS	Adj MS	F	P
Regression	13	249793	249793	19215	3034,1	0,000000
F	1	65027	857	857	135,3	0,000000
M	1	169383	107651	107651	16998,6	0,000000
V3	1	10537	8906	8906	1406,3	0,000000
Wh	1	2837	2344	2344	370,1	0,000000
Ws	1	397	300	300	47,4	0,000000
Δ	1	1132	1271	1271	200,8	0,000000
E	1	169	84	84	13,2	0,000315
E*M	1	146	100	100	15,8	0,000084
E*V3	1	96	152	152	24,1	0,000001
E*Δ	1	16	18	18	2,8	0,093206
E*Wh	1	50	41	41	6,4	0,011574
E*Ws	1	3	2	2	0,3	0,555264
E*F	1	0	0	0	0,0	0,895733
Error	352	2229	2229	6		
Total	365	252022				

Table 14: SHIP 1 ANOVA table

From the ANalysis Of Variace (ANOVA) *Table 14*, supposing the $p-value<0,05$, we deduce that the regressor considered are in relation with the response variables Y. Moreover, it's possible to notice that the variables $E\cdot\Delta, E\cdot W_S, E\cdot F$, are not relevant. The negligible importance of these variables from a statistic point of view is due small number to the voyages in combinator mode which diesel generators are turned on. These voyages are carried out during the summertime in which the choice to adopt a combinator mode during sailing instead of a constant rpm is due to the necessity to reach high speeds, and which, as explained in (Chap. 2), cannot be done the second way. During the summertime in fact the ship sails with more load than during the rest of the year. Moreover the good weather conditions mean the absence of the transversal component W_S and of stabilizer fins in use.

Residuals analysis

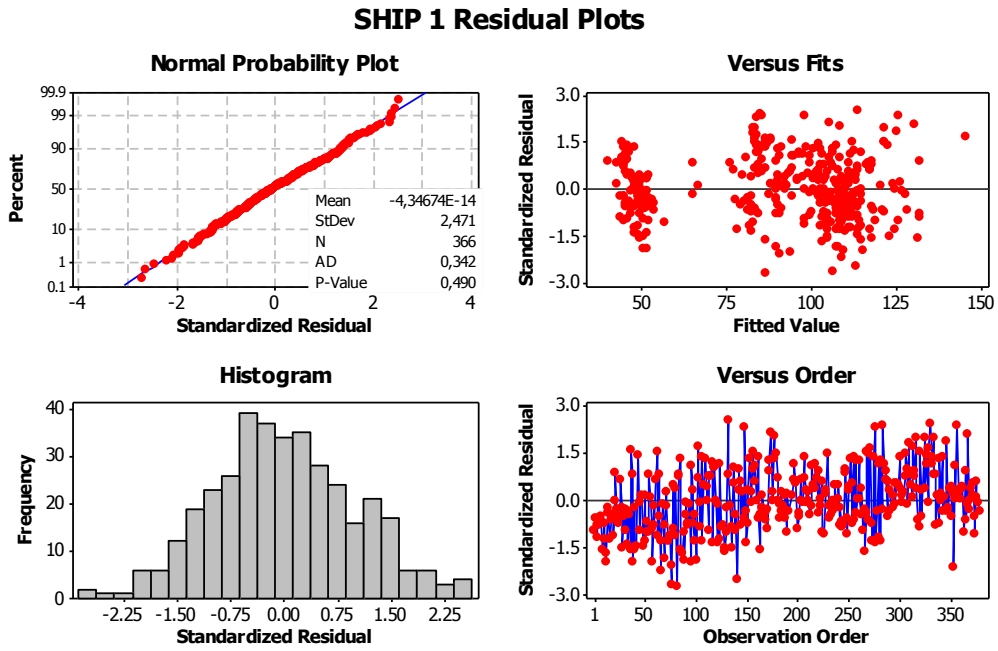

Figure 46: SHIP 1, analysis of the residual plots

Ship 2 Analysis

Equation model

$$\begin{aligned} Y = &-97,39+0,43F+0,27Miglia+0,003V^3+0,51W_f \\ &+0,23W_s+0,002\Delta+101,57E-0,05E\cdot M-0,001E\cdot V^3 \\ &-0,003E\cdot\Delta-0,29E\cdot W_f-0,09E\cdot W_s+1,61E\cdot F \end{aligned} \tag{34}$$

main results of the regression analysis

SHIP 2	β'_{i0}	β'_{i1}	β'_{i2}	β'_{i3}	β'_{i4}	β'_{i5}	β'_{i6}
i		M	V^3	W_h	W_s	Δ	F
0	-97,391	0,267	0,003	-0,509	0,234	0,002	0,426
1	10,146	0,212	0,002	-0,798	0,143	-0,001	2,080
β'_{1J}	101,573	-0,054	-0,001	-0,003	-0,289	-0,091	1,602
Std Dev (Mt)	2,45		R^2	99,26 %		R^2_{Adj}	99,23 %

Table 15: SHIP 2, regression analysis main results

ANOVA

Source	DF	Seq SS	Adj SS	Adj MS	F	P
Regressione	13	269811	269811	20754,7	3454,7	0,000000
F	1	78717	1128	1128,4	187,8	0,000000
M	1	176068	76121	76120,7	12670,7	0,000000
V3	1	10738	6436	6436,5	1071,4	0,000000
Wh	1	2448	2423	2423,1	403,3	0,000000
Ws	1	504	344	344,1	57,3	0,000000
Δ	1	408	546	545,9	90,9	0,000000
E	1	525	61	60,9	10,1	0,001597
ExM	1	168	132	131,7	21,9	0,000004
ExV^3	1	0	55	55,1	9,2	0,002648
ExΔ	1	37	27	26,6	4,4	0,036035
ExWh	1	56	58	58,2	9,7	0,002011
ExWs	1	12	2	2,2	0,4	0,542300
ExF	1	130	130	129,8	21,6	0,000005
Errore	334	2007	2007	6,0		
Totale	347	271818				

Table 16: SHIP 2 ANOVA table

From the ANalysis Of Variace (ANOVA) *Table 16*, made on the basis of the data for SHIP 2, we deduce that the unique un important variable is $E \cdot W_s$. Differently from SHIP 1, SHIP 2 has carried out a higher number of voyages in combinator mode, not only in the summertime and that's why the two variables $E \cdot \Delta$ and $E \cdot F$ for this ship are significant.

Residuals Analysis

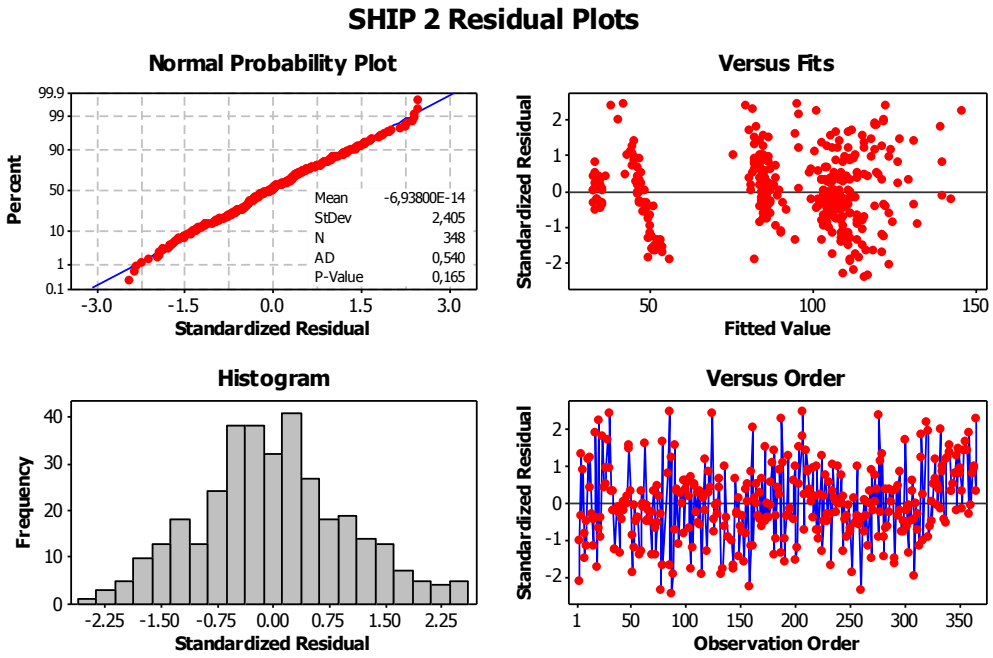

Figure 47: SHIP 2, a*nalysis of the residual plots*

The four-in-one residual plot displays four different residual plots together in one graph window. This layout can be useful for comparing the plots to determine whether your model meets the assumptions of the analysis. The residual plots in the graph include:

- Histogram - indicates whether the data is skewed or whether outliers exist in the data.
- Normal probability plot - indicates whether the data are normally distributed, if other variables are influencing the response, or if outliers exist in the data.
- Residuals versus fitted values - indicates whether the variance is constant whether, a nonlinear relationship exists, or whether outliers exist in the data.
- Residuals versus order of the data - indicates whether there are systematic effects in the data due to time or data collection order.

Model residuals for ship *SHIP 1* have a Normal distribution with average μ equal to zero and standard deviation σ equal to 2,51 [Mt], while for ship *SHIP 2* they have a Normal distribution with average μ equal to zero and standard deviation σ equal to 2,45 [Mt].
The obtained results confirm the hypothesis the regression model is based on.

2. Technological interpretation of outliers

During the monitoring problems can occur regarding the probably presence of abnormal values. An outlier is an extreme observation; one that is considerably different from the majority of the data. The outliers can have moderate to severe effects on the regression model.

Outliers are carefully investigated to see if a reason for their unusual behaviour can be found. Sometimes outliers are "bad" values, occurring as a result of unusual but explainable events. Examples include faulty measurement or analysis, incorrect recording of data, and the failure of a measuring instrument. In this case, the outliers are deleted from the data set.

Thus, during the monitoring, before we reach the final regression model, such outliers are discovered, technologically interpreted and then eliminated. Often a simple graphic method helps finding out such abnormal values.

The graphic method used during this analysis is the boxplot; it also highlights the presence of outliers.

The outliers can be univariate, which means they have an extreme value for a single variable or multivariate if they have an unusual combination of values on a certain number of variables. In concrete terms they are such values that appear particularly extreme compared to the other values of the sample.

The effect of outliers on the regression model may be easily checked by dropping these points and refitting the regression equation. We may find the value of the regression coefficients or the summary statistic such as the *t* or *F* statistic, R^2, and the residual mean square may be sensitive to the outliers.

A situation in which a relative small percentage of the data has a significant impact on the model may be not acceptable to the user of regression equation. For this reason during the monitoring it's important to find out such values, to interpreted them technologically and to repeat the regression analysis with a database without the outliers. In the case of the study, outliers are such voyages where the predicted fuel consumption for the model is very far from the observed consumption.

In *Table 17* the outliers of both ships are scheduled.

Ship	***No. of outlier voyages***
SHIP 1	200; 204; 266; 283; 324; 348; 350; 351; 387; 450; 481
SHIP 2	27; 82; 83; 84; 126; 135; 141; 142; 143; 199; 207; 255; 263; 293; 323; 324; 352; 361; 367

Table 17: outliers

To allow a technological interpretation of the outliers (*Table 18 and Table 19*), boxplots were drawn up and give the distribution of each regressor of the model. It is important to point out the variables M and F have been divided on the base of the routes run by the ships subject of study. This division is important as if you consider miles *M*, these cannot be merged in a model because the routes are not the same length. Moreover, as the voyage time is different for each route, the stabilizer fins *F* have been divided in the same way as the miles. In the following tables you will find in red the values of the explaining variables higher than quartile Q3, in blue the values lower than quartile Q1.

SHIP 1 – Technological interpretation of outliers

Voyage no.	Route	M [NM]	V [Knots]	W_h [Knots]	W_s [Knots]	Δ [Mt]	F [ore]
200	B-C	**340**			**11,10**	**25793**	**4,30**
204	B-C				**20,22**		**9,35**
266	B-A		**20,00**	**1,66**		**24000**	
283	A-B	**476**			**23,21**	**24278**	**20**
324	A-B		**21,00**			**24322**	
348	A-B		**22,70**	**0,56**	**0,31**		
350	A-B		**22,87**	**0,17**	**4,48**		
351	B-A	**474**	**20,00**	**31,20**	**15,06**		**23,30**
356	B-A	**480**	**20,25**		**17,47**	**26294**	**22,00**
387	C-B	**301**		**11,92**	**21,70**	**25668**	**6,30**
450	C-B	**346**		**12,10**	**21,81**		**11,10**
481	C-B		**22,66**	**16,20**	**21,31**		**12,45**

Table 18: SHIP 1, outliers interpretation

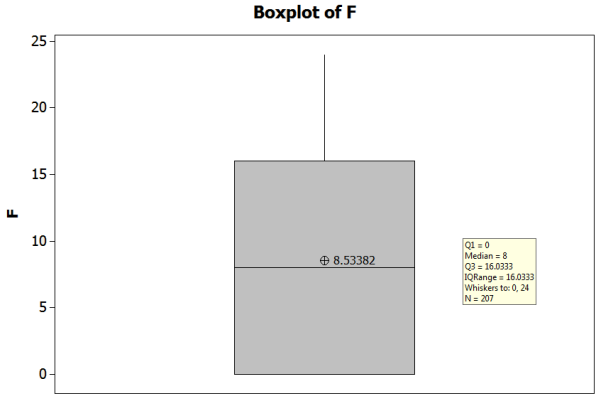
Boxplot of F
F
25
20
15
10
5
0
8.53382
Q1 = 0
Median = 8
Q3 = 16.0333
IQRange = 16.0333
Whiskers to: 0, 24
N = 207

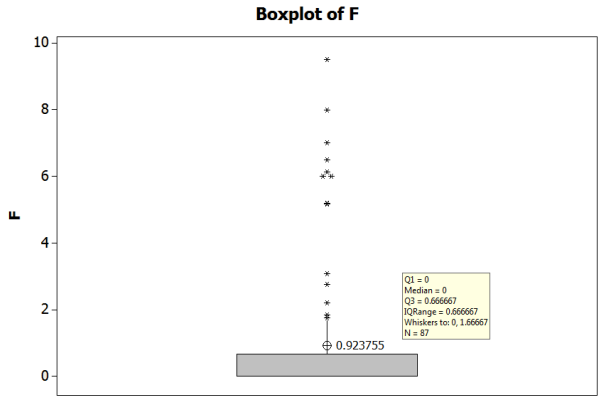
Boxplot of F
F
10
8
6
4
2
0
0.923755
Q1 = 0
Median = 0
Q3 = 0.666667
IQRange = 0.666667
Whiskers to: 0, 1.66667
N = 87

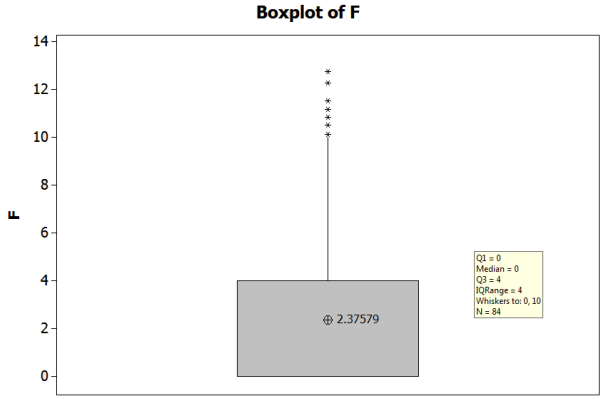
Boxplot of F
F
14
12
10
8
6
4
2
0
2.37579
Q1 = 0
Median = 0
Q3 = 4
IQRange = 4
Whiskers to: 0, 10
N = 84

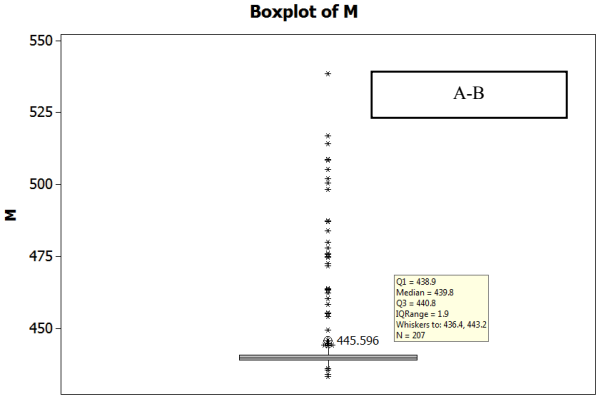
Boxplot of M
M
550
525
500
475
450
A-B
445.596
Q1 = 438.9
Median = 439.8
Q3 = 440.8
IQRange = 1.9
Whiskers to: 436.4, 443.2
N = 207

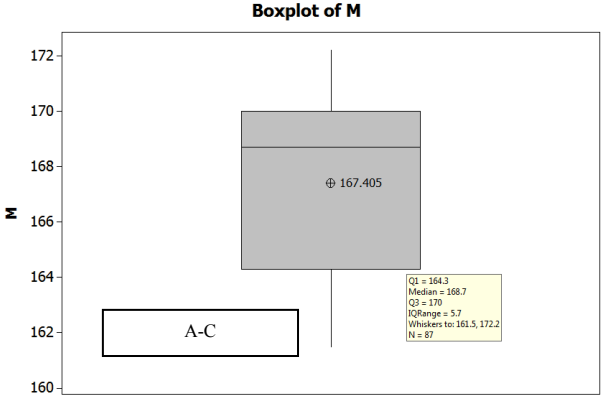
Boxplot of M
M
172
170
168
166
164
162
160
167.405
A-C
Q1 = 164.3
Median = 168.7
Q3 = 170
IQRange = 5.7
Whiskers to: 161.5, 172.2
N = 87

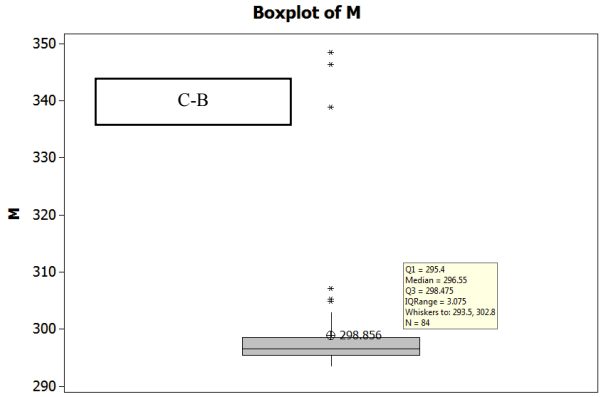
Boxplot of M
M
350
340
330
320
310
300
290
C-B
298.856
Q1 = 295.4
Median = 296.55
Q3 = 298.475
IQRange = 3.075
Whiskers to: 293.5, 302.8
N = 84

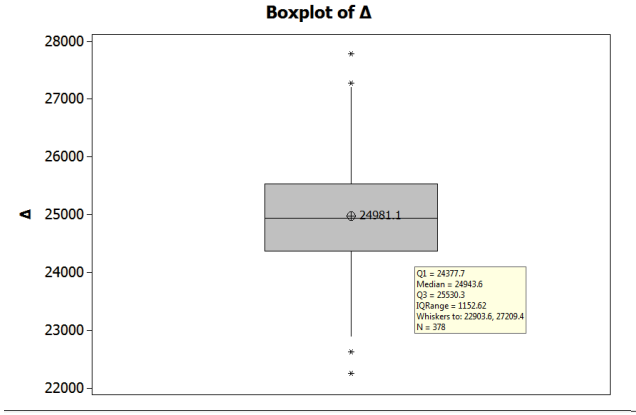
Boxplot of Δ
Δ
28000
27000
26000
25000
24000
23000
22000
24981.1
Q1 = 24377.7
Median = 24943.6
Q3 = 25530.3
IQRange = 1152.62
Whiskers to: 22903.6, 27209.4
N = 378

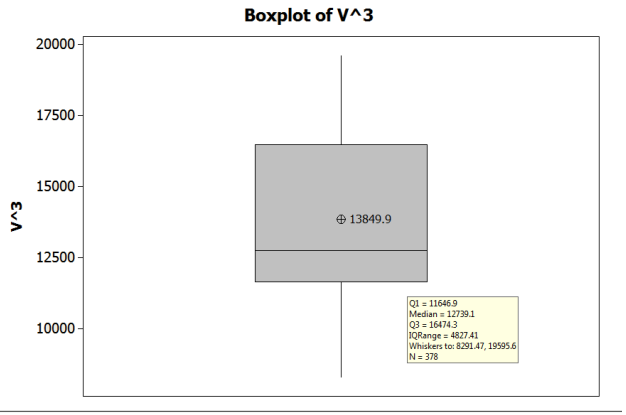
Boxplot of V^3
V^3
20000
17500
15000
12500
10000
13849.9
Q1 = 11646.9
Median = 12739.1
Q3 = 16474.3
IQRange = 4827.41
Whiskers to: 8291.47, 19595.6
N = 378

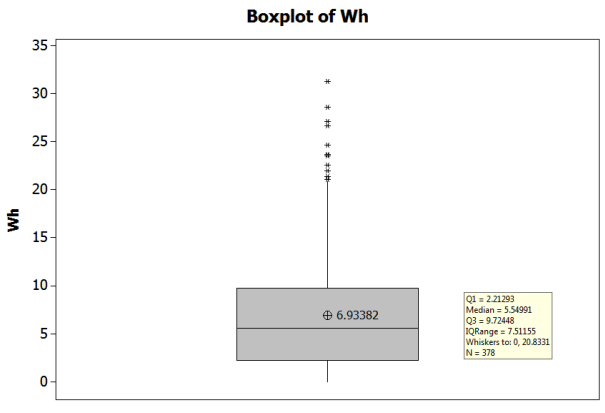
Boxplot of Wh
Wh
35
30
25
20
15
10
5
0
6.93382
Q1 = 2.21293
Median = 5.54991
Q3 = 9.72448
IQRange = 7.51155
Whiskers to: 0, 20.8331
N = 378

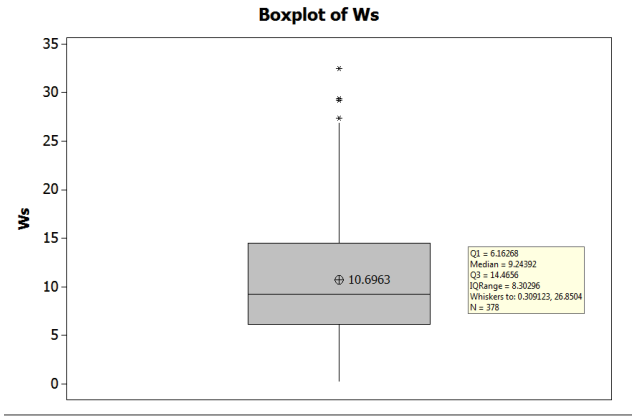
Boxplot of Ws
Ws
35
30
25
20
15
10
5
0
10.6963
Q1 = 6.16268
Median = 9.24392
Q3 = 14.4656
IQRange = 8.30296
Whiskers to: 0.309123, 26.8504
N = 378

SHIP 2 – Technological interpretation of outliers

Voyage no.	Route	M [NM]	V [Knots]	W_h [Knots]	W_s [Knots]	Δ [Mt]	F [ore]
27	B-A	**490**	**22,43**	**12,10**	**24,25**		**16,50**
82	A-C	**169**		**16.24**	**27,61**		**6,75**
83	C-A	**315**				**26000**	
84	B-A			**23,43**	**15,90**	**27000**	**14,50**
126	C-B	**304**		**15,56**	**15,87**	**24451**	**2,50**
135	B-A			**0,47**	**4,01**	**25827**	
141	A-C		**19,93**	**21,30**			
142	C-B			**16,43**	**13,94**		
143	B-C	**438**		**10,71**		**26337**	
199	C-A			**3,19**			
207	A-B	**467**	**21,28**	**0,02**			
255	A-B	**468**				**24250**	
263	B-A	**491**		**1,21**	**22,26**		
293	B-A	**437**			**24,43**		
323	A-B	**511**	**21,58**	**14,65**	**23,50**		**23,00**
324	B-A	**547**	**21,27**		**23,41**	**25903**	**25,00**
352	B-A	**481**			**25,28**		**19,92**

361	A-B	**457**	**21,50**	**12,64**	**23,21**	**18,33**
367	A-B		**21,55**	**16,50**	**19,06**	**19,67**

Table 19: SHIP 2, outliers interpretation

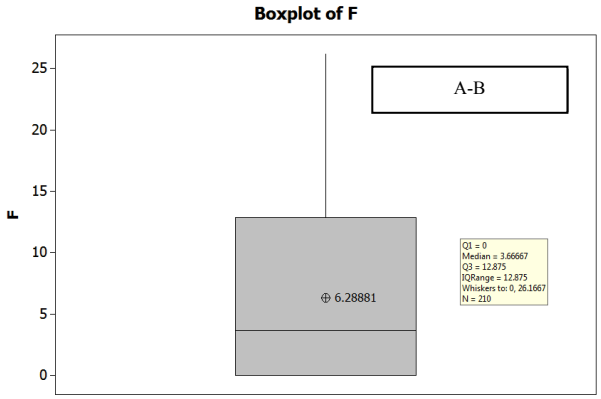
Boxplot of F
A-B
F
Q1 = 0
Median = 3.66667
Q3 = 12.875
IQRange = 12.875
Whiskers to: 0, 26.1667
N = 210
6.28881

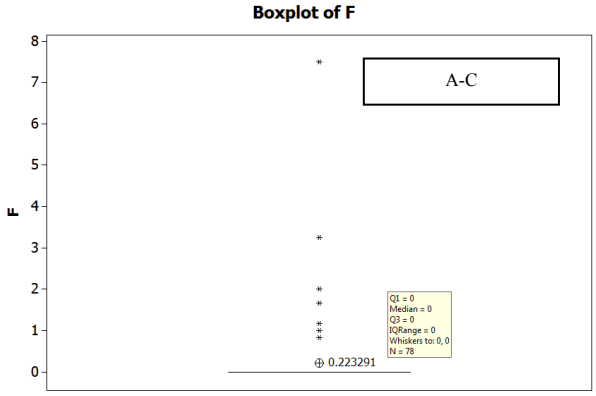
Boxplot of F
A-C
F
Q1 = 0
Median = 0
Q3 = 0
IQRange = 0
Whiskers to: 0, 0
N = 78
0.223291

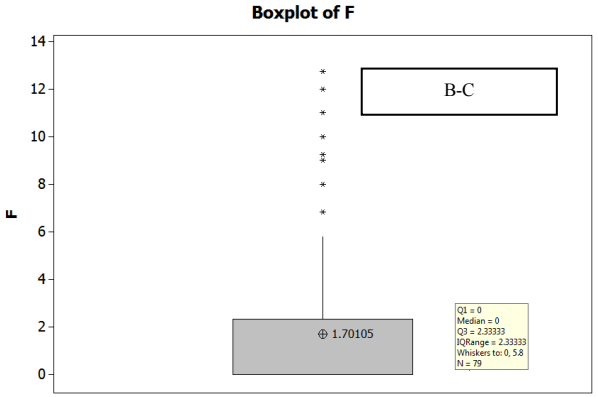
Boxplot of F
B-C
F
Q1 = 0
Median = 0
Q3 = 2.33333
IQRange = 2.33333
Whiskers to: 0, 5.8
N = 79
1.70105

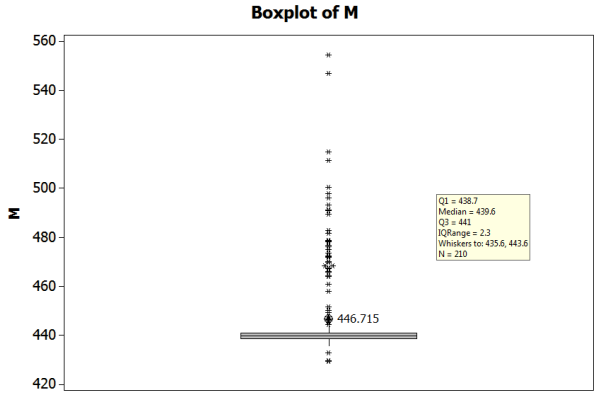
Boxplot of M
M
Q1 = 438.7
Median = 439.6
Q3 = 441
IQRange = 2.3
Whiskers to: 435.6, 443.6
N = 210
446.715

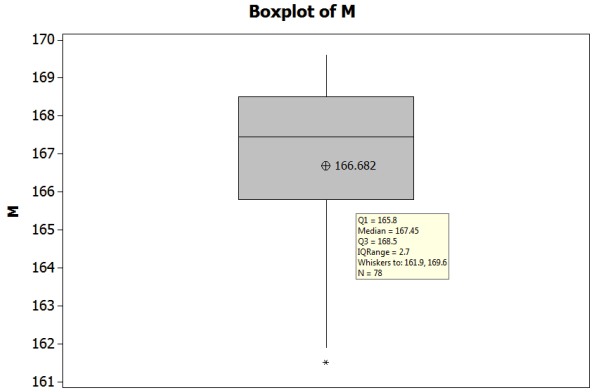
Boxplot of M
M
Q1 = 165.8
Median = 167.45
Q3 = 168.5
IQRange = 2.7
Whiskers to: 161.9, 169.6
N = 78
166.682

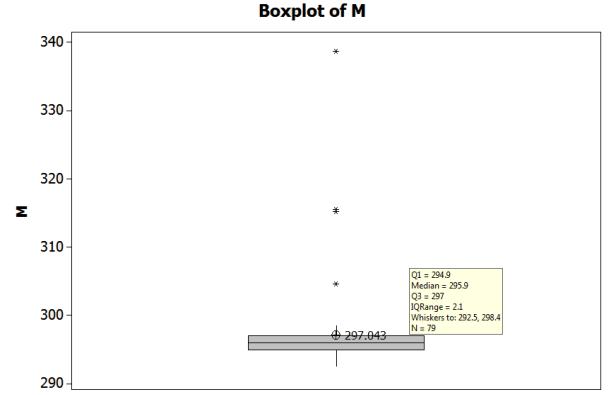
Boxplot of M
M
Q1 = 294.9
Median = 295.9
Q3 = 297
IQRange = 2.1
Whiskers to: 292.5, 298.4
N = 79
297.043

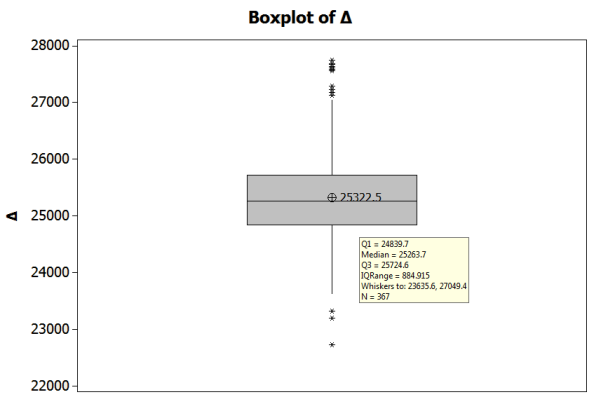
Boxplot of Δ
Δ
28000
27000
26000
25000
24000
23000
22000
25322.5
Q1 = 24839.7
Median = 25263.7
Q3 = 25724.6
IQRange = 884.915
Whiskers to: 23635.6, 27049.4
N = 367

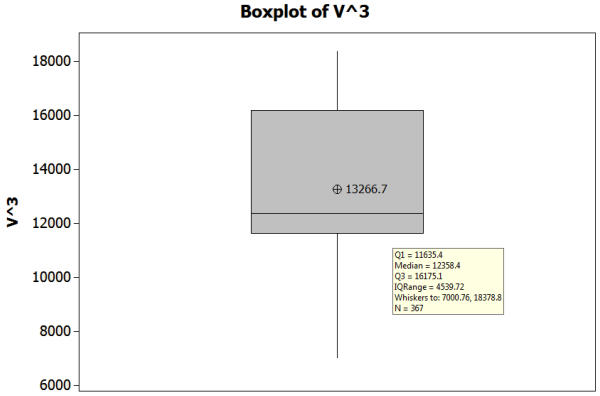
Boxplot of V^3
V^3
18000
16000
14000
12000
10000
8000
6000
13266.7
Q1 = 11635.4
Median = 12358.4
Q3 = 16175.1
IQRange = 4539.72
Whiskers to: 7000.76, 18378.8
N = 367

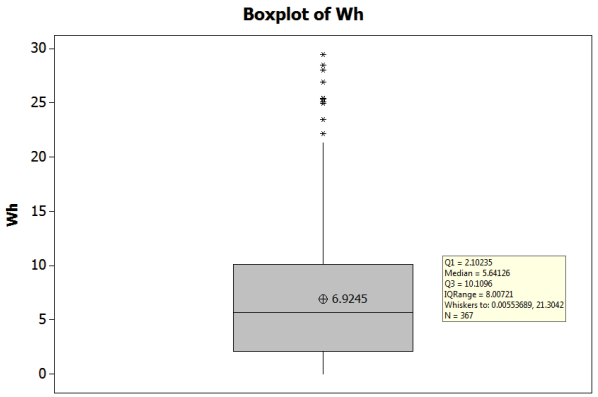
Boxplot of Wh
Wh
30
25
20
15
10
5
0
6.9245
Q1 = 2.10235
Median = 5.64126
Q3 = 10.1096
IQRange = 8.00721
Whiskers to: 0.00553689, 21.3042
N = 367

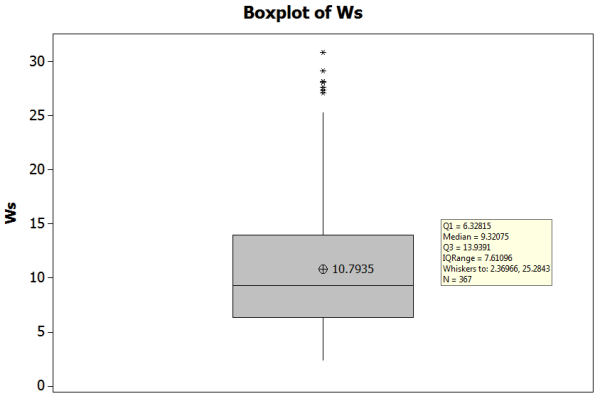
Boxplot of Ws
Ws
30
25
20
15
10
5
0
10.7935
Q1 = 6.32815
Median = 9.32075
Q3 = 13.9391
IQRange = 7.61096
Whiskers to: 2.36966, 25.2843
N = 367

3. Consumption prediction and technological interpretation of the voyages out of the prediction limits

For each voyage (with even VN) the actual fuel consumption is compared to the prediction limits calculated by (21).

As an example, *Figure 48 and Figure 49* show the actual fuel consumption, the prediction intervals calculated on the basis of the data collected during the monitoring periods defined in *Figure 48*, corresponding to $(VN\,603 \div VN\,623)$ for SHIP 1 and *Figure 49* $(VN\,539 \div VN\,559)$ for SHIP 2, respectively. In these figures, numeric values are omitted, but scales are left unchanged.

When the actual consumption falls outside the prediction limits ($VN\,606, 608, 609, 623$ for SHIP 1 and $VN\,523, 542, 543, 546, 550, 552, 553, 555, 556, 559$ SHIP 2) a possible problem may have occurred.

Plausible causes are listed below:

- SHIP 1, $VN\,606$: the lower fuel consumption is explained by bad weather conditions on the quarter, with following sea and wind, which are not explicitly considered in the model.
- SHIP 1, $VN\,608, 623$: the voyages is an outlier since during the navigation the ship switched from constant rpm mode to combinator mode only on the starboard shaft (Figure 2). Therefore, the starboard shaft generator must be necessarily powered off (i.e. $P_1^E = 0$). Since the operation mode has been considered constant during the whole voyage, the estimated fuel consumption results less than the actual one. In the VN 623 stabilizer fins were being used because of side wind.
- SHIP 1, $VN\,609$: the higher fuel consumption is explained by the ship overload, two days of very poor weather condition with high wind speed blowing from bow dial which makes long sea waves. Moreover ship used stabilizer fins all voyage long.
- SHIP 2, $VN\,550, 555$: the higher fuel consumption is explained by two consecutive days of weather conditions characterized by on the wind quarter with mean speed of 30 knots and long sea-wave. The stabilizer fins were being used because of side wind.
- SHIP 2, $VN\,556$: the higher fuel consumption is explained also by ship overload and seven consecutive days of weather condition characterized by the wind quarter with mean speed of 25 knots and long sea-wave. The stabilizer fins were being used because of side wind.
- SHIP 2, $VN\,559$: the higher fuel consumption is explained by two days of bad weather conditions and long sea-waves. Moreover the ship had very high SOG and stern down trim.
- SHIP 2, $VN\,539$: the higher fuel consumption is explained by very high SOG and stern down trim.
- SHIP 2, $VN\,542$: the higher fuel consumption cannot be technologically explained.
- SHIP 2, $VN\,543$: An error displacement calculation may have occurred.

— SHIP 2, *VN* 546 : the higher fuel consumption is explained by very high SOG, ship overload and stabilizer fins used all voyage long.

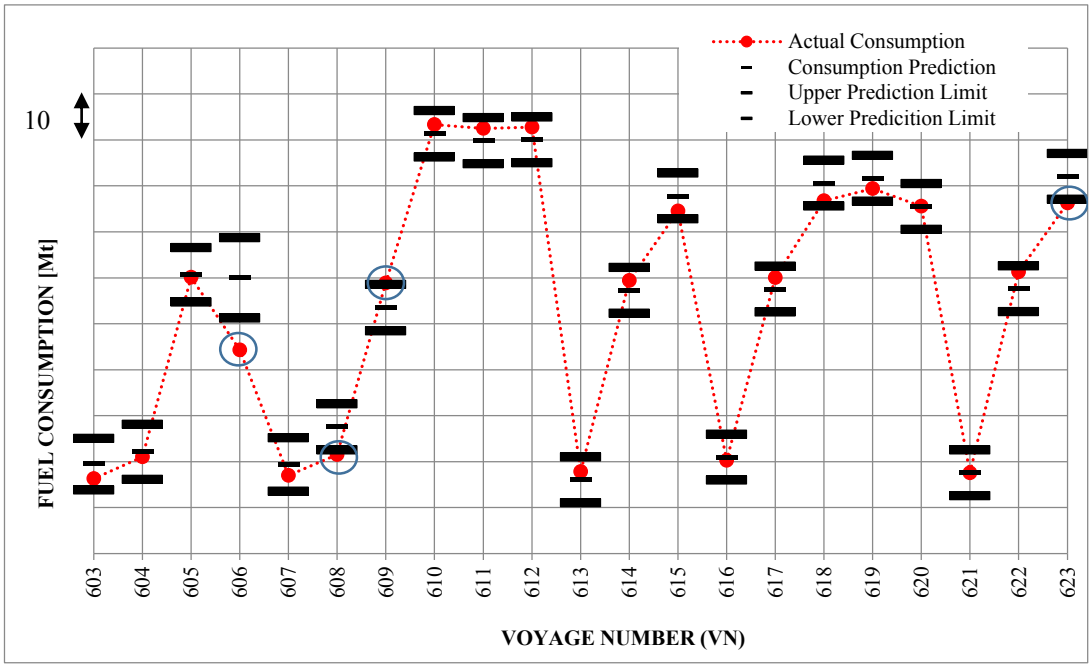

Figure 48: SHIP 1 – Actual fuel consumption and prediction intervals

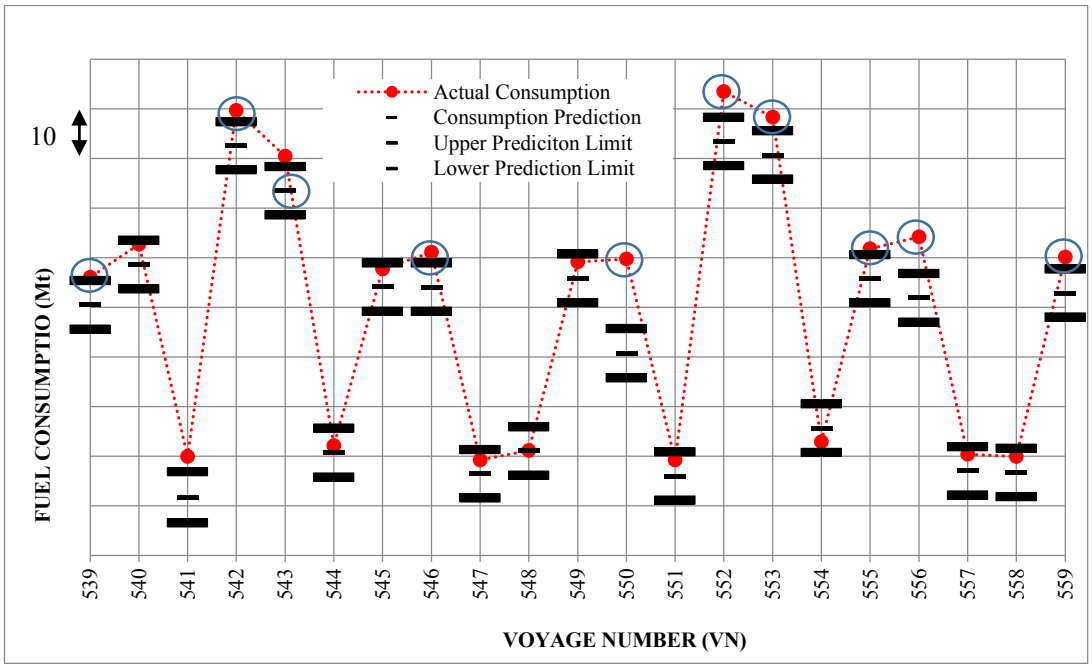

Figure 49: SHIP 2 – Actual fuel consumption and prediction intervals

By comparing the actual fuel consumption after a specific imporvement operation (e.g. hull form optimization, hull cleaning and propeller polishing, ultra smooth coating, improving propulsion

efficiency, engine maintenance operation, improving power plant efficiency) the proposed model can be utilized to demonstrate its significant effect.

For example, in order to evaluate the effectiveness of the dry-dock operation performed on the SHIP 1 from *Figure 50*, the actual fuel consumption after such operation ($VN\,675 \div 701$) is compared with the prediction limits calculated through (21) on data collected during the monitored period ($VN\,157 \div 537$) see *Figure 45*. We can observe that the actual fuel consumption falls significantly below the lower prediction limit. This could be significant evidence of a well executed dry-dock operation (hull cleaning).

On the countrary, in *Figure 51*, for SHIP 2 we observe that the actual fuel consumption from $VN\,377$ to $VN\,407$ after the dry-dock operation (hull cleaning) (see *Figure 45*) falls inside the prediction limits. This would alert the management that a problem may have occurred in hull cleaning, likely due to the use of too high pressure water and/or the unusual washing delay of about 72 hours.

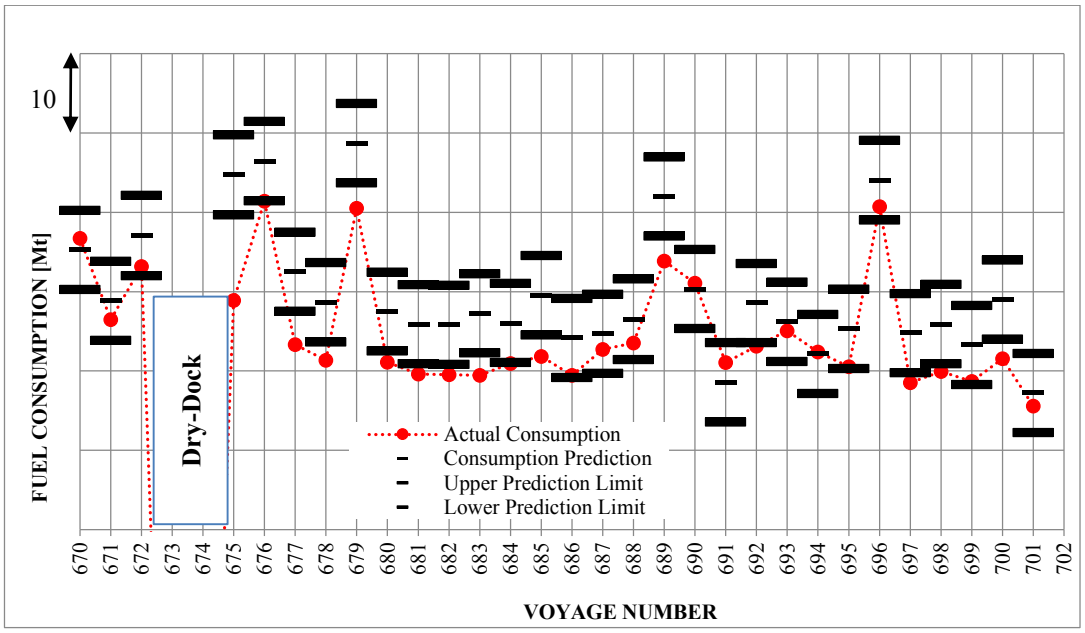

Figure 50: SHIP 1 – Actual fuel consumption and prediction intervals pre and after Dry-Dock operation

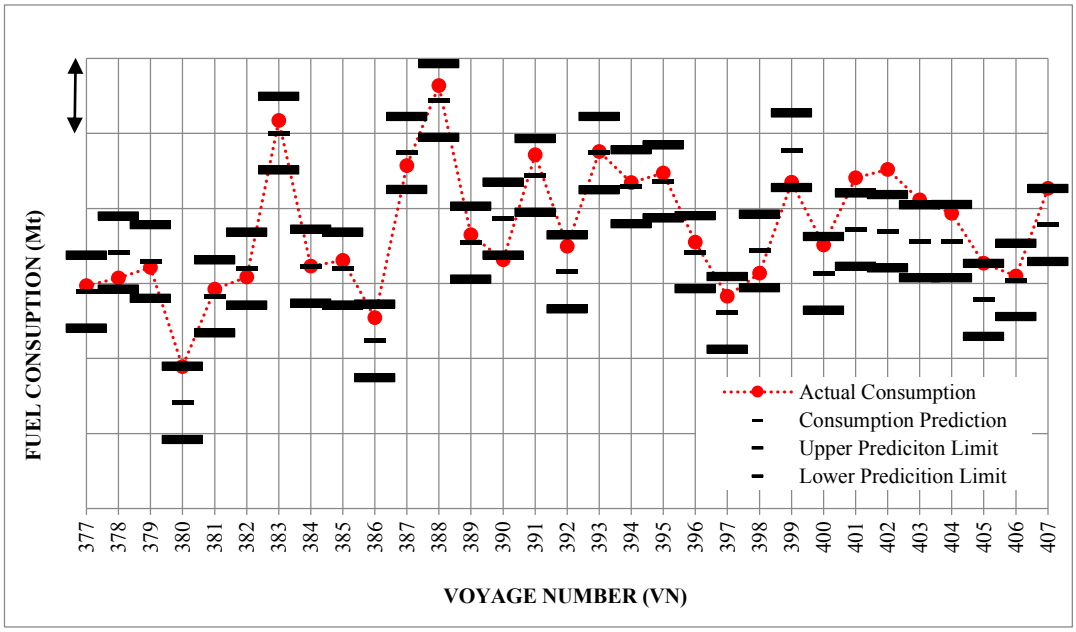

Figure 51: SHIP 2 – Actual fuel consumption and prediction intervals after Dry-Dock operation

4. Regression models comparison

In this paragraph we wish to compare two regression models.

Before approaching the regression model shown before, we started from another model in [10], called RINA model.

In RINA model, we take into consideration only the following variables, which have the main influence on the fuel consumption Y in (Mt) from a technological point of view:

Variable	Description	Unit of measurement
V	Ship Average Speed Over Ground	(*Knots*)
M	Sailed Distance	(*NM*)
W	Weather Condition Beaufort scale	
Δ	Displacement	(*Mt*)

Table 20: RINA model variables

In RINA model, the variables $V, M \text{ e } \Delta$ are collected by DAQ (quantitative variables) as well as W (categorical/qualitative variable) deducted from noon reports. Thus we introduce the dummy variables [30] reported in Table 20 for each wind speed class of Beaufort scale.

W	D_1	D_2	D_3	D_4	D_5	D_6	D_7	D_8
1	1	0	0	0	0	0	0	0
2	0	1	0	0	0	0	0	0
3	0	0	1	0	0	0	0	0
4	0	0	0	1	0	0	0	0
5	0	0	0	0	1	0	0	0
6	0	0	0	0	0	1	0	0
7	0	0	0	0	0	0	1	0
8	0	0	0	0	0	0	0	1
9	0	0	0	0	0	0	0	0

Table 21: RINA model dummy variables

Therefore the regression model is expressed in the following form:

$$
\begin{aligned}
Y = {} & \beta_0 + \beta_1 M + \beta_2 V^3 + \beta_3 \Delta + \\
& + \beta_{10} D_1 + \beta_{11} M D_1 + \beta_{12} V^3 D_1 + \beta_{13} \Delta D_1 + \\
& + \beta_{20} D_2 + \beta_{21} M D_2 + \beta_{22} V^3 D_2 + \beta_{23} \Delta D_2 + \\
& + \beta_{30} D_3 + \beta_{31} M D_3 + \beta_{32} V^3 D_3 + \beta_{33} \Delta D_3 + \\
& + \beta_{40} D_4 + \beta_{41} M D_4 + \beta_{42} V^3 D_4 + \beta_{43} \Delta D_4 + \\
& + \beta_{50} D_5 + \beta_{51} M D_5 + \beta_{52} V^3 D_5 + \beta_{53} \Delta D_5 + \\
& + \beta_{60} D_6 + \beta_{61} M D_6 + \beta_{62} V^3 D_6 + \beta_{63} \Delta D_6 + \\
& + \beta_{70} D_7 + \beta_{71} M D_7 + \beta_{72} V^3 D_7 + \beta_{73} \Delta D_7 + \\
& + \beta_{80} D_8 + \beta_{81} M D_8 + \beta_{82} V^3 D_8 + \beta_{83} \Delta D_8 + Z
\end{aligned}
$$

Or equivalently:

$$
Y = \begin{cases}
\beta_0 + \beta_1 M + \beta_2 V^3 + \beta_3 \Delta + Z & if \quad W = 9 \\
\beta_{10} + \beta_{11} M + \beta_{12} V^3 + \beta_{13} \Delta & if \quad W = 1 \\
\beta_{20} + \beta_{21} M + \beta_{22} V^3 + \beta_{23} \Delta & if \quad W = 2 \\
\beta_{30} + \beta_{31} M + \beta_{32} V^3 + \beta_{33} \Delta & if \quad W = 3 \\
\beta_{40} + \beta_{41} M + \beta_{42} V^3 + \beta_{43} \Delta & if \quad W = 4 \\
\beta_{50} + \beta_{51} M + \beta_{52} V^3 + \beta_{53} \Delta & if \quad W = 5 \\
\beta_{60} + \beta_{61} M + \beta_{62} V^3 + \beta_{63} \Delta & if \quad W = 6 \\
\beta_{70} + \beta_{71} M + \beta_{72} V^3 + \beta_{73} \Delta & if \quad W = 7 \\
\beta_{80} + \beta_{81} M + \beta_{82} V^3 + \beta_{83} \Delta & if \quad W = 8
\end{cases} \tag{35}
$$

where $\beta_{ij}^{'} = \beta_i^{'} + \beta_j^{'}; \quad i = 1,...,8 \; j = 0,...,3$ and $\beta_{9j}^{i} = \beta_j$. In fact if all the dummy variables D_i are zero, from (10) the regression equation is

$$Y = \beta_0 + \beta_1 M + \beta_2 V^3 + \beta_3 \Delta + Z \tag{36}$$

then represents the fuel consumption corresponding to wind speed of Beaufort force 9.

In Table 22 and in Table 23 are shows the main parameter of the regression analysis for SHIP 1 and SHIP 2, for RINA model and Thesis model, relative to equal monitoring period, respectively.

SHIP 1

Parameters	RINA model	Thesis model
S	3,11	2,51
R^2	98,71%	99,12%
R^2_{adj}	98,72%	99,08%
R^2_{pred}	98,23%	99,05%
PRESS	4288	2400

Table 22: SHIP 1, the main regression parameters for models

SHIP 2

Parameters	RINA model	Thesis model
S	3,77	2,45
R^2	98,44%	99,26%
R^2_{adj}	98,30%	99,23%
R^2_{pred}	97,89%	99,12%
Press	5836	2404

Table 23: SHIP 2, the main regression parameters for models

From the results obtained from the two regression models it appears clear that the parameters received from the Thesis model make it preferable to the RINA model. In fact the use of variables $W_h \, \text{e} \, W_s$, and of variable E, has a positive effect and allows for better results on each ship where the new model was implemented.

The Figure 52 hereafter shows a comparison between the prediction intervals calculated as difference between Upper Limit and Lower Limit expressed in (Mt) of fuel, of the RINA model and those of the Thesis models for each voyage “i”. Please note that the prediction intervals of Thesis model are much smaller, that means a higher accuracy in the prediction.

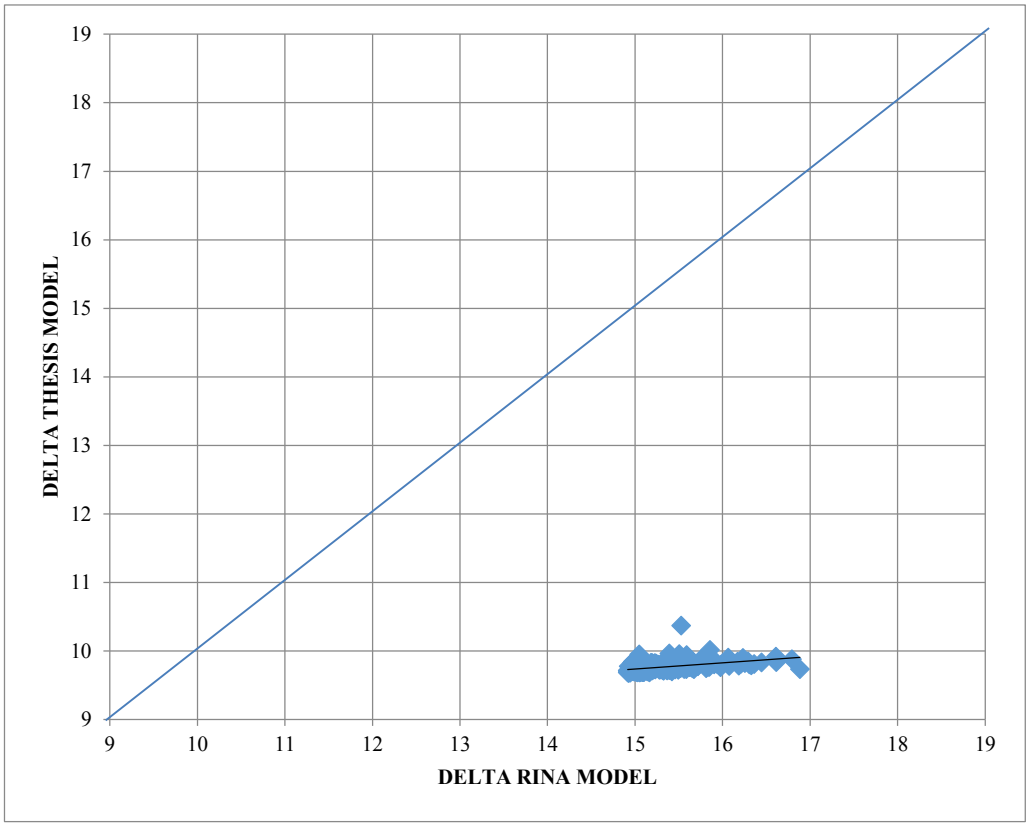

Figure 52: prediction interval, thesis model Vs RINA model

Explicitly note that the data considered in this paper overlap those in [10]. Voyages are identified with the same *VNs*. It can be worth noting that the actual fuel consumption of the voyages with VN $392, 394$ and 398 falls outside the prediction limits calculated in [10] (*Figure 54*) but inside those calculated in this paper (*Figure 53*).

In particular, voyage with VNs 392 and 398, are characterized by high side wind component on quarter and stabilizer fins activated during the whole voyage. In this condition, the model in [10] (*Figure 54*) overestimates fuel consumption prediction, probably because the characterization of the wind using through the Beaufort scale is less accurate than the characterization using W_h and W_s.

The VNs 394 is characterizes quartering sea with long waves and as a consequence of 3 days of bad weather and very low W_s, the stabilizer fins were being used. The model in [10] (Figure 54) underestimates the fuel consumption prediction because the stabilizer fins are not considered.

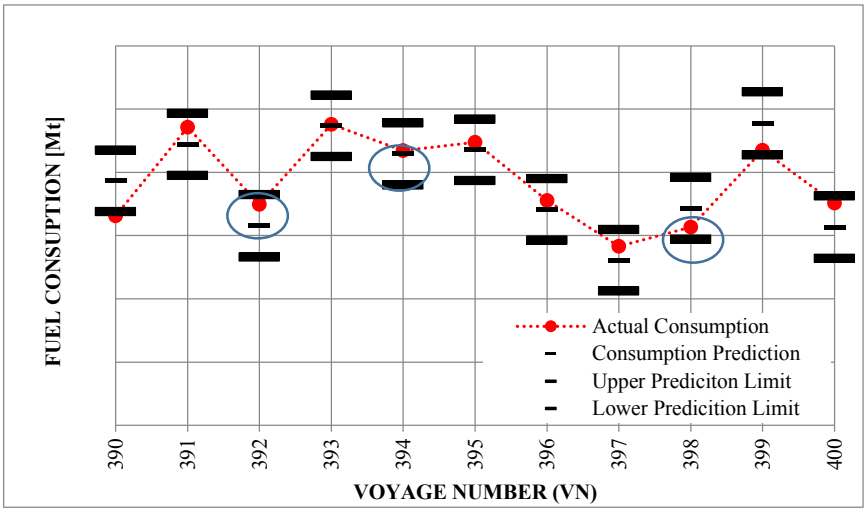

Figure 53: SHIP 2 Actual fuel consumption and prediction interval in thesis model

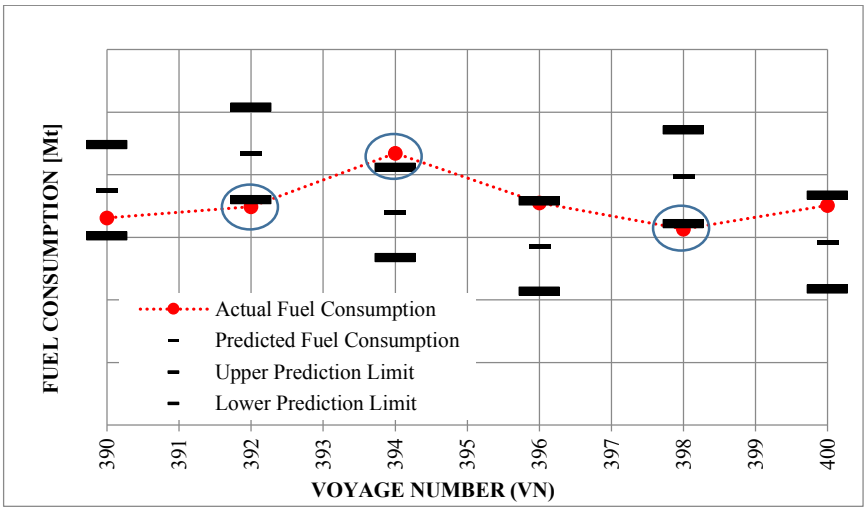

Figure 54: SHIP 2 Actual fuel consumption and prediction interval in [10] model

CONCLUSIONS

This study shows how engineering and statistical knowledge can be integrated and catalyses process innovation. Moreover, it allows for a continuous learning from data, which produces a significant improvement of the ship energy efficiency via design of experiments and regression analysis.

The Design Phase shows the strategic role in technological process innovation of a systematic approach in the industrial design of experiment. The team approach has been the real driving force of pre-experimental activities.

Moreover, technological interpretation of the results has allowed practitioners to gain technological knowledge and to see the added value of a systematic approach to planning for a design industrial experiment.

Since the obtained results arise from a systematic approach, they enable future experimental work focused on optimization and reliability to be planned.

Through the use of the Design of Experiment instead with traditional approach (OFAT) it has been possible to estimate the effects due to the change the two different control factors (design parameters) on the total response variable regarding the displacement.

The same approach can be used to yield information for the design of each ship or part of it.

From DoE we found that the best planning combination of control factors regarding hull resistance is the one with step number 1, step height 2 and static tau -1°, which gave the following hull resistance values measured in the towing tank test

Model speed V_m *[m/s]*	Ship speed V_s *[Knots]*	Model hull resistance R_{tm} *[Kg]*
4,631	28,5	8,162 ± 0,108
8,050	49,5	13,842 ± 0,186

Table 24: towing tank test

Through the open water efficiency η_h and η_0 calculated in chapter 2, power prediction with towing tank was carried out as shown in *Table 25*

Ship Speed V_M [Knots]	Effective Power in the towing tank test P_E [kW]	Open water propeller efficiency η_0	Hull efficiency η_t	Power Delivered P_D [kW]
28,5	101	0,67	0,80	189
49,5	267	0,73	0,99	272

Table 25: power prediction

Comparing the results obtained in **Errore. L'origine riferimento non è stata trovata.**, we deduce that our stepped hull at a speed of 49,5 knots ($F_\nabla = 7$) will have a Transport Efficiency $E_T = 3$. Consequently, the efficiency of the designed hull is higher than the ones already proposed in the literature.

In the Operation Phase, the statistical approach presented in this study helps practitioners to exploit navigation information usually available on modern ships in order to predict fuel consumption, and therefore CO_2 emissions, for given specific set of sailing parameters.

In order to predict fuel consumption and therefore carbon dioxide emission by exploiting the navigation information usually available on modern ships, a statistical model is introduced based on multiple regression analysis. For each voyage the actual fuel consumption can be compared with the consumption prediction and the prediction limits obtained through the proposed model. If the prediction interval does not include the actual fuel consumption, the management would be alerted of any change (improvement/decrease) in ship performance or the possible need for further data analysis.

In fact, only with a proper and continuous monitoring of specific variables, it is possible to support sail management in decision making.

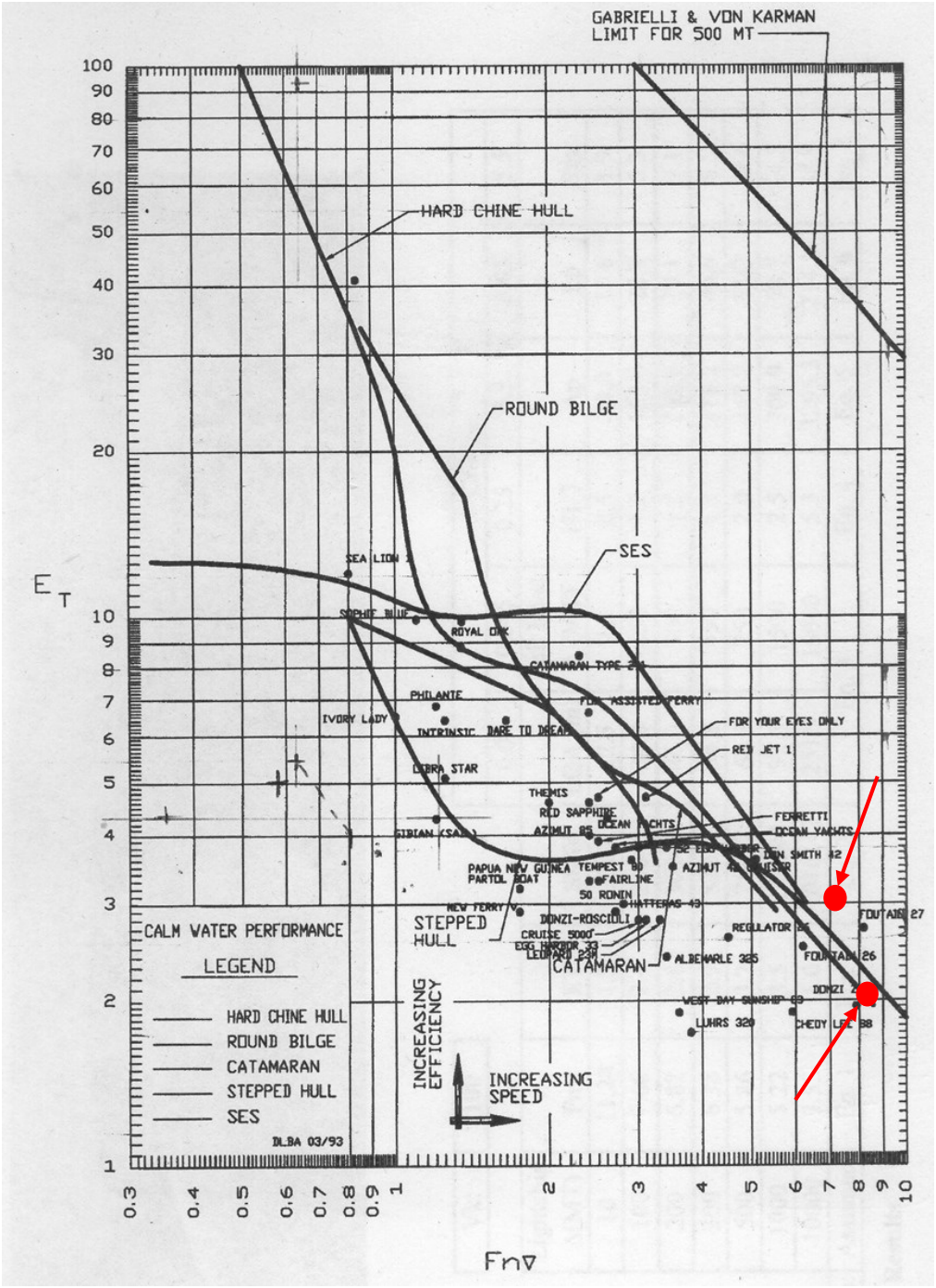

Figure 55: diagram of transport efficiency Vs volumetric Froude

REFERENCES

[1] Gabrielli G. and von Kàrmàn T., "What price speed? Specific power required for propulsion of vehicles," *Mechanical Engineering, ASME,* vol. 72, no. 10, 1950.

[2] Jong J., Smith R., Hatano L. and Hillmansen S., "What price speed - revisited," *Ingenia,* no. 22, March 2005.

[3] IMO, Second IMO GHG study final, 2009.

[4] IMO, Air pollution and greenhouse gas (GHG) emission from international shipping, Marpol Annexe VI, 12/09/2012.

[5] IMO, 2012 Guidelines on the method of calculation of the attenined energy efficiency design index (EEDI) for a new ship, MEPC.212 Annex 8, 02/03/2012.

[6] IMO, 2012 Guideline on survey and certification of the energy efficiency desig index (EEDI), MEPC.214 (63) Annexe 10, 02/03/2012.

[7] IMO, Guidelins for calculation of reference lines for use with the energy efficiency design index (EEDI), MEPC.215 (63) Annex 11, 2012.

[8] IMO, 2012 Guideline for development of a ship energy efficiency management plan (SEEMP), MEPC.213 (63) Annex 9, 02/03/2012.

[9] IMO, Guidance for the development of a ship energy efficiency management plan (SEEMP), MEPC.1/Circ. 683, 17/08/2009.

[10] BOCCHETTI D., LEPORE A., PALUMBO B. e VITIELLO L., A statistical control of the ship fuel consumption, London UK: The Royal Institution of Naval Architects, International conference on the design, construction and operation of passenger ships, 20-21 Nov 2013.

[11] DNV, DNV fuel saving guidelines, 2012.

[12] IMO, Guidelins for voluntary use of the ship energy efficiency operational indicator (EEOI), MEPC. 1/CIRC 684, 17/08/2009.

[13] SNAME, Transaction, 1911.

[14] M. D. Coleman D.E., «A systematic approach to planning for a design industrial experiment,» vol. 35, 1993.

[15] Akers, «Dancing a fine line,» *Professional Boat Builder,* Oct/NOV 2003.

[16] Peters M, «Peter on (fast) powerboats part 2,» *Professional Boat Builder,* n. 127, Oct/Nov 2010.

[17] Acampora B, «SM racer: designand operation of one of the world's fastest monohulls,» *MT ,* vol. 32, July 1995.

[18] P. Clement E.P., «Stepless and stepped planing hulls graph for performance prediction and design, report n° 1490,» DTMB, 1964.

[19] Clement E.P., «A lifting approach to planing boat design, report n 1902,» 1964.

[20] SNAME, Principles of naval architecture, vol. second, Edward V Lewis.

[21] M. M. Savitsky D., «Surface contourn associated with the forebody wake of stepped planing hulls,» *MT SNAME,* vol. 47, Jan 2010.

[22] Garland W.R., «Stepped planing hull investigation,» *Trans.,* 2011.

[23] M. K. Garland W.R., «A numerical study of a two-dimensional stepped planing surface,» *JSPD,* vol. 28, 2012.

[24] F. A. Brizzolara S., «Design of planing hulls with longitudinal steps: CFD in support of traditional semi-empirical methods,» in *Design and Construction of Super and Mega Yacht*, Genova, 2013.

[25] Clement E.P., «A configuration for a stepped planing boat having minimum drag (Dynaplane Boat),» International Hydrofoil Society, 2006. [Online].

[26] ITTC, «Guidelines for Uncertainty Analysis in Resistance Towing Tank Tests,» in *Recommended Procedure and Guidelines*, 2008.

[27] M. S. B. F. B. A. C. S. Vitiello L, «Stepped hulls: model experimental tests and sea trial data,» in *NAV 2012*, Napoli, 2012.

[28] D. C. Montgomery, Design and Analysis of Experiments 5 th edition, Wiley, 1997.

[29] PEDERSEN B.P. e LARSEN J., Modeling of ship propulsion performance, WMTC, 2009.

[30] MONTGOMERY D., PECK E. e VINING G., Introduction to Linear Regression Analysis 5th ed, Mc-Graw-Hill, 2008.

[31] MONTGOMERY D., RUNGER G. e HUBELE N., Engineering statistic 5th ediion, Wiley & Sons, 2011.

[32] W. Z. Yang E.Z., «Metamodel approach for reliability-based design optimization of a steel catenary riser,» *JMST,* 2011.

[33] VAN MANEN J.D. e VAN OOSSANEN P., Principles of naval architecture, chapter 5 resistance, SNAME.

[34] P. D. C. E. S. F. Tahara Y., «Single and multiobjective desgn optimization of a fast multihull ship: numerical and experimental results,» *JMST,* 2011.

[35] PESCETTO A., SEBASTIANI L. e (CETENA), Energy management: a holistic operational strategy to enhance ship energy efficiency of ship in service, NAV 2012 .

[36] PEDERSEN B.P. e LARSEN J., Prediction of full scale propulsion power using artificial neural networks, 2009.

[37] CHEN H., A new approach to ship speed performance monitoring and prediction, SNAME Spring Meeting/Star symposium, 1989 April.

[38] Bertram Volker e Mohammed S. Seif, «New developments for fast unconventional marine vehicles,» 2006.

[39] «Atti di Guidonia,» Roma, 1938.

[40] Akagi S., «Syntetic aspects of transport economy and transport vehicle performance with reference to high speed marine vehicles,» in *FAST 91*, 1991.

FIGURE INDEX

TABLE INDEX

Acknowledgements

I would like to thank the following people:
Prof. Pasquale Erto, Prof Salvatore Miranda, il Prof Biagio Palumbo and Antonio Lepore (researcher) for believing in me, for supporting my doctorate thesis at every stage with patience and experience, contributing in a determining way to my development;
Dario Bocchetti (manager) and Andrea d'Ambra (engineer) of Energy Saving Department of Grimaldi Group, for their support of any kind during the research in the energy ship performance monitoring;
Vincenzo Nappo (CEO) of MVmarine for providing their resources to build the many craft model for towing tank test and a your rigid inflatable boats for many sea trial;
Maurizio Mirabile (CEO) of HPSystem.it for providing their resources to build the data acquisition hardware and software for outboard marine engine thrust;
Prof. Fabrizio Ricci for providing their resources to design and calibration of load cells for thrust of outboard marine engine;
Prof. Domenico Coiro for providing their resources to build the propeller model;
Mario e Davide Comitangelo for ship propeller reverse engineering and for load cells build;
Marco di Palma (Ph.D. st.) for all hull model and propeller model design;
Dr Andrea Bove for his deepen technological and scientific support in experiment phase
Flavio Balsamo (researcher) for his support during sea trials;
Antonio Alfano, Biagio Scotto D'Abbusco, Vitale Esposito, Lucio Iadicicco, Pasquale Zuppaldi e Pasquale Cioffi, technician of model basin for their collaboration during the towing tank tests;
Thanks also the thesis students Ida Pellegrino, Francesco Scognamiglio, Giovanni Scotto di Carlo e Dario Lo Noce, who daily have collaborated in all my works.

Ringraziamenti

Ringrazio:
il Prof. Pasquale Erto, il Prof Salvatore Miranda, il Prof Biagio Palumbo e l'Ing. Antonio Lepore per aver creduto in me, per avermi offerto indicazioni e consigli preziosi, per avermi seguito in tutte le fasi con pazienza ed esperienza, contribuendo in modo determinante alla mia formazione.
l'Ing. Dario Bocchetti e l'Ing. Andrea d'Ambra della compagnia di navigazione Grimaldi S.p.a. per aver messo a disposizione collaborazione e risorse per lo studio del monitoraggio dei consumi di combustibile;
l'Ing. Vincenzo Nappo della MVmarine per la realizzazione dei tanti modelli di carene provati in vasca navale e per la disponibilità di un suo gommone per le numerose prove in mare;
Maurizio Mirabile della HPSystem.it per la realizzazione della scheda e del software di acquisizione dati per la misura della spinta dei motori fuoribordo;
il Prof. Fabrizio Ricci per la progettazione e la taratura delle celle di carico;
il Prof. Domenico Coiro per la sponsorizzazione della realizzazione del modello di elica;
Mario e Davide Comitangelo per il reverse engineering dell'elica e per la costruzione delle celle di carico;
l'Ing. Marco di Palma per la collaborazione nel disegno e nella progettazione di tutti i modelli di carene ed elica;
il Dott. Andrea Bove per il supporto tecnico scientifico durate tutte le sperimentazioni in laboratorio;
l'Ing. Flavio Balsamo per il supporto tecnico scientifico durante le prime sperimentazioni in mare;
Antonio Alfano, Biagio Scotto D'Abbusco, Vitale Esposito, Lucio Iadicicco, Pasquale Zuppaldi e Pasquale Cioffi, i tecnici della vasca navale per la collaborazione durante gli esperimenti;
inoltre ringrazio Ida Pellegrino, Francesco Scognamiglio, Giovanni Scotto di Carlo e Dario Lo Noce, i tesisti che quotidianamente hanno collaborato in tutte le mie attività.